Louisiana Transportation Research Center

Final Report 590

Assessment of the Traffic Speed Deflectometer in Louisiana for Pavement Structural Evaluation

by

Mostafa A. Elseifi, Ph.D., P.E.
Zia Uddin Ahmed Zihan

LSU

4101 Gourrier Avenue | Baton Rouge, Louisiana 70808
(225) 767-9131 | (225) 767-9108 fax | www.ltrc.lsu.edu

TECHNICAL REPORT STANDARD PAGE

1. Report **FHWA/LA.18/590**	**2. Government Accession No.**	**3. Recipient's Catalog No.**
4. Title and Subtitle **Assessment of the Traffic Speed Deflectometer in Louisiana for Pavement Structural Evaluation**	**5. Report Date** March 2018 **6. Performing Organization Code** LTRC Project Number: 14-2P SIO Number: DOTLT 100009	
7. Author(s) **Mostafa A. Elseifi and Zia U.A. Zihan**	**8. Performing Organization Report No.**	
9. Performing Organization Name and Address Department of Civil and Environmental Engineering Louisiana State University Baton Rouge, LA 70803	**10. Work Unit No.** **11. Contract or Grant No.**	
12. Sponsoring Agency Name and Address Louisiana Department of Transportation and Development P.O. Box 94245 Baton Rouge, LA 70804-9245	**13. Type of Report and Period Covered** **Final Report** **14. Sponsoring Agency Code** LTRC	
15. Supplementary Notes **Conducted in Cooperation with the U.S. Department of Transportation, Federal Highway Administration**		

16. Abstract

Many state agencies have recognized the importance of incorporating pavement structural conditions in the selection of maintenance and rehabilitation (M&R) strategies along with functional indices. The Traffic Speed Deflectometer (TSD) has emerged as a continuous pavement deflection-measuring device as it operates at traffic speed and reduces lane closure and user delays. The objective of this study was to assess the feasibility of using TSD measurements at the network-level for pavement conditions structural evaluation in Louisiana and in backcalculation analysis. To achieve the objectives of the study, TSD and FWD measurements were collected in District 05 of Louisiana and data were available from experimental programs conducted at the MnROAD research test facility and in Idaho. Based on the results of the analysis, it is concluded that the deflection reported by both FWD and TSD for the same locations are statistically different, which was expected given the differences in loading characteristics and load type between the two devices. It is also concluded that surface roughness has a notable effect on TSD field measured deflections. The present study successfully developed a model to predict in-service Structural Number (SN) based on TSD deflections at 0.01-mile interval of a road section. The model was successfully developed and validated with SN calculated based on TSD and FWD deflection data obtained from two contrasting data sets from Louisiana and Idaho. Furthermore, the estimated percentage loss in structural capacity from the model was in good agreement with the percentage loss calculated from FWD. The importance of considering structural indices along with functional indices was demonstrated based on statistical analysis and extracted cores. Core samples showed that the sections that were predicted to be structurally deficient suffered from asphalt stripping and debonding problems. Yet, some of these sections were in very good functional conditions. A methodology was developed to incorporate TSD measurements in the backcalculation analysis and for predicting pavement layer moduli. The proposed Artificial Neural Network (ANN) model showed acceptable accuracy in predicting the corresponding FWD deflections (TSD*) from TSD deflection measurements with a coefficient of determination of 0.90. In addition, the backcalculated moduli from FWD and TSD* deflection measurements were in good agreement. The ANN model was also validated by comparing the critical pavement responses, number of cycles for fatigue failure, and Structural Health Index (SHI) calculated from FWD and TSD* measurements.

17. Key Words Traffic Speed Deflectometer, Structural Evaluation, Falling Weight Deflectometer, Pavement Management System		**18. Distribution Statement** **Unrestricted. This document is available through the National Technical Information Service, Springfield, VA 21161.**	
19. Security Classif. (of this report)	**20. Security Classif. (of this page)**	21. No. of Pages 118	22. Price

Project Review Committee

Each research project will have an advisory committee appointed by the LTRC Director. The Project Review Committee is responsible for assisting the LTRC Administrator or Manager in the development of acceptable research problem statements, requests for proposals, review of research proposals, oversight of approved research projects, and implementation of findings.

LTRC appreciates the dedication of the following Project Review Committee Members in guiding this research study to fruition.

LTRC Administrator

Kevin Gaspard, P.E.
Senior Pavement Research Engineer

Members

Simone Ardoin
Xingwei Chen
Christophe Fillastre
Amy Giddens
Hector Santiago
Don Weather

Directorate Implementation Sponsor

Christopher P. Knotts, P.E.
DOTD Chief Engineer

Assessment of the Traffic Speed Deflectometer in Louisiana for Pavement Structural Evaluation

by

Mostafa A. Elseifi, Ph.D., P.E.
Professor
Department of Civil and Environmental Engineering
Louisiana State University
3240N Patrick Taylor Hall
Baton Rouge, LA 70803
e-mail: elseifi@lsu.edu

and

Zia Uddin Ahmed Zihan
Graduate Research Assistant
Department of Civil and Environmental Engineering
Louisiana State University
3256 Patrick Taylor Hall
Baton Rouge, LA 70803
e-mail: zzihan1@lsu.edu

LTRC Project No. 14-2P
State Project No. DOTLT 100009

conducted for
Louisiana Department of Transportation and Development
Louisiana Transportation Research Center

March 2018

ABSTRACT

Many state agencies have recognized the importance of incorporating pavement structural conditions in the selection of maintenance and rehabilitation (M&R) strategies along with functional indices. To measure in-service pavement structural capacity, surface deflection under a defined load has been typically used. The Traffic Speed Deflectometer (TSD) has emerged as a continuous pavement deflection-measuring device as it operates at traffic speed and reduces lane closure and user delays.

The research objective of this study was to assess the feasibility of using TSD measurements at the network-level for pavement conditions structural evaluation in Louisiana and in backcalculation analysis. To achieve the objectives of the study, TSD and Falling Weight Deflectometer (FWD) measurements were collected in District 05 of Louisiana and data were available from experimental programs conducted at the MnROAD research test facility and in Idaho. TSD measurements were compared with FWD deflection measurements to evaluate the level of agreement and difference between the two devices. Based on this evaluation, a SN predictive model was developed and validated to assess the structural conditions of in-service pavements. The model was then used to identify structurally sound and structurally deficient in-service pavements. Furthermore, a methodology was developed and was validated to backcalculate the layer moduli from TSD measurements.

Based on the results of the analysis, it is concluded that the deflection reported by both FWD and TSD for the same locations are statically different, which is reasonable given the differences in loading characteristics and load type between the two devices. It is also concluded that surface roughness has a notable effect on TSD field measured deflections.

The present study successfully developed a model to predict in-service SN based on TSD deflections at 0.01-mile interval of a road section. The model was successfully developed and validated with SN calculated based on TSD and FWD deflection data obtained from two contrasting data sets from Louisiana and Idaho. Furthermore, the estimated percentage loss in structural capacity from the model was in good agreement with the percentage loss calculated from FWD. The importance of considering structural indices along with functional indices was demonstrated based on statistical analysis and extracted cores. Core samples showed that the sections that were predicted to be structurally deficient suffered from asphalt stripping and debonding problems. Yet, some of these sections were in very good conditions according to their functional indices.

A methodology was developed to incorporate TSD measurements in backcalculation analysis and for predicting pavement layer moduli. The proposed Artificial Neural Network (ANN) model showed acceptable accuracy in predicting the corresponding FWD deflections (TSD*) from TSD deflection measurements with a coefficient of determination of 0.90. In addition, the backcalculated moduli from FWD and TSD* deflection measurements were in good agreement. The Root Mean Square Error (RMSE) was 12.5%, 13.2%, and 10.2% for the AC moduli, base moduli, and subgrade moduli, respectively. The ANN model was also validated by comparing the critical pavement responses, number of cycles for fatigue failure, and Structural Health Index (SHI) calculated from FWD and TSD* measurements.

ACKNOWLEDGMENTS

The authors recognize the efforts of Chad Murnane with ARRB Group Inc., who cooperated with the research team during this project. This was critical for interpreting the TSD measurements collected in this study. The authors would also like to acknowledge the remarkable effort of Kevin Gaspard and Zhongjie "Doc" Zhang of the Louisiana Transportation Research Center (LTRC).

The U.S. Department of Transportation (USDOT), Federal Highway Administration (FHWA), and DOTD through LTRC financially supported this research project.

IMPLEMENTATION STATEMENT

Based on the findings and the results of this project, TSD measurements were found beneficial to the state Pavement Management System (PMS) by successfully identifying sections that were predicted to be structurally deficient and by addressing their repair needs based on their deficiencies. Some of these sections were in very good conditions according to their functional indices. The proposed SN model is implementation-ready in routine overlay design if TSD measurements are conducted regularly by the state.

TABLE OF CONTENTS

LIST OF TABLES

LIST OF FIGURES

INTRODUCTION

In-service pavement conditions are typically described by a number of functional factors such as surface distresses, roughness, and rutting, which do not necessarily describe the structural conditions of a pavement. As roads are being subjected to loads higher than the design traffic loads and to extreme weather events, the increasing rate of deterioration necessitates the incorporation of a structural capacity indicator in Pavement Management System (PMS) for effective rehabilitation and maintenance decision-making. Structural capacity is a valuable input in the design of asphalt concrete (AC) overlays and for identifying structurally deficient pavements. It also important in selecting treatment methods and in making cost-effective pavement maintenance and rehabilitation decisions *[1-3]*.

Pavement deflection under a given static or moving load is a fast and reliable method to evaluate pavement structural capacity. Deflection is also an important measurement that is used in numerous pavement deterioration models *[4]*. Pavement deflection is typically measured by applying a defined load using the Falling Weight Deflectometer (FWD). In FWD testing, an impact circular load is applied to the pavement surface at a predefined frequency. This stationary device uses multiple sensors located at different distances from the load to measure pavement surface deflections. Pavement layer moduli can be backcalculated from the deflection basin obtained from FWD testing *[5, 6]*. While FWD allows measuring deflections with a high accuracy, it requires lane closures causing traffic delays and safety concerns. This has limited the use of FWD to project level applications and has led to the introduction of Traffic-Speed Deflection Devices (TSDD) including the Traffic Speed Deflectometer (TSD) and the Rolling Wheel Deflectometer (RWD) *[7]*. A recent Strategic Highway Research Program 2 (SHRP2) study identified the TSD and the RWD as the most promising continuous deflection measurement devices *[8]*.

The traffic speed deflectometer was evaluated in the present study in assessing in-service pavement structural conditions at the network level. The TSD can measure pavement deflection at traffic speeds, which enable large spatial coverage and can generate continuous deflection profiles rather than measuring deflection at discrete points *[9]*. Another advantage of TSD is, unlike RWD, it allows complete measurement of the deflection basin. Since TSD allows the measurement of the complete deflection basin, it could also be used in the backcalculation analysis of layer moduli *[10]*.

The present study was conducted to evaluate TSD based on deflection measurements obtained from three field-testing programs conducted in District 05 of Louisiana, at the MnROAD test facility in Minnesota, and in Idaho. Based on these measurements, the study

evaluated the feasibility and effectiveness of TSD for structural pavement evaluation at the network-level. The study also developed a methodology to predict in-service Structural Number (SN) and to incorporate TSD measurements in the backcalculation analysis of layer moduli.

Literature Review

Pavement-conditions data collection by DOTD evolved from windshield surveys in the 1970s to videotaping the pavement surface in 1992, and then to automatic distress data collection in 1995. At present, distress data are collected and analyzed every two years for the road network in Louisiana. DOTD PMS data collection protocol includes collection of roughness, rutting, cracking, patching, and faulting data from all the nine districts of Louisiana. Each control section is divided into $1/10^{th}$ of a mile and distress data are collected and are reported at 0.1-mile interval along a control section. An index scale that ranges from zero to 100 is then used to report and describe pavement surface conditions where a value of zero represents very poor conditions and a value of 100 indicates excellent conditions *[2]*.

The need for considering pavement structural conditions along with functional conditions has been recognized in the past decade by various state agencies, which supported the incorporation of a structural condition index in PMS to assist in decision-making processes. The traffic speed deflectometer, a Doppler-laser based continuous deflection measurement device, has emerged as a promising method to measure vertical surface deflection velocity continuously along a road section. The TSD consists of an articulated truck that uses a rear axle of 22,000 lbs. to load the pavement structure. The operational speed of the device is up to 60 mph; the TSD concept is based on the measurement of the deflection velocity rather than the absolute deflection at the road surface *[9, 11]*.

Overview of the Traffic Speed Deflectometer

In early 2000s, the traffic speed deflectometer was introduced as a continuous deflection measuring device by Greenwood Engineering, which showed promising potential in assessing pavement structural conditions. The TSD is a continuous laser-based deflection measurement device that loads the pavement and measures vertical deflection velocity using Doppler lasers at four or six points *[9, 11]*. At these discrete points, when the preliminary vertical surface deflection velocity collected by the Doppler lasers is divided by the instantaneous horizontal TSD vehicle speed, the deflection slope is obtained *[12]*. The deflection slope is then converted to actual pavement deflection by curve fitting or numerical integration *[10]*. Figure 1 illustrates the TSD vehicle used in the experimental program described in this study.

Figure 1
TSD vehicle used in the experimental program in Louisiana

As shown in Figure 1, the TSD consists of an articulated truck applying 22,000 lbs. on the rear axle; pavement response to the rear axle is measured as the vertical deflection velocity by fixed Doppler lasers mounted on a servo-hydraulic beam. The servo-hydraulic beam can move with the movement of the trailer, which allows the Doppler lasers to maintain a fixed height from the surface of the pavement. To address thermal fluctuations during testing, a constant 68°F (20°C) temperature is maintained in the servo-hydraulic beam. The TSD can collect one measurement every 0.00001-mile (0.787 in.) of road section at a rate of 1000 Hz while travelling at a traffic speed of up to 60 mph *[13]*. The maximum temporal resolution of the TSD is 1-millisecond and typical spatial resolution after processing is 0.0006-mile *[14]*. In the United Kingdom, TSD data are commonly reported at 0.006-mile and are stored at 0.0006-mile (39.37 in.) averages *[13]*.

The operation of the TSD is based on the vertical deflection velocity measurements rather than the actual surface deflections *[8, 15]*. The measured deflection velocity depends on the speed of the TSD; this dependency can be eliminated by dividing the vertical deflection velocity by the instantaneous horizontal TSD speed, which allows obtaining the deflection slope at each location of TSD measurement. The unit for measuring the deflection velocity and vehicle speed are millimeter per second and meters per second, respectively *[16]*. A good correlation has been reported by Simonin et al. between the center deflection and the calculated deflection slope *[17]*.

Along a pavement section, weak and sound locations can be identified through the deflection slopes but the estimation of the extent of weakness or soundness, which could assist in selecting maintenance and rehabilitation treatment methods, requires the pavement surface deflection. Pavement surface deflection can be calculated at any point from the center deflection (deflection under load) up to a radial distance by integrating the deflection slopes. Structural condition indicators such as the Base Damage Index (BDI) and Surface Curvature Index (SCI) can also be calculated using the calculated surface deflection *[18]*.

Deflection Measuring Technique of FWD and TSD

The deflection measuring techniques for FWD and TSD are quite different. Even if both devices apply the same load magnitude, the measured deflection is conceptually different. The stationary FWD device applies an impact load to the surface of the pavement and measures the deflection at the center of the applied load and at multiple locations with varying distances from the center of the load. The FWD uses a circular plate to load the pavement as shown in Figure 2(a). In contrast, the TSD operates at a traffic speed up to 60 mph and loads the pavement through its rear axle. Over the right wheel, Doppler lasers are mounted to measure the deflection velocity between the dual tires. Doppler lasers measure the deflection velocity at the midpoint between the tires as shown in Figure 2(b).

(a) FWD testing using a circular plate

(b) TSD measuring deflection velocity between the dual tires

Figure 2
Deflection measuring technique of FWD and TSD *[19, 20]*

While FWD applies a circular loading with a uniform contact pressure, TSD applies an elliptical-shape loading using regular tires with non-uniform contact pressure. Hence, pavement responses are expected to be different due to the different loading mechanisms for TSD and FWD *[19]*. It is also noted that a dynamic load of a five-axle truck-semitrailer can vary by almost 33% of the load of that truck when measured in a static scale *[21]*. As

previously noted, TSD measurements are reported as deflection slopes (calculated by dividing the vertical deflection velocity by the horizontal velocity of TSD), whereas FWD measures the actual vertical deflection. The TSD deflection calculation procedure is further discussed in the "Methodology" section of this report.

TSD and FWD Comparisons

As previously noted, there is a fundamental difference between the TSD and FWD loading mechanisms, which could lead to notable differences in the measured deflection values obtained from these two devices. With respect to loading operations, TSD operates with a moving load at traffic speeds, whereas, FWD load is stationary. Furthermore, TSD measured deflections could be highly influenced by the irregularities in the surface such as roughness and other pavement distresses *[8, 22]*. Previous studies compared the SCI and BDI derived from TSD slope measurements and FWD deflection measurements *[23]*. The study found significant bias between these two devices and recommended using the Limit of Agreement (LOA) method to compare the measurements from the two devices *[23]*. In Australia and New Zealand, a research study found a strong correlation between TSD and FWD deflection measurements *[24]*. Another study compared between the TSD and FWD measured deflections in Virginia *[25]*. The comparison indicated a similar trend in deflections between the two devices. The study suggested that the structural conditions along the tested road was successfully reflected in the measurements of the two devices; see Figure 3.

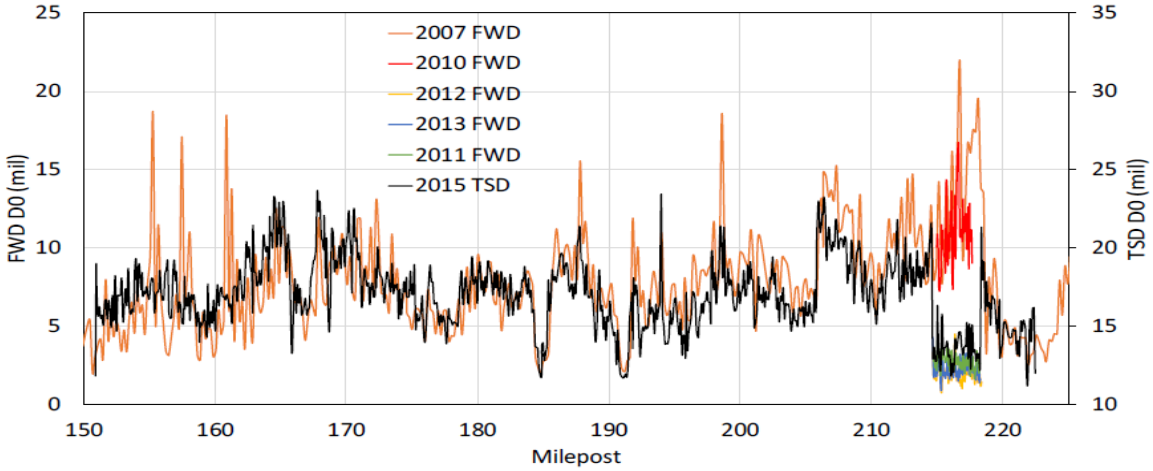

Figure 3
Comparison of TSD and FWD D0 on I81 South in Virginia

TSD Measurements Dependency on Speed

In a previous study, the variation of TSD measurements with its operating speed was investigated *[26]*. TSD testing was conducted at two different traffic speeds of 30 and 45

mph on low volume roads (LVR) and at 45 and 60 mph on the Mainline. Results indicated that the measured deflection is sensitive to speed of loading. It was found that the coefficients of variation of the deflection slopes were about 24% less at 30 mph than at 45 mph along the LVR and were around 38% greater at 60 mph than the COVs at 45 mph on the Mainline. The developed graphs for the COVs in the LVR and Mainline are shown in Figure 4 and Figure 5. However, another research study concluded that TSD measures "real" pavement response, even at low speed (<20 mph) *[27]*.

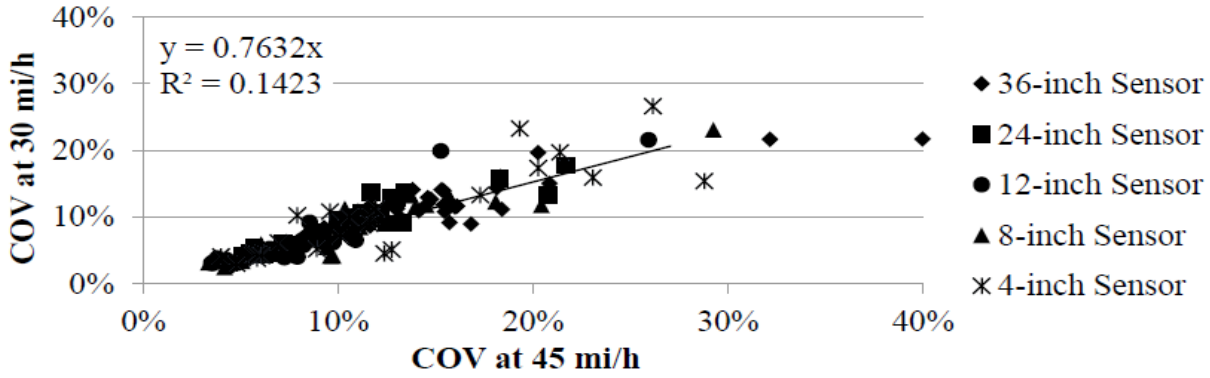

Figure 4
Comparison deflection slope COVs in LVR *[26]*

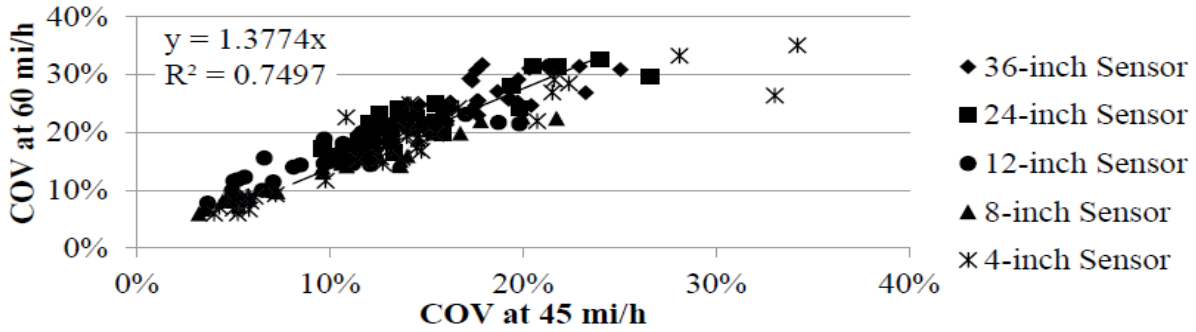

Figure 5
Comparison deflection slope COVs in the Mainline *[26]*

TSD Measurement Dependency on Pavement Structure

The correlation of TSD slope measurements to pavement stiffness and surface roughness was investigated in a previous study *[26]*. TSD slope measurements were collected for different pavement sections and the COVs of the deflection slopes were calculated for each section. The average FWD central deflection was also measured for these sections. Pavement stiffness was represented by the FWD central deflection in the analysis; the greater the FWD

central deflection, the lower the pavement stiffness. The authors reported that the COVs from the first four sensors decreased with the increase in FWD central deflection for the flexible pavement sections; see Figure 6. For the rigid pavement sections, the COVs of the deflections slopes were found to be relatively higher than for the far sensor locations; see Figure 7. However, it is our opinion that the reported trends were not strongly evident, possibly due to the variation in the pavement structure concurrently with the variation in surface roughness. Pavement surface roughness was also correlated to the COVs of the TSD measurements. However, no strong correlation was observed, as shown in Figure 8 and Figure 9.

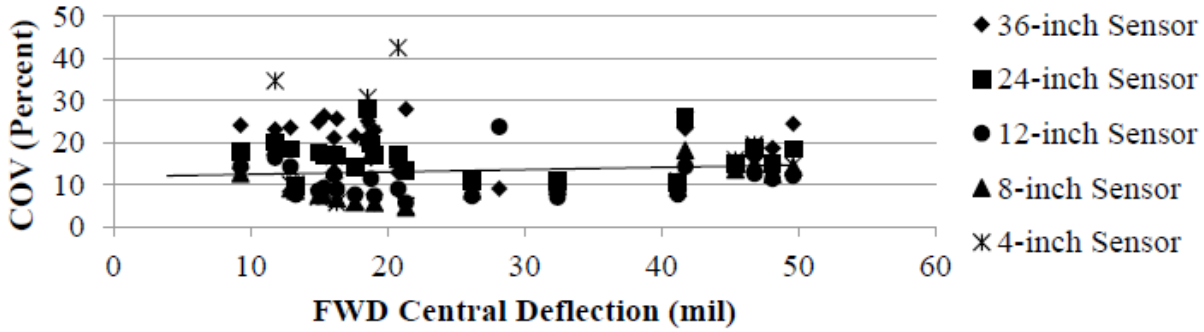

Figure 6
TSD measurements variation with pavement stiffness on flexible pavement *[26]*

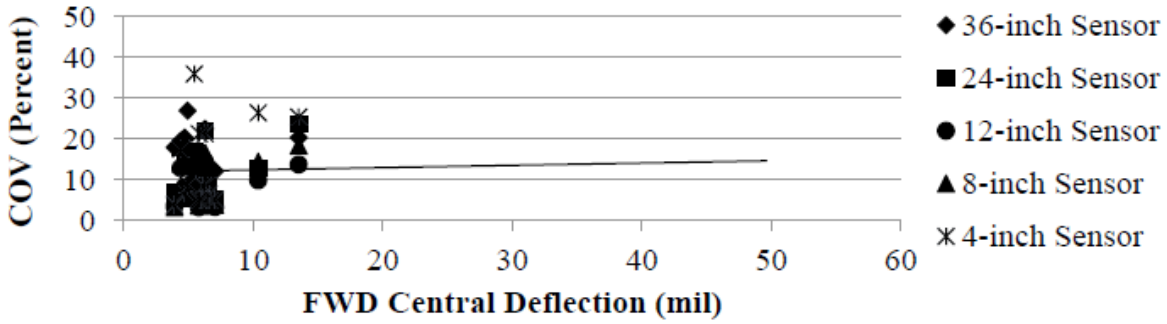

Figure 7
TSD measurement variation with pavement stiffness on rigid pavement *[26]*

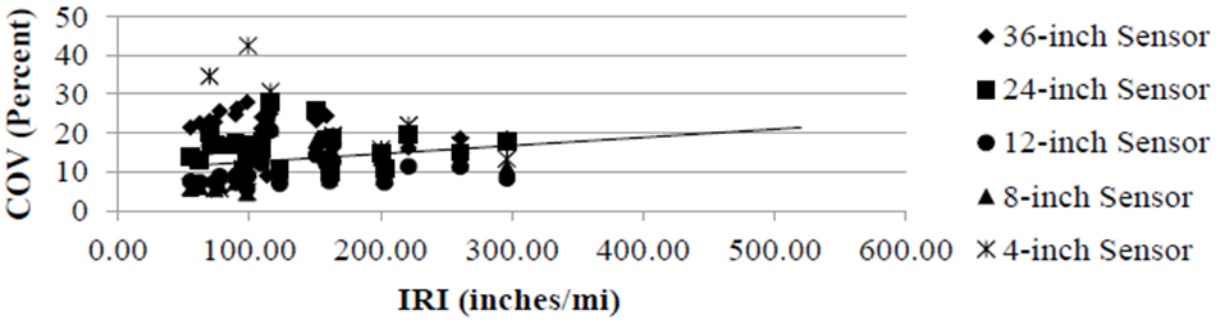

Figure 8
TSD measurement variation with pavement roughness of flexible pavement *[26]*

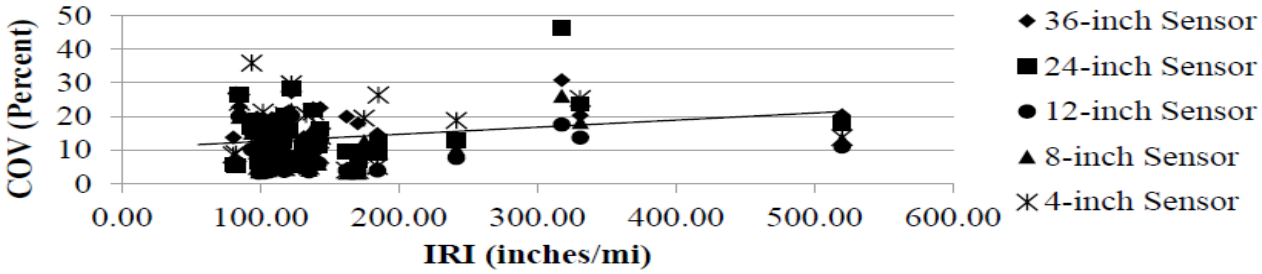

Figure 9
TSD measurement variation with pavement roughness of rigid pavement *[26]*

As previously noted, axle load can be dynamically amplified due to vehicle suspension type, travelling speed, tire contact pressure, tire thread pattern, axle and wheel configuration, and pavement stiffness. It was found that a rough pavement surface could cause a 50% increase in the static axle load, which explains the accelerated deterioration of rough pavements. A number of studies used a Dynamic Load Coefficient (DLC) to represent the dynamic amplification of static axle load. Statistically, DLC can be defined as one standard deviation from the mean static axle load. The typical value for DLC has been reported as 0.05 to 0.4 from previous studies *[1]*. For different vehicle suspension types and tire configurations, the DLC was correlated to different parameters as follows:

$$DLC^{*} = \frac{\kappa^{*}R^{*}IRI}{2} \quad (1)$$

where,

DLC* = DLC value for the normal distribution of the axle load;

κ = coefficient related mostly to the suspension type (assumed $\kappa = 0.0016$);

R = truck speed [km/h]; and

IRI = International Roughness Index [m/km].

From equation (1), it can be noticed that with the increase in IRI and traffic speed, the DLC also increases, which causes dynamic amplification of the load. A probabilistic approach using 10,000 Monte Carlo simulation trials has been conducted to account for the random effects of pavement roughness. A normal distribution of the dynamic axle load for TSD vehicle was developed using equation (1); see Figure 10. F_{stat} is the average static axle load and F_{left} and F_{right} accounts for the left and right side of the vehicle. From this distribution, it is observed that the static axle load increases by around ± 20% due to surface roughness *[1]*.

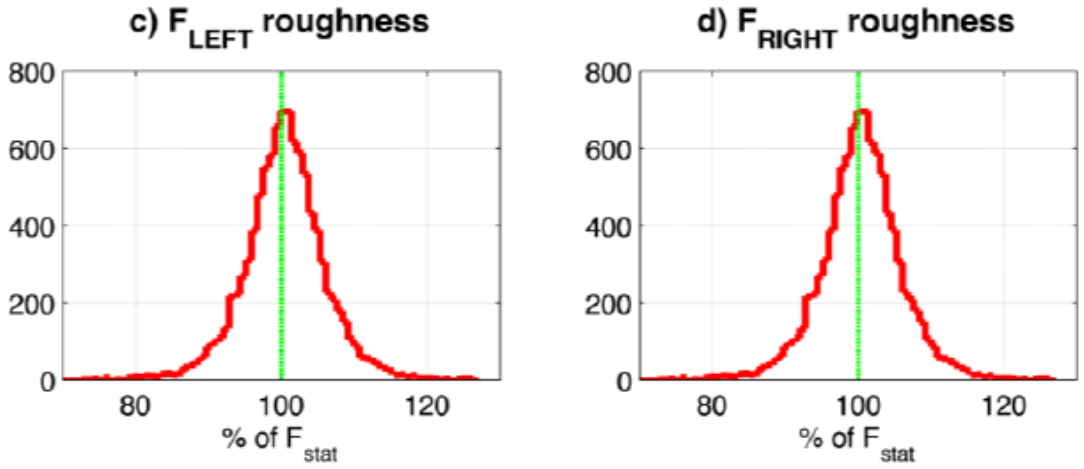

Figure 10
Wheel dynamic load distribution caused by roughness *[1]*

Prediction of Backcalculated Layer Moduli from TSD Data

Pavement layer moduli can assist state agencies in making more informed decisions at the network level. Through an online survey, it was reported that around 69% of the agencies commonly backcalculate pavement layer moduli from surface deflections *[7]*. Typical backcalculation tools generally assume linear elastic properties for the pavement layers and adopt only FWD loading characteristics to compute pavement responses. Therefore, these conventional programs may not be appropriate for direct use with TSD data due to the difference in loading mechanisms; i.e., FWD generates an impact load on the pavement surface while TSD applies a moving load at varying traffic speeds *[19]*. However, very few research studies have been conducted to address this issue and the proposed approaches were not computationally practical for regular use by state agencies. Yet, these studies are informative and useful to support further research on this issue.

Backcalculation of Layer Moduli Using TSD Deflection Velocities. In this approach, a 3D Move simulation was conducted to calculate the TSD deflection velocities. Important TSD testing features were incorporated in 3D Move such as the dynamic loading nature of TSD; i.e., non-uniform contact pressure distribution of tires, non-circular loaded area; vehicle speed, and viscoelastic properties of AC layer. 3D Move uses layer moduli as an input in the simulation. In this approach, the inputs were altered by trial and error to match the 3D Move output deflections to the TSD measured deflections. The trial and error process is certainly tedious, especially for network level pavement evaluation. However, TSD loading characteristics were well defined and simulated in this approach. The main advantage of this approach is the use of TSD deflection velocities. Since TSD deflection velocities are directly measured from TSD testing, this approach did not require the use of any algorithm to calculate the surface deflections and was independent of the error associated with the calculation. However, the error associated with the calculation of surface deflection is generally small. The results of this approach are shown in Table 1.

Table 1
Backcalculated pavement layer moduli from TSD and FWD data using deflection velocity method *[19]*

Pavement Section ID	Layer	Backcalculated moduli from TSD deflection velocities (ksi)	Backcalculated moduli from FWD deflections (ksi)
MnROAD Cell 19	AC	70-112*	178
	Base	16	17.3
	Subgrade	36	35.8
	Stiff Layer	Fixed	1000
MnROAD Cell 34	AC	211-305*	525
	Base	7	5.1
	Subgrade	16	17.3
	Stiff Layer	Fixed	1000

** Dynamic modulus at 75ºF for frequencies ranging between 5 and 45 Hz.*

Linear Elastic Analysis Approach. Another method was suggested by Nasimifar et al. using the Linear Elastic Approach (LEA), which uses TSD surface deflection instead of deflection velocities *[19]*. This approach was conducted using 3D Move but with more simplified assumptions of TSD characteristics such as circular loaded area and AC material simulated as linear elastic. However, dual circular loads were used to account for TSD tires and non-uniform contact stress distribution. The results obtained with this approach were

considered satisfactory by the authors. The advantage of this approach is that the computational effort is significantly reduced as compared to the first approach. The backcalculated moduli obtained from this approach are shown in Table 2.

Table 2
Backcalculated pavement layer moduli from TSD and FWD data using LEA approach *[19]*

Pavement Section ID	Layer	Backcalculated moduli using LEA approach (ksi)	Backcalculated moduli from FWD deflections (ksi)
MnROAD Cell 19	AC	133	178
	Base	14.7	17.3
	Subgrade	34.2	35.8
	Stiff Layer	1000	1000
MnROAD Cell 34	AC	364	525
	Base	5.9	5.1
	Subgrade	24.9	17.3
	Stiff Layer	1000	1000

The referenced study also compared the aforementioned two approaches by backcalculating the layer moduli of two other pavement sections from Pennsylvania and Idaho. The results using both approaches are presented in Table 3. The study recommended using the LEA approach rather than the deflection velocity method because of the computational requirements of using trial and error using 3D Move in network level evaluation.

Table 3
Further validation of the two approaches on Pennsylvania and Idaho pavement sections *[19]*

Pavement Section ID	Layer	Backcalculated moduli using deflection velocity method (ksi)	Backcalculated moduli using LEA approach (ksi)
Penn Route 144	Asphalt	181-267*	270
	Base	43	41
	Subgrade	22	20.5
	Stiff Layer	1000	1000
Idaho State Highway 22	Asphalt	325-480*	416
	Base	31	39
	Subgrade	12	11
	Stiff Layer	1000	1000

** Dynamic modulus at 75ºF for frequencies ranging between 5 and 45 Hz.*

In the present study, a simple methodology was developed to backcalculate the layer moduli from TSD measurements. TSD measured deflections were converted using an Artificial Neural Network (ANN) model to the corresponding FWD deflections. The ANN model output could then be used in the already established and easily available backcalculation software for predicting the layer moduli. An overview of the ANN method is presented.

Artificial Neural Networks

Artificial Neural Networks (ANNs) are widely used as computational modelling tools; these networks work similar to the mechanism of the human biological nature of neurons to model practical complex world problems. It is globally accepted and is widely used because of its unique features such as non-linearity, which allows fitting complex data, noise tolerance in the input data, adaptability with complicated data patterns, and ability to generalize data, which facilitates the implementation of the model to unlearned data. Moreover, there are several types of ANNs, which can solve problems with various characteristics *[28]*.

An ANN consists of a genetic flexible training algorithm that learns how to make decisions based on given information *[29]*. ANNs' use has increased tremendously in solving complex civil engineering problems in the last three decades *[30]*. They can be very generic, accurate, and convenient mathematical models with high capability in simulating numerical model components *[31]*. ANN is useful with either small or large database; yet, large databases are preferable when modelling with ANNs. Furthermore, ANN models can be continuously updated with the addition of new data *[32]*.

The Feed-Forward ANN. The feed forward ANN is mostly used for regression analysis and function approximation. This type of ANN consists of an input layer (i), one or more hidden layers (j), and an output layer. In the input layer, multiple independent variables can be defined; similarly, the output layer known as the target layer can be fed with one or more dependent variables. The hidden layers adjust and update the weights to process the data until the desired output is produced *[29]*. Each of these layers may contain multiple processing units, which are known as "neurons," and the neurons in a layer are linked with all other previous neurons layers *[33]*. A "weight" is assigned to each connection among these neurons and a "bias" is assigned to each of these neurons. A general layout of a feed-forward ANN is demonstrated in Figure 11.

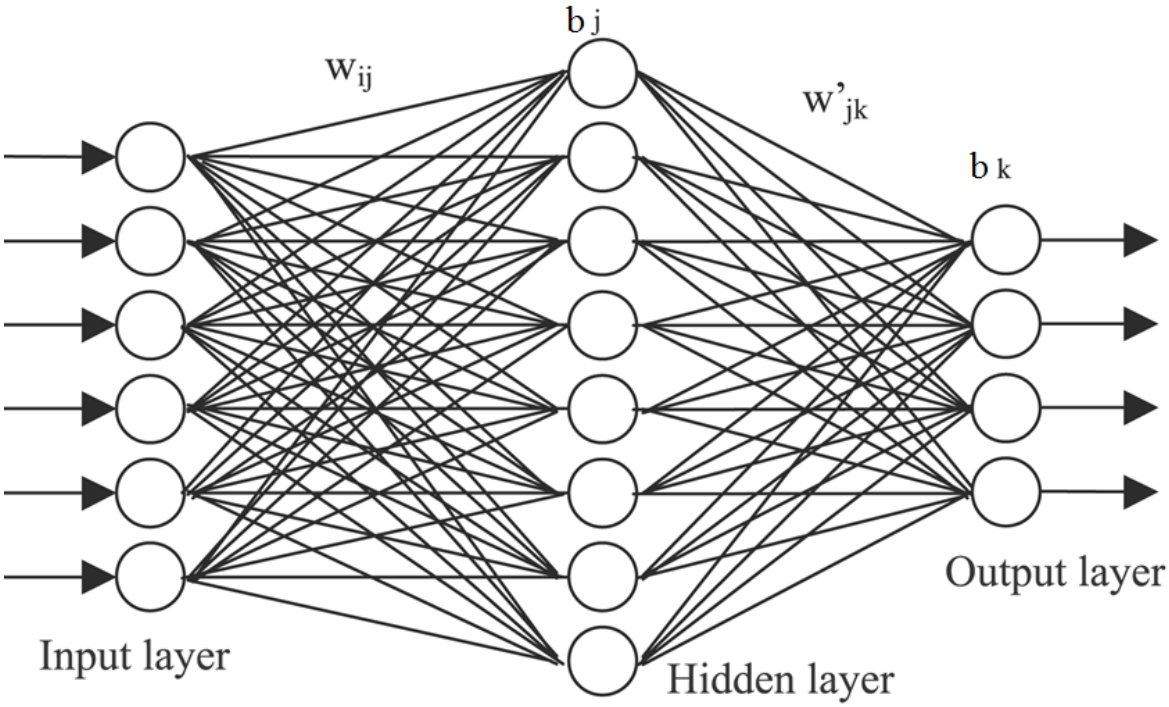

Figure 11
Example of feed-forward neural network structures *[2]*

ANN Back-Propagation. Learning or training of input data in ANN is the process where biases and weights are calculated to match the desired output data. Back-propagation is the most common algorithm for error optimization in the learning and training phases of ANN. Back-propagation algorithm uses the assigned weights and biases to each network connections and neurons to calculate the output. The error is calculated by comparing the calculated output to the target values. This algorithm optimizes the error by changing the weights and biases and generates the output with the least possible errors depending on the

training and transfer functions considered in ANN *[2]*. The mechanism of back-propagation algorithm is shown in Figure 12. Equation (2) illustrates the function used to calculate the error from the network output:

$$E = \frac{1}{2}(t - y)^2 = \frac{1}{2}[t - f(w, b, x)]^2 \quad (2)$$

where,

E= error function;

y = network output;

t = target value;

w= network weights;

b= network biases; and

x= independent variables.

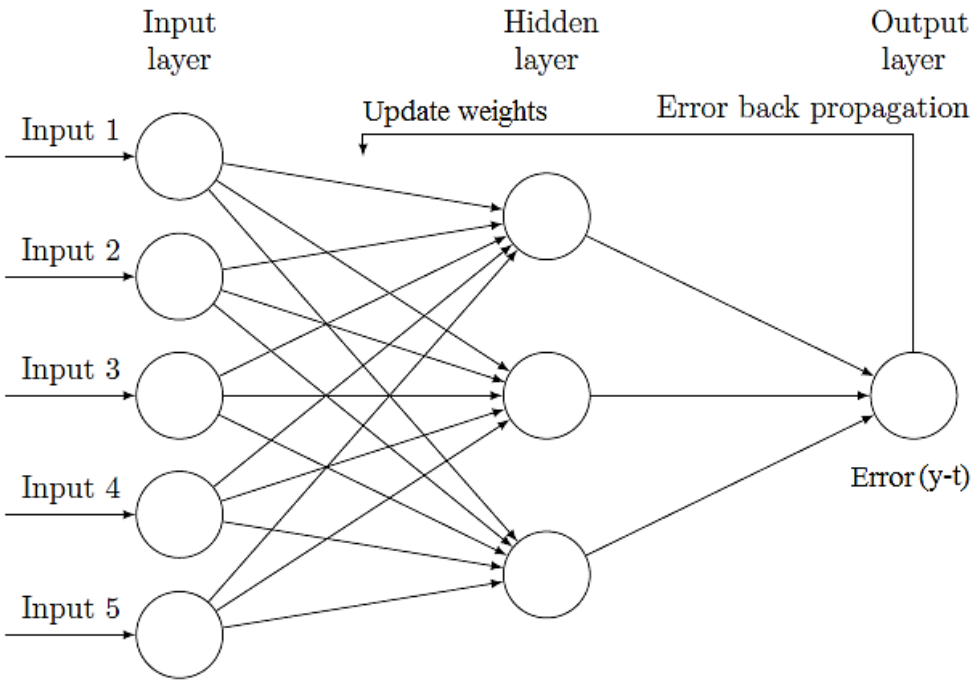

Figure 12
Back-propagation algorithm *[2]*

Back-propagation procedure uses different training algorithms. Each training algorithm has their individual characteristics of learning the data. Training algorithms also have different

data learning rate, storage requirements, and computational time. The selection of training function depends on the type of problem to be modeled and input sample characteristics. A general overview of the most common training functions is shown in Table 4.

Table 4
Overview of the training functions in ANN *[34]*

Training Functions	**Descriptions**
Gradient Descent with Variable Learning Rate	
TRAINGD	This training function is used in incremental-mode training and is generally slow.
TRAINGDM	This back-propagation algorithm with momentum is used in incremental-mode training and is generally faster than TRAINGD.
TRAINGDX	Gradient descendent with momentum and adaptive linear BP. Faster training than TRAINGD, but it can be used only in batch-mode training.
TRAINGDA	TRAINGDA is faster than TRAINGD and TRAINGDM and can be used in batch-mode training.
Resilient BP	
TRAINR	Random-order incremental update Resilient BP. Simple batch-mode training algorithm with fast convergence and minimal storage.
TRAINRP	Resilient BP (RPROp) used in batch-mode training, fast convergence, and minimal storage requirements.
Conjugated Gradient Descent	
TRAINCGF	Smallest storage requirement among the conjugate gradient algorithms.
TRAINCGP	Slightly larger storage requirements and faster than TRAINCGF.
TRAINCGB	Slightly larger storage requirements faster convergence than TRAINCGP
TRAINSCG	Very good general-purpose training algorithm.
Quasi-Newton Algorithm	
TRAINBFG	BFGS quasi-Newton method, fast convergence.
TRAINOSS	One-step secant BP method. Compromise between conjugate gradient methods and quasi-Newton methods.
Levenberg-Marquardt	
TRAINLM	Levenberg-Marquardt algorithm. fastest training algorithm for networks.
Automated Regularization	
TRAINBR	Bayesian regularization. Modification of the Levenberg-Marquardt training algorithm to produce networks that generalize well.

Transfer functions are used in ANN to learn the non-linearity of the data. Transfer functions are applied to the input neurons to generate output neurons. Three commonly used transfer functions are logistic sigmoidal function (logsig), tan sigmoidal function (tansig), and "hardlim" transfer functions. The output for each transfer function has different properties. For example, logsig produces output between zero to +1, tansig function produces outputs between -1 to +1 and hardlim function is used to make decision and classification of input sample data. Equations (3) and (4) define the ANN logsig and tansig transfer functions:

$$\text{logsig}(x)=\frac{1}{1+e^{-x}} \tag{3}$$

$$\text{tansig}\,(x)=\frac{e^{x}-e^{-x}}{e^{x}+e^{-x}} \tag{4}$$

Structural Capacity Indicator Models

The need for considering structural conditions along with functional conditions in pavement management has been recognized in the past decade by various state agencies. The FWD allows practitioners to assess the structural conditions of in-service pavements *[1]*. Research studies have also developed methodologies to evaluate the structural conditions of in-service pavement and its structural number based on surface deflections measured using FWD and RWD. A recent pooled funded study has also developed a methodology for predicting the Effective Structural Number (SN_{eff}) from TSD measurements using Rohde's (1994) method *[25, 35]*, which includes estimating the Structural Index of Pavement (SIP) using equation (5):

$$SIP = D_0 - D_{1.5Hp} \tag{5}$$

where,

D_0 = peak deflection under the 9,000-lbs. load;

$D_{1.5Hp}$ = deflection at lateral distance 1.5 times the pavement depth; and

Hp = pavement depth (thickness of all layers above the subgrade).

Afterwards, SN_{eff} is predicted from the following equation (6):

$$SN_{eff}= K_1\, SIP^{k_2}\, H_p{}^{k_3} \tag{6}$$

where,

For asphalt pavements, $k_1 = 0.4728$, $k_2 = -0.4810$, and $k_3 = 0.7581$.

In the developed methodology, D_0 was corrected to a reference temperature of 68°F (20°C) using the procedure described by Lukanen et al. (2000) *[36]*. The pooled-fund study also developed thresholds for assessing pavement structural conditions based on the derived parameters, SCI_{300} and Deflection Slope Index (DSI), from TSD measured deflections. The thresholds were used to classify pavement conditions as good, fair and poor. SCI_{300} and DSI were derived from TSD deflections based on equations (7) and (8):

$$SCI_{300} = D_0 - D_{300} \quad (7)$$

$$DSI = D_{100} - D_{300} \quad (8)$$

where,

D_0 = deflection at the point of load application (mid-point between the dual tires);

D_{100} = deflections at 100 mm (3.93 in.) from the center of the applied load; and

D_{300} = deflections at 300 mm (11.81 in.) from the center of the applied load.

SCI_{300} and DSI were corrected to a reference temperature of 70°F according to the methodology developed by Rada et al. *[25]*. The suggested thresholds for pavement conditions evaluation based on these parameters are shown in Table 5.

Table 5
Thresholds for SCI_{300} and DSI from TSD measurements

Road Category	AC layer thickness, in.	Threshold for Poor		Threshold for Fair	
		SCI_{300} (mil)	DSI (mil)	SCI_{300} (mil)	DSI (mil)
Interstate	>9	3.7	3.0	2.7	2.2
Primary	6-9	6.2	5.2	4.9	4.0
Secondary	3-6	9.7	7.7	7.3	5.8

The pooled-fund study also compared the SN_{eff} estimated from TSD deflections with the PMS SN_{eff} from Pennsylvania and found significant discrepancy between TSD SN_{eff} and PMS SN_{eff}, see Figure 13. Pennsylvania PMS SN_{eff} is calculated according to the AASHTO 1993 design method with a reduction of layer coefficients with pavement age. As suggested by the authors, this may indicate that PMS SN_{eff} does not accurately predict the effective pavement SN since good agreement was found between FWD and TSD deflections *[25]*.

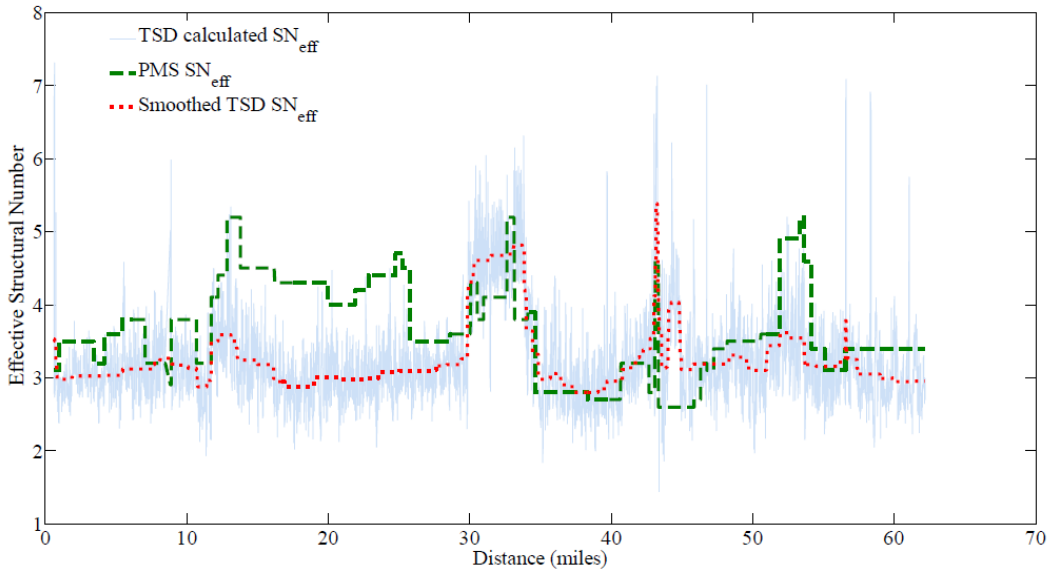

Figure 13
Comparison between TSD SN_{eff} and Pennsylvania PMS SN_{eff}

The AASHTO equation for estimating the SN requires trial and error and numerical methods, which makes it complicated to use *[37]*. A SN model was developed by Gedafa et al. based on FWD center deflection measurements along with other performance indices data from PMS in Kansas. The road network was divided into 23 categories and different regression models were developed for each of the road categories using the center deflection, pavement depth, and surface condition indices. Afterwards, an overall SN model was proposed with a coefficient of determination (R^2) of 0.77. It was suggested that either RWD or FWD center deflection measurements could be used in the overall model:

$$SN= 6.3763- 0.3364\ d_0 + 0.0062d_0^2 – 0.0805D+0.01D^2-0.0008(d_0*D) - 0.4115\ \log (EAL) + 0.1438\ (\log (EAL))^2 + 0.0836ETCR-0.0091\ EFCR+0.0004\ EFCR^2 -0.4061\ Rut \quad (9)$$

where,

SN= pavement structural number;

d_0= center deflection (mils);

D= pavement depth (in.);

EAL = Equivalent standard daily traffic;

EFCR/ETCR=equivalent fatigue/transverse cracking; and

Rut=rut depth (in).

A SN-predictive model was developed by Elbagalati et al. based on the RWD average center deflection, deflection standard deviation along the pavement length at 0.1-mile interval, asphalt layer thickness, and traffic volume. The model accuracy was evaluated and indicated a Root-Mean Square Error (RMSE) of 0.8 and a coefficient of determination (R^2) of 0.8. The model was then used to identify structurally deficient pavement sections assuming a 50% loss in structural capacity *[38]*. Equation (10) presents the developed SN model based on RWD deflection measurements:

$$SN_{RWD0.1} = -14.72 + 27.55 * \left(\frac{Ac_{th}}{D_0}\right)^{0.04695} - 2.426 * \ln SD + 0.29 * \ln ADTPLN \quad (10)$$

where,

Ac_{th} = Asphalt layer(s) thickness of the pavement structure (in.);

D_0 = Avg. RWD deflection measured each 0.1-mile (mils);

SD = Standard deviation of the RWD deflection each 0.1-mile;

ADTPLN= Average Annual Daily traffic per lane (vehicle/day);

$SN_{RWD0.1}$ = Pavement SN based on RWD measurements defined each 0.16 km (0.1 mi.).

Schnoor et al. assessed flexible pavement structural conditions using a simple SN model, which was developed based on derived parameters from FWD deflection measurements; i.e., area under the pavement profile and the base layer index; see equation (11) *[39]*:

$$SN = e^{5.12} A_{UPP}{}^{-0.78} BLI^{0.31} \quad (11)$$

where,

A_{upp} = Area under pavement profile; and

BLI = Base layer index.

Other noteworthy SN models were also developed based on FWD and RWD deflection measurements and are presented in Table 6 *[39]*.

Table 6
Developed SN models based on FWD and RWD measurements

Method	SN models	Description
FWD center deflection based SN model *[37]*	$SN = 6.3763 - 0.3364\,d0 + 0.0062 * d_0{}^2 - 0.0805 * D + 0.01 * D^2 - 0.0008(d_0 * D) - 0.4115 \log(EAL) + 0.1438 * (\log(EAL))^2 + 0.0836 * ETCR - 0.0091 * EFCR + 0.0004 * EFCR^2 - 0.4061 * Rut$	SN= pavement structural number; d_0= center deflection (mils); D= pavement depth (in.); EAL = equivalent standard daily traffic; EFCR/ETCR=equivalent fatigue/transverse cracking; and Rut=Rut depth (in).
Backcalculated Moduli AASHTO NDT Method *[39]*	$SN = \sum_{i=1}^{n} h_i\, a_g \left(\frac{E_i}{E_g}\right)^{1/3}$	a_g = layer coefficient of standard materials; E_i = layer resilient modulus (MPa); E_g = layer resilient modulus of standard materials (MPa); and h_i = layer thickness (in.).
AASHTO Method II *[39]*	$D_0 = \frac{1.5P}{\pi lr}\left(\frac{(0.0045HP)^3}{SN^3}\left[1 - \frac{1}{(1+(HP/lr)^{1/2}}\right] + \frac{1}{E_{SG}(1+\frac{40000SN^2}{lr^2E_{SG}^{2/3}})^{1/2}}\right)$	D_0 = the peak FWD deflection (in.); P = FWD load (lbs.); H_p= layer thickness (in.); lr = load radius (in.); E_{SG} = subgrade modulus (psi).
Jameson's formula *[39]*	$SN = 1.69 + \frac{842.8}{(D_0 - D_{1500})} + \frac{42.94}{D_{900}}$	D_0 = the peak deflection (microns); D_{900}= Deflection at 900 mm from loading (microns); D_{1500}= Deflection at 1500 mm from loading (microns).
Asgari's formula *[39]*	$SNC = a0\,(D_0)^{a1}$	SNC = modified structural number; a0, a1 = Asgari coefficients; D_0 = Peak deflection (mm).
The Wimsatt formula *[39]*	$SN_{eff} = 0.0045\,(D)E_p^{0.333}$	D = Total layer thickness; E_p = Existing pavement modulus of the layers above subgrade.

As the use of FWD is limited at the network level and with the acceptance of continuous deflection measurement devices in many countries, a model is needed to predict SN from continuous devices such as TSD. The present study developed a SN-prediction model based on TSD deflections; the model can also be used to identify structurally deficient pavements.

Such information would benefit state agencies at the network-level in decision-making processes and in avoiding inaccurate selection of Maintenance and Rehabilitation (M&R) activities.

Limit of Agreement Method

Limit of Agreement (LOA) is a statistical method introduced by Bland and Altman, which is widely used to evaluate the difference between two sets of measurements by two independent devices *[40]*. The error between each set of measured data by the two devices can be calculated based on equations (12) and (13) as follows:

$$y_{i1} - y_{i2} = (s_{i1} - s_{i2}) + (e_{i1} - e_{i2}) \quad (12)$$

where,

y_{i1} = Measurement at location i obtained from device 1;

y_{i2} = Measurement at location i obtained from device 2;

s_{i1} = Actual value at location i obtained from device 1;

s_{i2} = Actual value at location i obtained from device 2;

e_{i1} = Error in measurement at location i for device 1;

e_{i2} = Error in measurement at location *i* for device 2.

$$D_i = B_i + E_i \quad (13)$$

where,

D_i = Difference in measurements between two devices;

B_i = Difference of systematic error of the two devices;

E_i = Difference of the random error of the two devices.

B_i can be considered constant for simple cases and if e_{i1}, e_{i2} are normally distributed as N (0, σ_1) and N (0, σ_2) respectively, then E_i can also be assumed normally distributed, N (0, σ). Therefore, in such cases, D_i will also be normally distributed as N (B, σ) where B is the constant difference of systematic error of the two devices and σ is the standard deviation. The standard deviation can be calculated as follows:

$$B = \sum_{i=1}^{N} \frac{B_i}{N} \quad (14)$$

$$\sigma^2 = \sum_{i=1}^{N} \frac{(B - B_i)^2}{N-1} \quad (15)$$

The plot of difference between the measurements is evaluated by D_i versus the average measurements of the two devices. This type of plot is very useful in identifying the lack of agreement between two device measurements and the relationship between true measurements and the error in device measurements. However, if the true value is unknown, the mean of the two devices can be assumed as the mean value. For example, for a set peak expiratory flow rate (PEFR) data measured by two flow-measuring meters, the plot in Figure 14 presents the concept of the Limit of Agreement method. According to this figure, one may conclude that the two meters show considerable lack of agreement up to a difference of 800 l/min. If there is no relationship between the measurement difference and the mean, the lack of agreement can also be summarized using the calculated bias from the two data sets. The difference between the two data sets are expected to be within the confidence limits constructed for the data set; typically, within d-2s and d+2s (Figure 14) or d-1.96s and d+1.96s for normally distributed differences, where d is the mean difference and s is the standard deviation of the differences *[40]*.

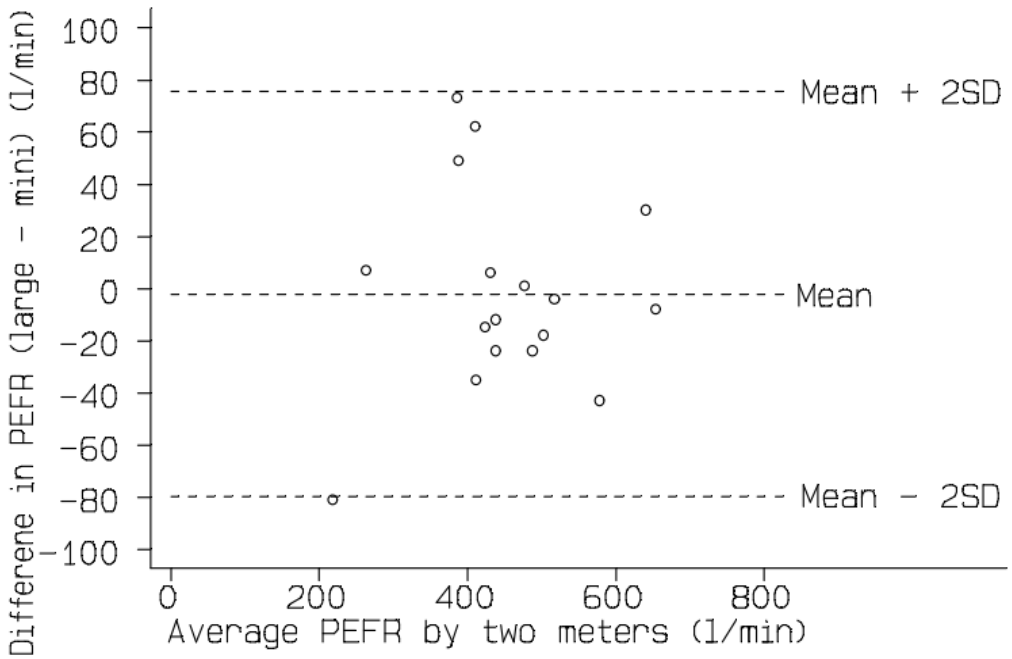

Figure 14
Example of Limit of Agreement (LOA) method *[39]*

OBJECTIVES

The objective of this study was to assess the feasibility of using TSD measurements at the network-level for pavement conditions structural evaluation in Louisiana and in backcalculation analysis.

SCOPE

To achieve the objectives of the study, TSD and FWD measurements were collected in District 05 of Louisiana and data were available from experimental programs conducted at the MnROAD research test facility and in Idaho. TSD measurements were compared with FWD deflection measurements to evaluate the level of agreement and difference between the two devices. Based on this evaluation, a SN predictive model was developed and validated to assess the structural conditions of in-service pavements. The model was then used to identify structurally sound and structurally deficient in-service pavements. Furthermore, a methodology was developed and was validated to backcalculate the layer moduli from TSD measurements.

METHODOLOGY

Figure 15 presents the general layout of the adopted methodology to achieve the objectives of this study. Nondestructive testing of in-service pavements was conducted using both TSD and FWD in District 05 of Louisiana. TSD and FWD measurements were also obtained through FHWA for recently conducted testing programs at the MnROAD test facility and in Idaho. Soundness of TSD measurements was evaluated and data were processed and filtered to calculate the surface deflections. After processing and filtering the TSD raw measurements, the deflection data were compared to the FWD deflection measurements to evaluate whether the two sets of measurements are statistically equivalent or different. TSD deflection data were also used to develop a SN-predicting model and the model's efficiency in identifying structural deficient pavement locations was evaluated by comparing the model prediction to the conditions of extracted cores from the pavement sections. An artificial neural network model was then developed to convert TSD measured surface deflections to the corresponding FWD deflections. The converted data were then used in ELMOD backcalculation software to predict the layer moduli directly from TSD deflection measurements. Evaluation and validation of the proposed methodology was conducted by comparing the critical pavement responses and structural health conditions based on the backcalculated moduli from FWD and TSD measurements.

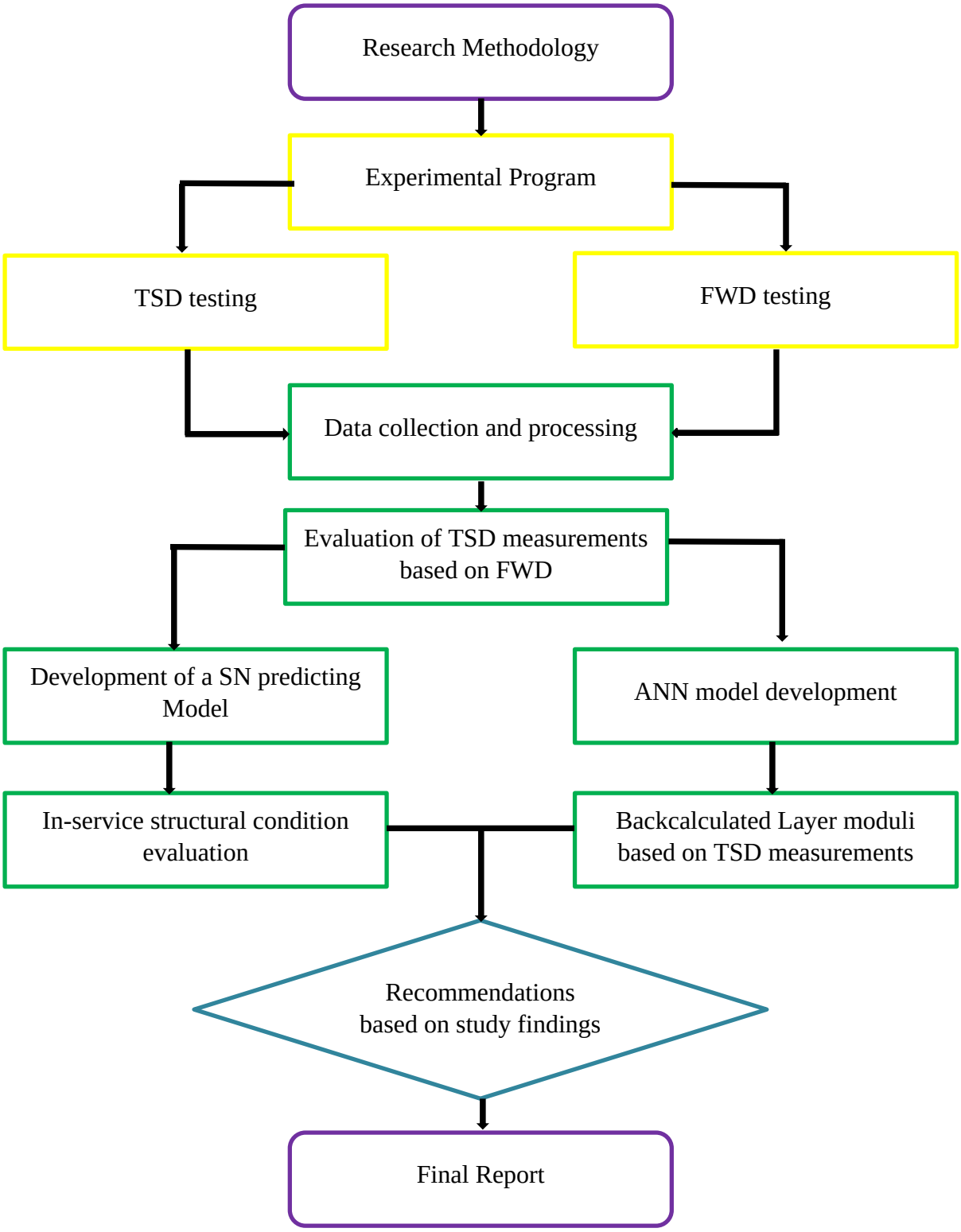

Figure 15
General layout of the developed methodology

Field Testing Program

Traffic speed deflectometer and falling weight deflectometer measurements were conducted in Louisiana in May 20 to 21, 2016. FWD and TSD measurements were conducted successfully with no significant problems to report. Due to the size limitations of the data collected in Louisiana, data were also obtained from FHWA for two recently completed testing programs conducted at the MnROAD test facility in Minnesota and in Idaho.

TSD Testing Program in Louisiana

In 2016, a TSD device operated by the Australian Road Research Board (ARRB), known as iPAVe, was used to measure vertical deflection velocity, horizontal speed of the vehicle, air temperature, and pavement surface temperature in six parishes of District 05 in Louisiana. Measurements were collected for 13 control sections at 0.01-mile interval. FWD measurements were also collected for the same control sections at 0.1-mile interval for the evaluation and comparison with TSD measurements. The 13 selected sites in District 05 are presented in Figure 16.

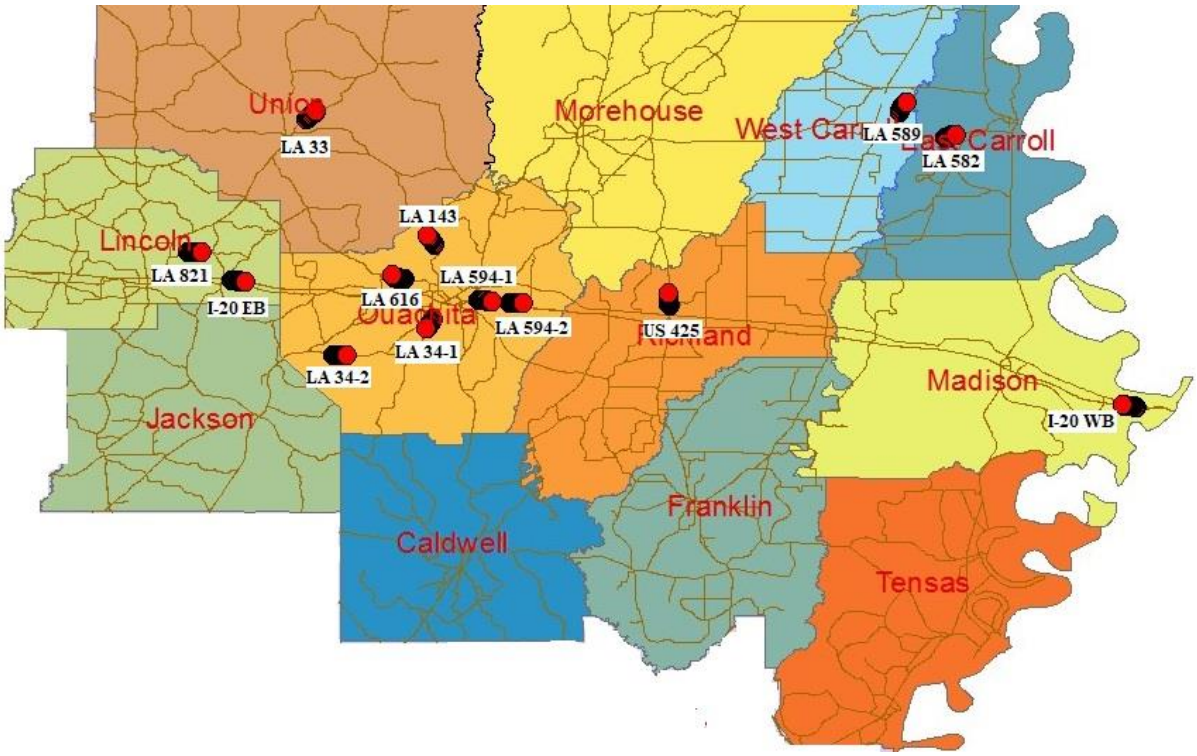

Figure 16
Locations of the TSD road segments in Louisiana (District 05)

The pavement surface and air temperature were recorded to an accuracy of +/-1°F and were reported within the TSD dataset. These measurements were made with a calibrated air temperature probe situated beneath the trailer chassis, above the ballast weight for the ambient air, and a calibrated infrared temperature sensor that measures pavement surface temperature in the outer wheel path location. The load is 'static' and is comprised of the base trailer mass itself, plus the mass of a main ballast weight of 7220 lbs. located under the belly of the trailer, and a small ballast weight of 475 lbs. situated underneath the rear of the trailer. These weights are balanced to provide a suitable center of gravity for the trailer road handling, as well as the nominal equal load over each wheel set. Figure 17 shows a typical arrangement of loading in the TSD device. It is to be noted that for the testing in Louisiana, the rear ballast weight (475 lbs.) was removed to comply with axle weight regulations, which resulted in a reduced load of 10,000 lbs. on each wheel set. Strain gauges were mounted on the rear axle to measure the bending moment on the loaded axle on both the left and right side. The load data were collected continuously and were averaged over the selected report interval, and were converted into a mass measurement, for both left and right side axles. The mass measure was derived from a load vs. signal equation derived from the strain gauge outputs, and was not a direct load cell weight or force measurement. The tolerance between actual and measured strain (weight) in a static setting is ± 440 lbs., which is acceptable considering the weight of the trailer, air pressure and suspension balancing valving, and engineering tolerance in the iPAVe chassis/suspension construction.

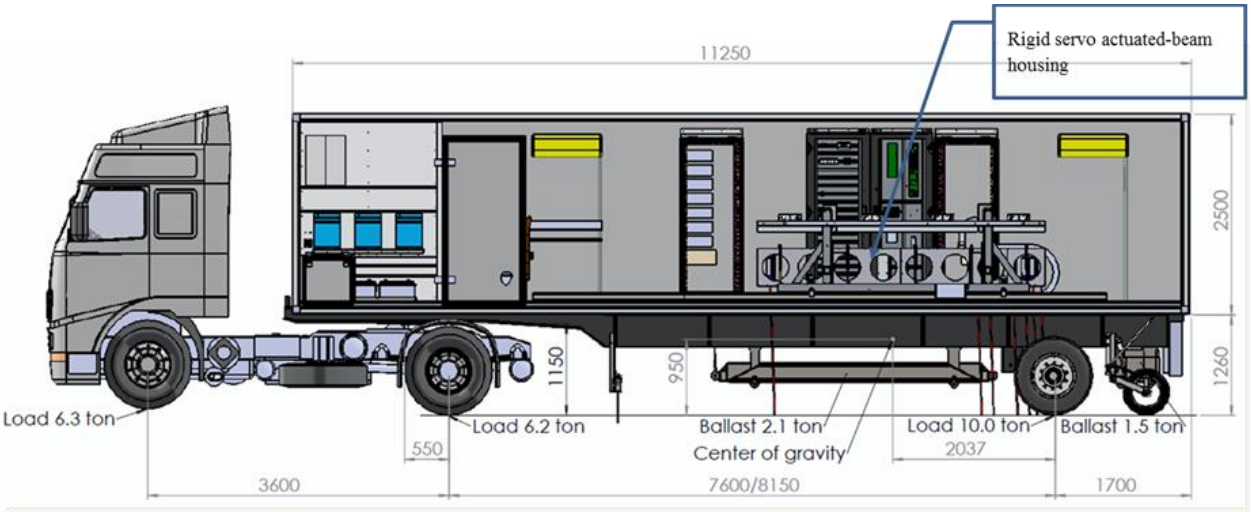

Figure 17
Typical loading configurations in the TSD device

The nominal load was set at 20,000 lbs. on the axle and was distributed on the left and right sides depending on the movement of the trailer Center of Gravity (CoG), the cross fall, and the grade of the road. Therefore, it varied dynamically within a range of a few percentages as the TSD travelled down the road. High-resolution horizontal velocity measurements (i.e., the travel speed of the iPAVe) are critical to deflection slope calculations. Distance and velocity are measured using a specialized odometer wheel assembly. Having a dedicated Distance Measuring Instrument (DMI) increases accuracy and limits error induced due to physical factors, such as tire loading, tracking, tire pressure, and thermal expansion. The overall accuracy of the DMI is defined with an error less than +/-0.1% and subsequent bias of less than 0.1%. The same odometer pulse count is used for all distance measurements within the iPAVe system. Measurements were reported for the 13 control sections at 0.01-mile intervals. FWD measurements were also collected for the same control sections at 0.1-mile intervals for the evaluation and comparison with TSD measurements.

TSD Loading Conditions for Louisiana

Travelling at normal traffic speed, TSD loads the pavement using its rear axle tires. The articulated Doppler lasers over the right wheel of the rear axles measures the deflection velocity along the midline between these dual tires. The applied load for these tires was reported through strain gauge measurements. TSD loading variation under static and dynamic conditions is discussed in this section.

TSD Load and Tire Pressure. The applied load by the TSD, loaded area of pavement surface, and tire contact pressure at static conditions, were measured. As shown in Figure 18, TSD applied a load of 20,360 lbs. on its rear axle and distributed this load evenly over its left and right dual tires producing a load of 9,800 lbs. and 10,560 lbs. on the left and right sides, respectively; see Figure 18. The contact tire pressure was reported at 115 psi in static conditions. It is to be noted that the ARRB TSD used in the testing program was intentionally slightly biased towards the right dual tire with a greater load to increase the deflection since it measures the deflection along the midline between the right dual tires.

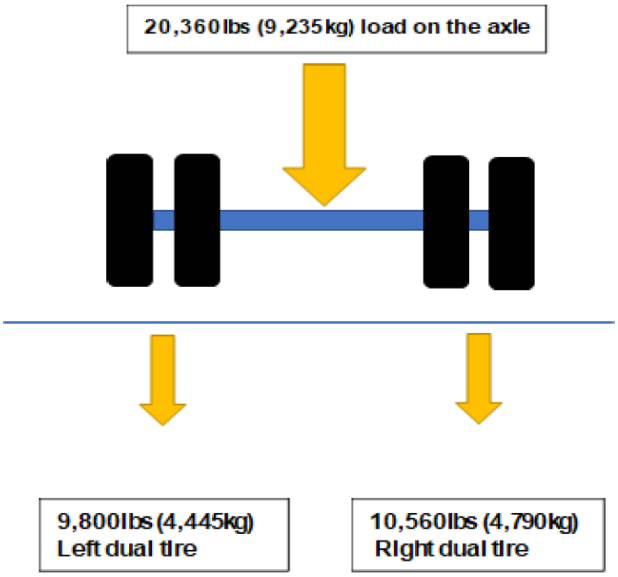

Figure 18
Load distribution between tires in the rear axle

Assuming the load on the right and left dual tire configurations is evenly distributed over each tire, the load on each tire shown in Table 7 can be calculated.

Table 7
Loads on each tire of the TSD

Tire location	Loads (lbs.)
Outer Left	4,900 lbs.
Inner Left	4,900 lbs.
Outer Right	5,280 lbs.
Outer Right	5,280 lbs.

The loaded area and tire dimensions were calculated by measuring the footprint from the outside the tire as shown in Figure 19. Tire longitudinal dimension (travel direction) was measured at 7.48 in. (190 mm) and at 9.45 in. (240 mm) in the transverse direction; see Figure 19. The spacing between the two tires was measured at 4.33 in. (110 mm).

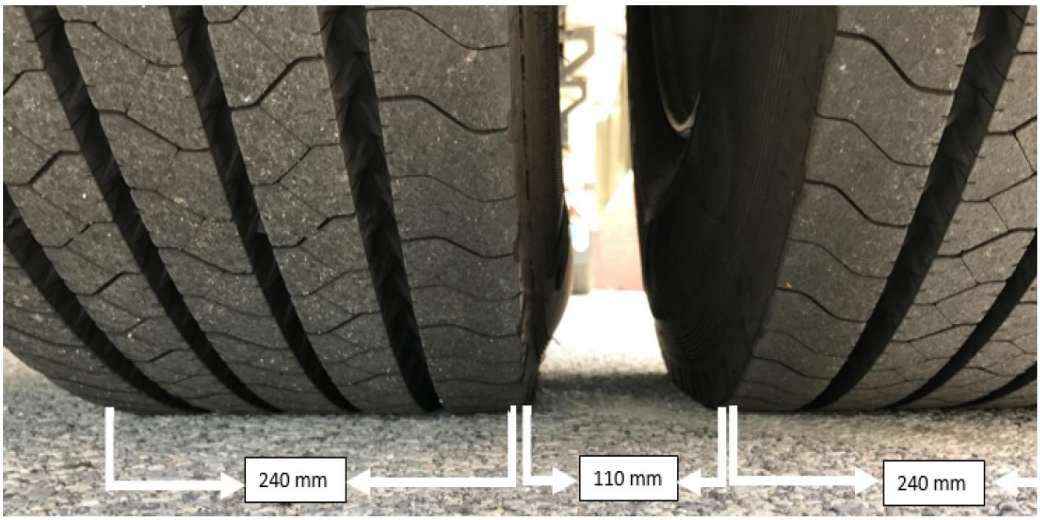

(a)TSD tire dimensions in transverse direction

(b)TSD tire dimensions in longitudinal (traffic) direction

Figure 19
Measured TSD tire dimensions

As previously noted, TSD loading, tire pressure, and loaded area vary significantly in dynamic conditions at the time of deflection velocity measurements. The loading profile for each processed data point was obtained through the strain gauges measurements.

FWD Testing Program in Louisiana

FWD testing was conducted in Louisiana within 24 hours of the TSD measurements to maintain the consistency in pavement and environmental conditions. FWD measurements were reported for the 13 test sites at an interval of 0.1-mile. Two loading drops were conducted for FWD at all test locations. The two drops varied within a load range of 9,700

to 10,200 lbs. and 24,200 to 24,700 lbs., respectively. The obtained deflections due to the drop with a load of 9,700 to 10,200 lbs. were used in this study and were normalized to a load of 9,000 lbs. Along with the deflection, FWD also measured the surface temperature during testing. Table 8 presents the details of the 13 test sections evaluated in the Louisiana testing program.

Table 8
General descriptions of the 13 test sites in Louisiana

Site ID	Control Section	Route	Parish	Pavement Type	Type of Treatment	Last Treatment Year	TSD Test Site Log-miles	Traffic
1	067-08	LA 34-1	Ouachita	Asphalt	A7- Asph Surf Treat	2003	5.55 - 6.95	2,400
2	067-09	LA 34-2	Ouachita	Asphalt	A3- Asph Ovly Pvmt	2001	3.35-4.75	11,714
3	451-05	I-20 eb	Lincoln	Composite	A3- Asph Ovly Pvmt	2005	22.25 - 23.95	35,528
4	326-01	LA 594-2	Ouachita	Asphalt	Z1- RCND AGGR SURF	2003	5.05 - 6.45	3,800
5	324-02	LA 616	Ouachita	Asphalt	A1-Asphalt New Pvmt	1995	3.55 - 4.95	11,000
6	831-05	LA 821	Lincoln	Asphalt	A3- Asph Ovly Pvmt	2009	2.05 - 3.25	1,030
7	071-02	US 425	Richland	Asphalt	A5- AC Ovly/In-place Base	2008	1.00 - 2.50	3,700
8	069-03	LA 33	Union	Asphalt	A7- AC Surf Treat	2006	3.05 - 4.45	2,536
9	315-02	LA 143	Ouachita	Asphalt	A3- Asph Ovly Pvmt	2004	6.00 - 7.50	4,100
10	333-03	LA 582	E Carroll	Asphalt	ZA- Asphalt Pavement Rehab	2003	3.00 - 4.50	4,60
11	862-14	LA 589	W Carroll	Asphalt	A5- AC Ovly/In-place Base	2009	4.00 - 5.50	3,20
12	326-01	LA 594-1	Ouachita	Asphalt	A3- Asph Ovly Pvmt	2006	2.00 - 3.50	3,800
13	451-08	I-20 wb	Madison	Composite	A6- AC Ovly Rubblized Pvmt	2013	29.3-30.8	25,600

Note: All sites were tested in the Primary direction except Site ID 2 and 13.

Table 8 – Continued.

ID	Surface Type	Base Type	Layer Thicknesses (in.)			Pavement Group	Core Conditions	IRI [2015] in./mile	PCI [2015]	Condition (PCI)
			Layer 1 (Surface)	Layer 2 (Base)	Layer 3 (Subbase)					
1	Asphalt	Stabilized Granular	8.5	9	0	Thick	---	111.6	77.9	Fair
2	Asphalt	Stabilized Granular	10	8	5	Thick	Stripping	68.8	89.3	Good
3	Asphalt	PCC+AC+Cement Stabilized	4	22.75	0	Medium	---	43.6	99.7	Very good
4	Asphalt	Stabilized Granular	4	7.5	0	Medium	---	55.6	97.6	Very good
5	Asphalt	Cement Stabilized	5	5	0	Medium	---	101.3	80.8	Fair
6	Asphalt	Granular	5	8	0	Medium	Stripping	87.3	92.7	Good
7	Asphalt	Stabilized Granular	8.5	8.5	0	Thick	---	72.8	92.5	Good
8	Asphalt	Crushed Gravel w/sand	7	3	8	Thick	---	95.3	83.5	Fair
9	Asphalt	Cement Stabilized Sand Clay Gravel	9.5	13.5	0	Thick	Separation	56.0	92.7	Good
10	Asphalt	Granular	9.5	8.5	0	Thick	Stripping	221.1	67.9	Poor
11	Asphalt	Stabilized Granular	1.75	15.75	0	Thin	---	95.0	91.0	Good
12	Asphalt	Stabilized Granular	8.5	8	19.5	Thick	---	67.5	90.2	Good
13	Asphalt	PCC+AC+Granular	5.25	18	0	Medium	Stripping	49.8	95.8	Very good

Idaho Testing Program

In September 2015, TSD measurements were conducted in Idaho by Greenwood Engineering of Denmark under FHWA pooled funded project TPF 5(282) *[41]*. TSD and FWD measurements were conducted for one road segment that was 13.4 mile in length. TSD measurements were reported at 0.006-mile interval and FWD measurements were reported at 100-ft. (0.02-mile) interval. Data were reported in one direction and six Doppler lasers were located at a distance of 3.9, 7.9, 11.8, 23.6, and 59 in. ahead of the rear axle of the vehicle to measure deflection velocity at different offsets. Another sensor, acting as a reference laser, was placed at a distance of 138 in. from the rear axle, which is beyond the deflection basin distance. Lasers were positioned on a beam that moved up and down in the opposite direction of the trailer movement to maintain a constant height from the road surface. A constant trailer temperature of 68°F (20°C) was maintained by a temperature control system in order to prevent thermal distortion of the steel beam.

The objective of the FWD testing program was to compare the measured deflections to TSD measurements. FWD measurements were collected within a month of the TSD survey using a Dynatest truck-mounted deflectometer. FWD testing was conducted on a 2-mile long road segment resulting in more than 100 FWD data points with an interval of 100 ft. Five load drops were conducted at each test location of the selected road segment. Out of the five drops, three were conducted at 12,000 lbs. and the remaining two were conducted at 9,000 lbs. Vertical deformation of the pavement surface due to the FWD drops was measured by seven sensors located at 0, 8, 12, 18, 24, 36, and 60 in. from the center of the load. Temperature of the pavement surface and air temperature, and GPS data were also collected to assist in the analysis.

MnROAD Testing Program

FWD and TSD measurements were collected at the MnROAD facility in Minnesota *[2]*. The surveyed road network consisted of a 3.5-mile mainline roadway (ML) with 45 sections and with "live traffic" as part of Interstate 94 near Albertville, Minnesota. In addition, a 2.5-mile closed-loop low volume roadway (LVR) consisting of 28 sections was also surveyed; the section lengths were typically about 500 ft. In addition to the test sections along the mainline and low volume road of the MnROAD, an 18-mile segment in Wright County was also tested. The segment is located about 20 miles from the MnROAD facility and was divided into nine sections.

Testing was conducted using the TSD, RWD, and the Euro-consult Curvimeter. FWD was also conducted and was used as a reference for comparison and evaluation purposes. Tested sections varied between flexible pavements, rigid pavements, and composite pavement

sections. Yet, the present study focused on the use of the TSD measurements in conducting backcalculation analysis of flexible pavements layer moduli, therefore, only TSD and FWD data collected on flexible pavements were considered. The flexible pavement test segments at which both FWD and TSD measurements were conducted consisted of 16 sections; six in the main line and 10 in the low volume roadway. The TSD and FWD deflection data for MnROAD were reported as an average over the 16 sections while the other testing program measurements were reported at a log-mile interval; hence, were analyzed separately.

Figure 20
MnROAD road facility in Minnesota

TSD Raw Measurements Processing

The TSD measures the velocity of the surface deflection under load using Doppler lasers rather than measuring the displacement directly. It collects vertical velocity (V_v) and horizontal velocity (V_h) continuously at a 0.001-mile interval as shown in Figure 21. The deflection slope was calculated at each measurement point by dividing the vertical deflection velocity by the horizontal velocity. Horizontal velocity is equivalent to the measured speed of the TSD.

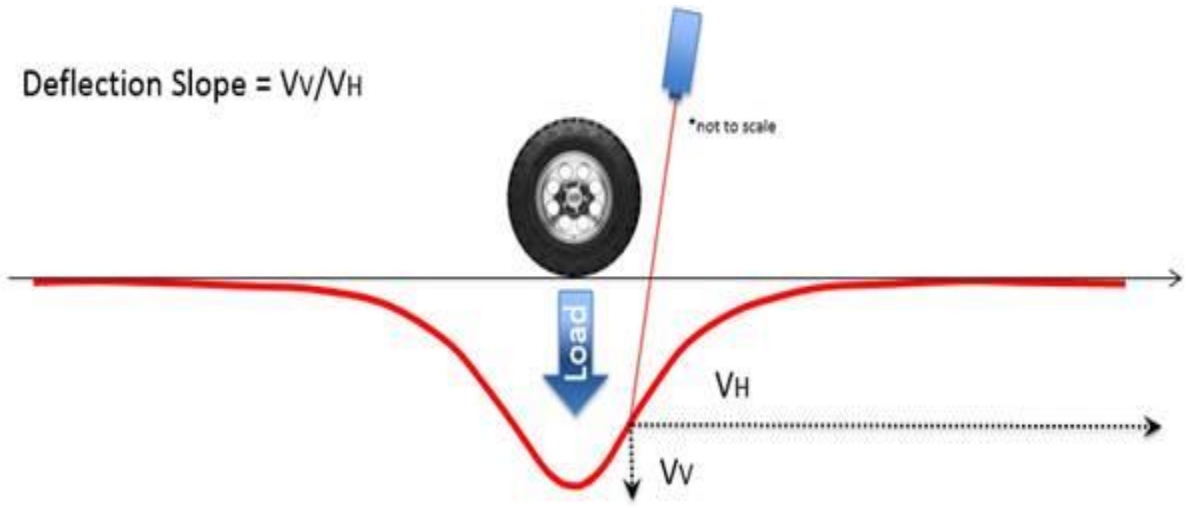

Figure 21
Schematic of Doppler lasers mechanism

Collected raw measurements (vertical deflection velocity and actual horizontal speed) of the TSD device were used to calculate the deflection basin at each milepost according to the methodology known as "Area under the Curve (AUTC)" proposed by Muller and Roberts *[10]*. According to this method, the vertical deflection velocity is divided by the actual speed of the vehicle to get the deflection slope; slopes are then plotted against TSD sensor locations; see Figure 22. Afterwards, the plotted curve is numerically integrated assuming the deflection slope is zero at locations 0 and 137.8 in. (3500 mm) from the load as shown in Figure 22. The slope value was then calculated at the selected locations with adequate curve fitting using the Piecewise Cubic Hermite function as suggested by the AUTC method. The deflections were then calculated at nine locations (i.e., 0, 8, 12, 18, 24, 36, 48, 60, 72 in. from the center of the load). An example of deflection basin computation is shown in Figure 23.

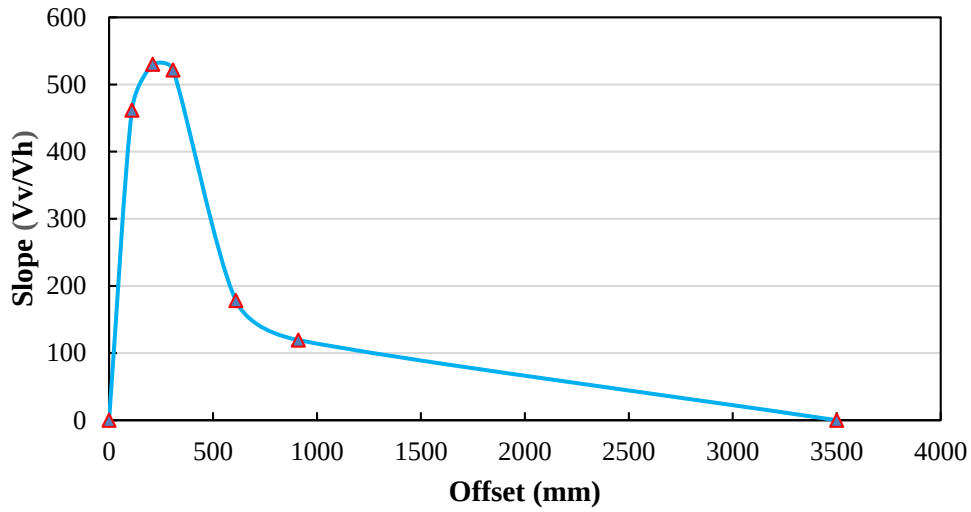

Figure 22
Numerically integrated slope over the offset distances

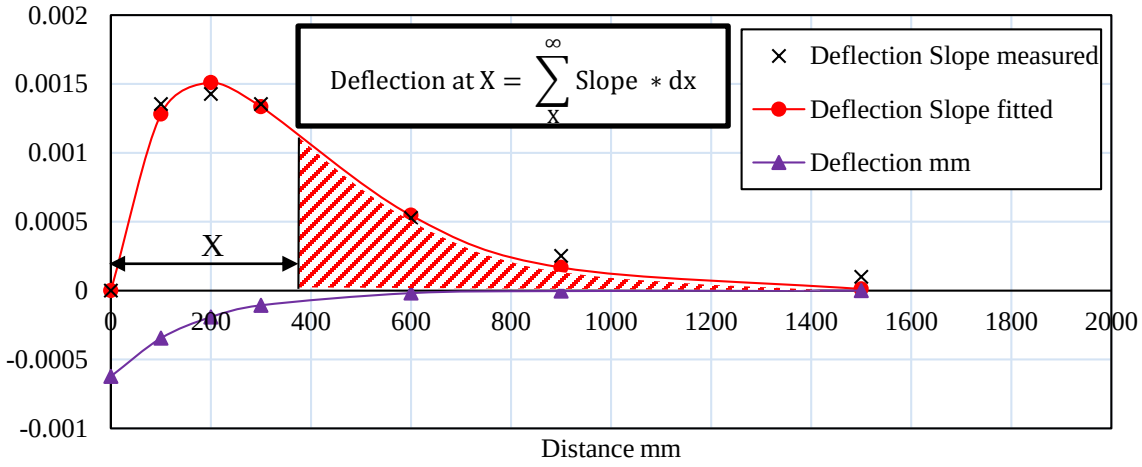

(a) AUTC method for calculating TSD deflection

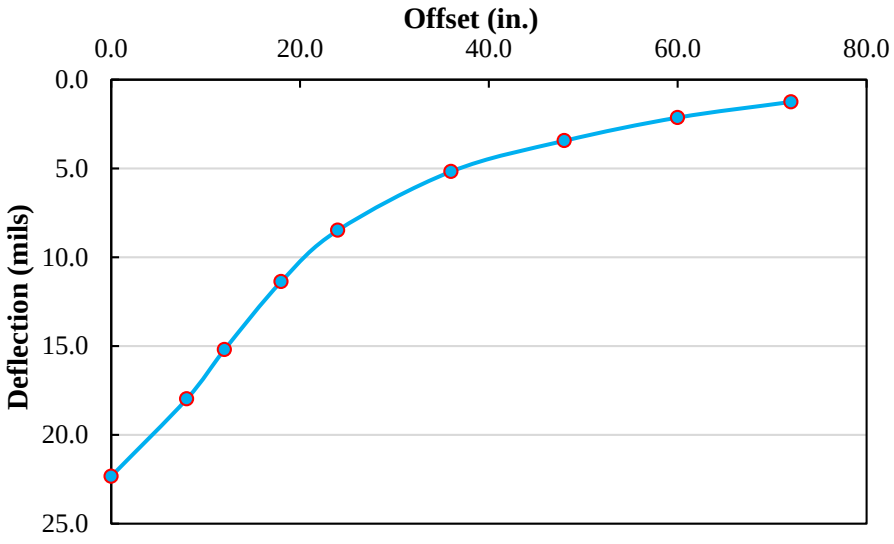

(b) Calculated deflection basin

Figure 23
Deflection basin computation

Temperature Correction for FWD and TSD measurements. FWD and TSD deflections were corrected to a reference temperature of 20°C. The Bells equation was used to calculate the pavement temperature at asphalt mid-depth *[36]*. Pavement surface deflections at radial offsets were then corrected using the methodology described in equations (16) to (18) based on the approach proposed by Kim and Park *[42]*.

$$\lambda_w = \frac{w_{T0}}{w_T} \tag{16}$$

where,

w_{T0} = the deflection corrected to temperature T_0;

w_T = the deflection at temperature T; and

λ_w = the deflection correction factor calculated as follows:

$$\lambda_w = 10^{-C(H_{ac})(T-T_0)} \tag{17}$$

where,

H_{ac} = Asphalt layer thickness; and

C = Regression constant calculated as follows:

$$C = -Ar + C_0 \quad (18)$$

where,

r = the radial distance from the center of the load; and

A = - 5.26x10^{-8} for U.S. Central Region; and

C_0 = 5.80x10^{-5} for U.S. Central Region.

Evaluation of TSD Measurements

Collected TSD and FWD measurements from the Louisiana experimental testing program were processed and filtered as described in the previous section for precise comparison and thorough evaluation. TSD measures deflections at 0.01-mile interval along a pavement sections while FWD measured deflections were reported at an interval of 0.1-mile. Hence, to match the data points where FWD deflection measurements were available, TSD deflections were also processed at 0.1-mile interval at the exact same locations of FWD testing. Furthermore, FWD deflections were measured at a distance of 0, 8, 12, 18, 24, 36, 48, 60 and 72 in. from the center of the plate load. Therefore, TSD deflections were processed from the deflection slopes at the same offset distances from the center of the load, which involves numerical integration of the slopes and subsequently, area under the curve computations. Two separate statistical methods were used to demonstrate and to evaluate the comparison of TSD and FWD deflections (i.e., significance test considering 95% confidence level and the Limit of Agreement Method *[39]*). Furthermore, the potential factors that could influence the TSD field measurements such as pavement roughness were evaluated by calculating the coefficient of variation (COV) within each section.

Development of a Methodology to Predict Layer Moduli Based on TSD Data

As part of the research activities in this study, a methodology was developed to utilize TSD measurements in the backcalculation of layer moduli for flexible pavements. There are clear differences between TSD and FWD such as difference in loading mechanisms and shape. Furthermore, backcalculation programs (e.g., Modulus and ELMOD) assume the load to be applied through a circular plate, which is not the case for the TSD. Therefore, the use of the

TSD deflection "as is" in a backcalculation software would not be realistic. In the present study, an ANN model was developed to convert the TSD deflection basin to a corresponding FWD deflection basin, which was referred to as TSD*. TSD and FWD measurements were obtained from the testing programs conducted in Louisiana and the MnROAD facility in Minnesota and were used to develop and to validate the ANN model.

Figure 24 presents a general overview of the adopted methodology to utilize TSD measurements in the backcalculation analysis. First, the TSD deflection velocity measurements were used to calculate the deflection basins through numerical integration. Then, both TSD and the FWD deflections were corrected to a reference temperature of 68°F (20°C). An ANN model with a topology of 9-5-9 was developed to establish a correlation between FWD and TSD deflection basins. Deflections obtained from the ANN model (TSD*) were then used to conduct the backcalculation analysis using ELMOD6 software.

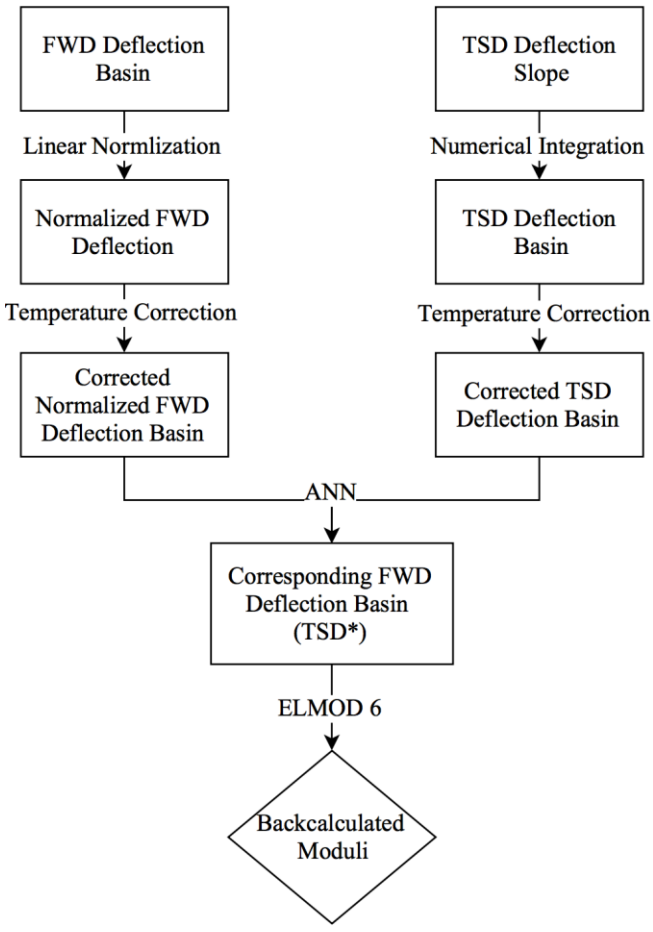

Figure 24
General overview of the ANN procedure

Evaluation and Validation of the Proposed Backcalculation Methodology. The use of the TSD-based backcalculated moduli was evaluated by conducting a comparison with the FWD-based backcalculated moduli in the following pavement analysis applications:

- Calculating critical pavement responses (stress-strain analysis);
- Pavement fatigue life prediction; and
- Structural health monitoring.

Development of TSD-Based Structural Capacity Indicators

This study developed a non-linear regression model for the prediction of in-service pavement SN and structural-deficiency at 0.01-mile interval. The proposed model was developed based on TSD surface deflection measurements calculated from the deflection slope by the AUTC method.

Measured deflections at nine offset distances referred as D_0, D_8, D_{12}, D_{18}, D_{24}, D_{36}, D_{48}, D_{60}, and D_{72} were initially used as independent variables along with the corresponding pavement total thickness (T_{th}), and the Average Daily Traffic (ADT). The SN calculated from the AASHTO 1993 method based on FWD and TSD deflections was used as the dependent variable in the development of the model. To ensure accuracy, several statistical analyses were conducted; i.e., pairwise correlation, significance testing using regression analysis, and multi-collinearity testing among all the independent variables. The model was successfully validated based on data points obtained from TSD and FWD measurements in Louisiana and Idaho. The validation and performance evaluation of the model was conducted by comparing its prediction with the SN calculated from FWD deflection measurements. Furthermore, model validation was conducted by evaluating SN prediction accuracy and residual plots. Extracted cores and functional indices data collected from the DOTD PMS were also used for evaluation of the model's ability in identifying structurally deficient locations.

DISCUSSION OF RESULTS

Assessment of TSD Measurements

TSD measurements were assessed based on FWD measurements conducted at the same test locations. Two analysis methods were conducted to identify if measurements from both devices are statistically equivalent (i.e., ANOVA and Limit of Agreement).

FWD and TSD Comparisons Using ANOVA

To compare FWD and TSD measured deflections, an Analysis of Variance (ANOVA) was conducted. TSD and FWD deflections were compared at the same locations within a control section at an interval of 0.1-mile. Before comparing the deflection measurements from FWD and TSD, both data sets were corrected to a reference temperature of 20°C (68°F). Afterwards, ANOVA was conducted using the SAS 9.4 software package. A 95% confidence level was assumed to identify significant differences; therefore, a P-value less than 0.05 would indicate significant difference between the measurements of the two devices. The results from the ANOVA are presented in Table 9 with their corresponding P-values. Significant differences were referred as "S;" whereas, non-significant differences were referred as "NS" in Table 9. Measurements were compared within each section and results indicated that significant differences exist between the measured deflections of TSD and FWD in most of the sections and at the different sensor locations. Yet, some of the comparisons showed non-significant differences between FWD and TSD measurements. Therefore, results should be compared concurrently with the findings of the Limit of Agreement, which is presented in the following section.

Table 9
Statistical differences between FWD and TSD using ANOVA

.

Control Section	(Pr > |t|)								
	D0	**D8**	**D12**	**D18**	**D24**	**D36**	**D48**	**D60**	**D72**
067-08	S (<.0001)	S (<.0001)	S (<.0001)	S (<.0001)	S (<.0001)	S (0.0005)	S (0.0049)	*NS (0.1482)*	*NS (0.3126)*
067-09	S (.0059)	*NS (0.2473)*	*NS (0.2944)*	S (.0126)	S (.0009)	S (<.0001)	S (<.0001)	S (<.0001)	S (<.0001)
451-05	S (<.0001)	S (<.0001)	S (<.0001)	S (<.0001)	S (<.0001)	S (<.0001)	S (<.0001)	S (0.0132)	S (0.0005)
326-01	S (<0.0001)	S (<0.0001)	S (<0.0001)	S (0.0063)	*NS (0.1186)*	*NS (0.7469)*	S (0.0220)	S (<.0001)	S (<.0001)
324-02	S (<.0001)	S (<.0001)	S (<.0001)	S (<.0001)	S (<.0001)	S (<.0001)	S (<.0001)	S (<.0001)	S (0.0003)
831-05	*NS (0.5973)*	*NS (0.4818)*	S (0.0123)	S (0.0011)	S (0.0010)	S (0.0013)	S (0.0024)	*NS (0.0621)*	*NS (0.5675)*
071-02	S (0.0003)	S (0.0022)	S (0.0161)	*NS (0.3616)*	*NS (0.9920)*	*NS (0.2486)*	S (0.0193)	S (<.0001)	S (<.0001)
069-03	S (0.0001)	S (<.0001)	S (<.0001)	S (<.0001)	S (<.0001)	S (<.0001)	S (<.0001)	S (0.0007)	*NS (0.1792)*
315-02	S (0.0148)	*NS (0.5158)*	*NS (0.7624)*	*NS (0.7590)*	*NS (0.7921)*	*NS (0.7663)*	*NS (0.7009)*	*NS (0.5202)*	*NS (0.3252)*
333-03	*NS (0.5380)*	*NS (0.6981)*	*NS (0.7078)*	*NS (0.2445)*	S (0.0168)	S (<.0001)	S (<.0001)	S (0.0007)	*NS (0.7355)*
862-14	S (<0.0001)	S (0.0002)	S (0.0028)	*NS (0.1576)*	*NS (0.3733)*	*NS (0.9903)*	*NS (0.2982)*	S (0.0035)	S (<.0001)
326-01	S (0.0203)	S (0.0104)	S (0.0052)	S (0.0253)	*NS (0.0960)*	*NS (0.4229)*	*NS (0.9348)*	*NS (0.0703)*	S (<.0001)
451-08	S (<.0001)	S (<.0001)	S (<.0001)	S (<.0001)	S (<.0001)	S (<.0001)	S (0.0006)	S (0.0475)	*NS (0.5107)*

Note: Non-significant relationships are marked in Yellow with P-value greater than 0.05.

Limit of Agreement Method

The Limit of Agreement Method is suitable to identify statistical differences between two device measurements at the same locations as suggested in the literature. As shown in the previous section, using typical statistical analysis, results showed significant differences at some locations while being statistically equivalent at other locations. Therefore, the Limit of Agreement (LOA) method was conducted to compare FWD and TSD measurements. According to the LOA method, the difference between FWD and TSD measurements were plotted against the mean of two measurements at each location. Since no true deflection value for those locations are known, the mean of the measurements were used in the developed plots. A consistent bias was used to summarize the agreement between these two device. The linear bias was calculated by taking the average of all differences in the measurement for the two devices. The upper and lower confidence limit was constructed using a 95% confidence level. The upper and lower confidence limits were calculated using equations (19) and (20):

95% Lower Confidence Limit: $\text{Lower CL} = \text{B} - 1.96 * \sigma$ (19)

95% Upper Confidence Limit: $\text{Upper CL} = \text{B} + 1.96 * \sigma$ (20)

where,

B= Bias, σ = Standard Deviation.

Plots were constructed combining all the data points at each offset distance from the applied load. The results shown in Figure 25 indicate statistical differences between the measurements by FWD and TSD. A significant number of data points deviated from the linear bias line and some data points exceeded the constructed upper and lower confidence limits. Hence, it can be concluded that the deflection reported by both FWD and TSD for the same locations are statically different, which is reasonable given the differences in loading characteristics and load type between the two devices.

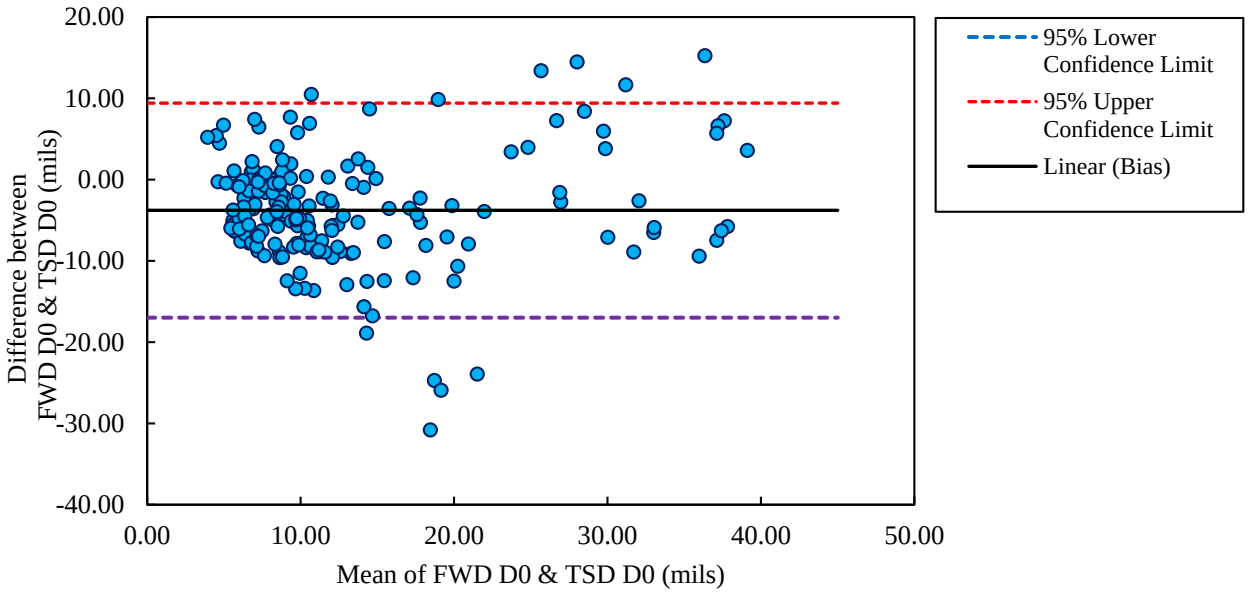

(a) Comparison of FWD D_0 and TSD D_0

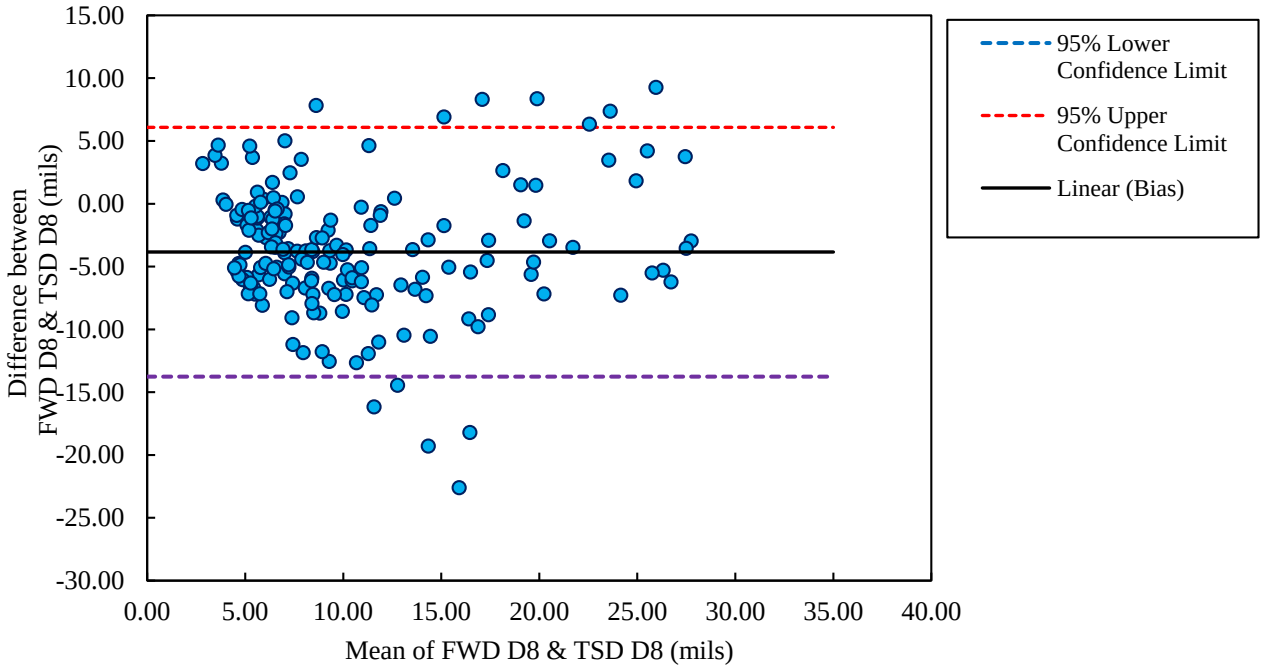

(b) Comparison of FWD D_8 and TSD D_8

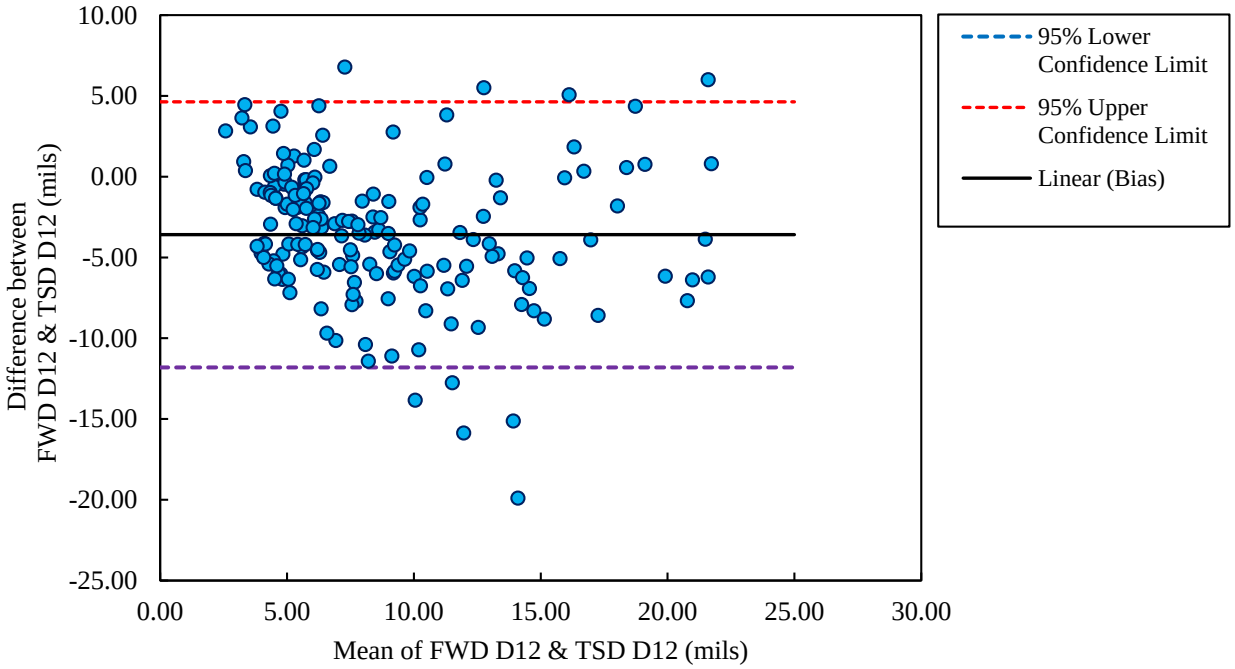

(c) Comparison of FWD D_{12} and TSD D_{12}

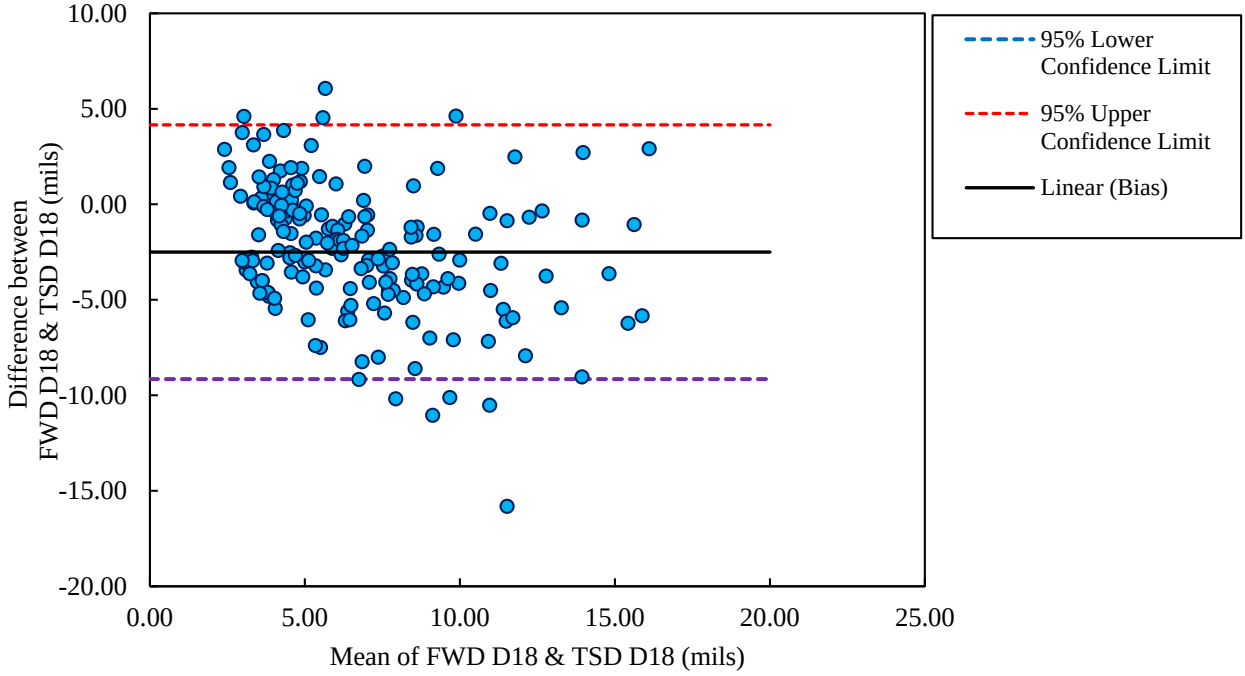

(d) Comparison of FWD D_{18} and TSD D_{18}

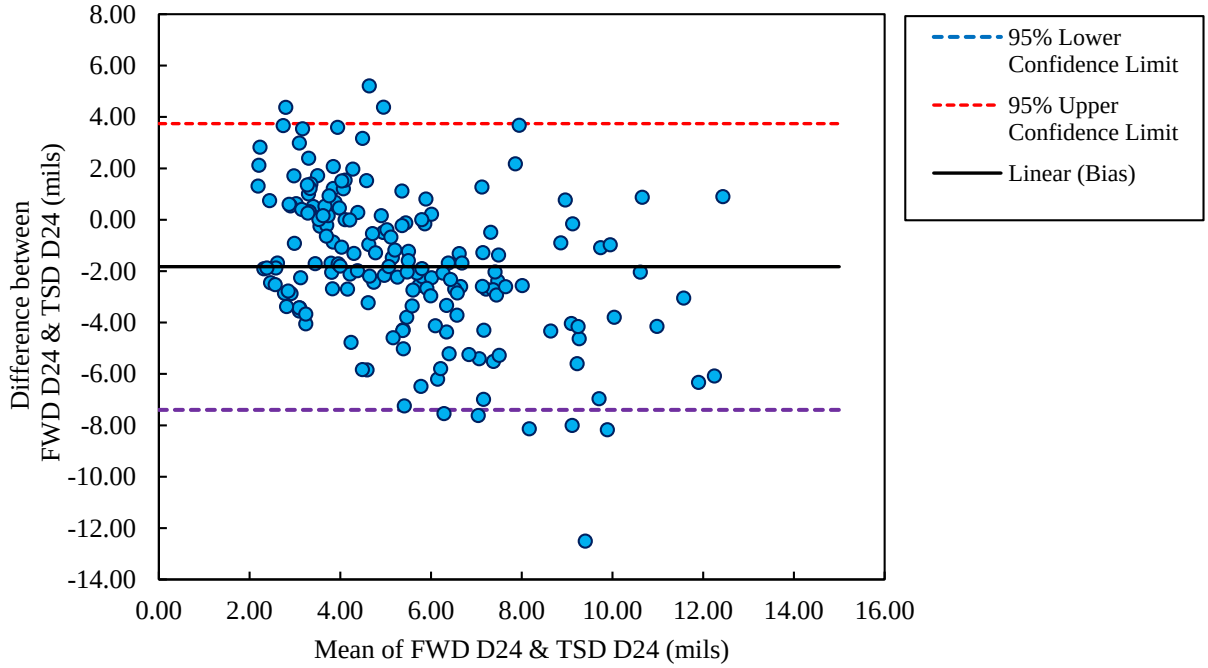

(e) Comparison of FWD D_{24} and TSD D_{24}

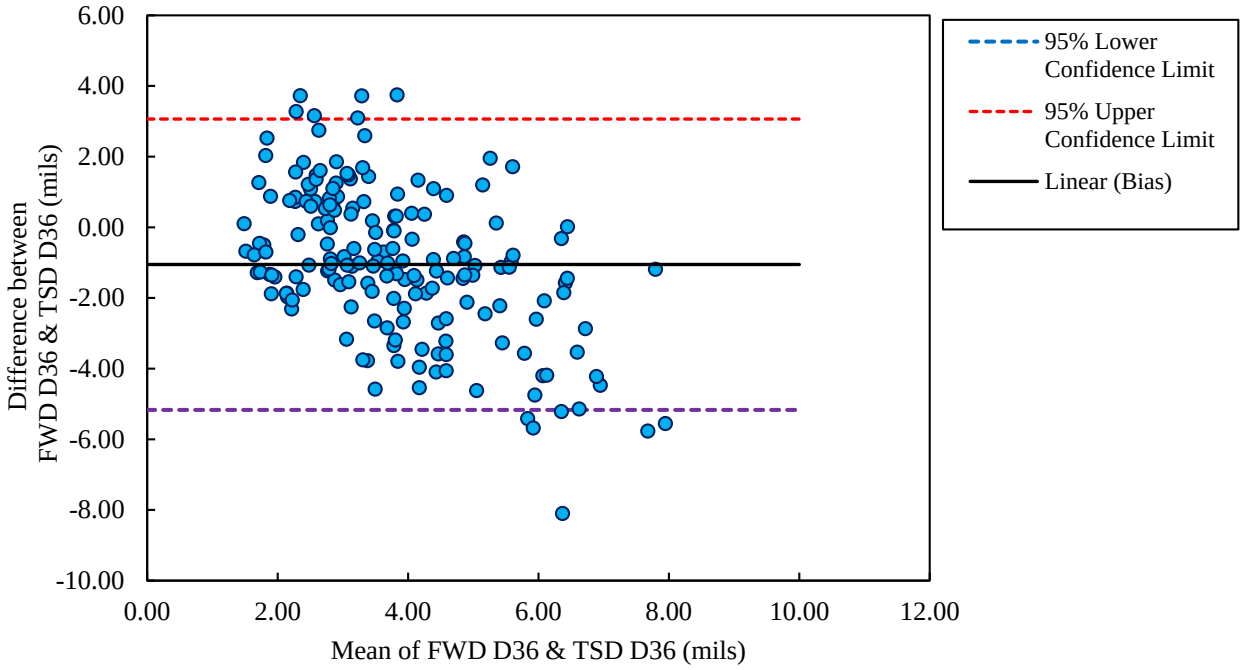

(f) Comparison of FWD D_{36} and TSD D_{36}

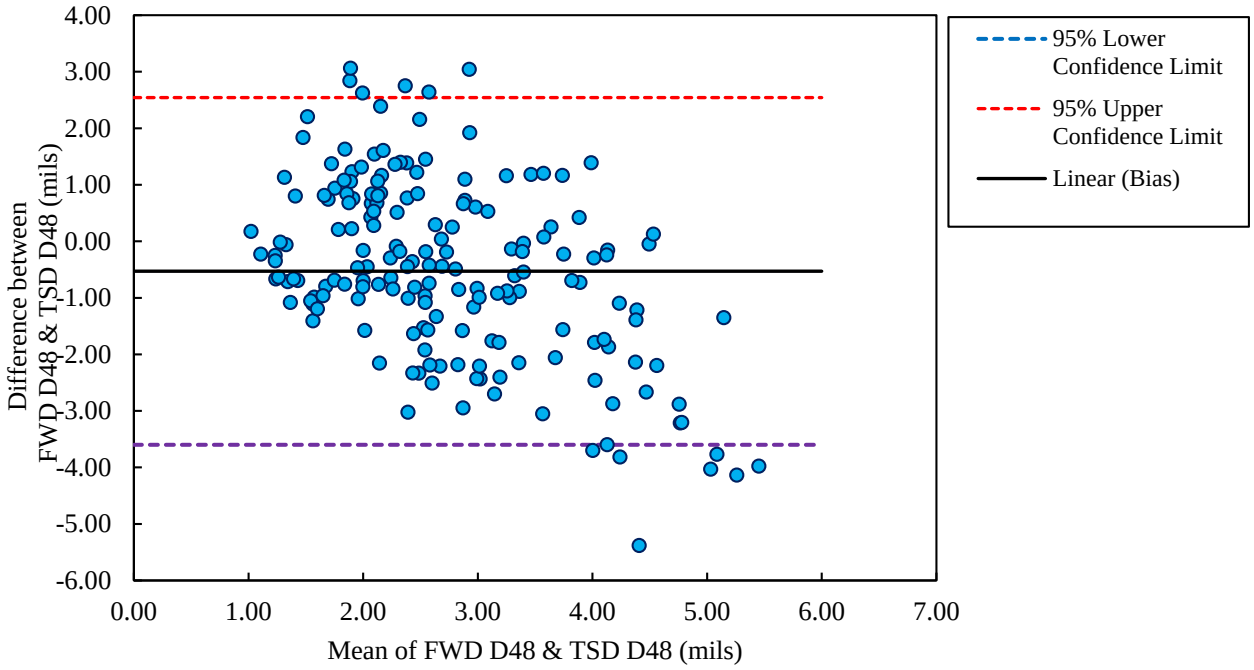

(g) Comparison of FWD D_{48} and TSD D_{48}

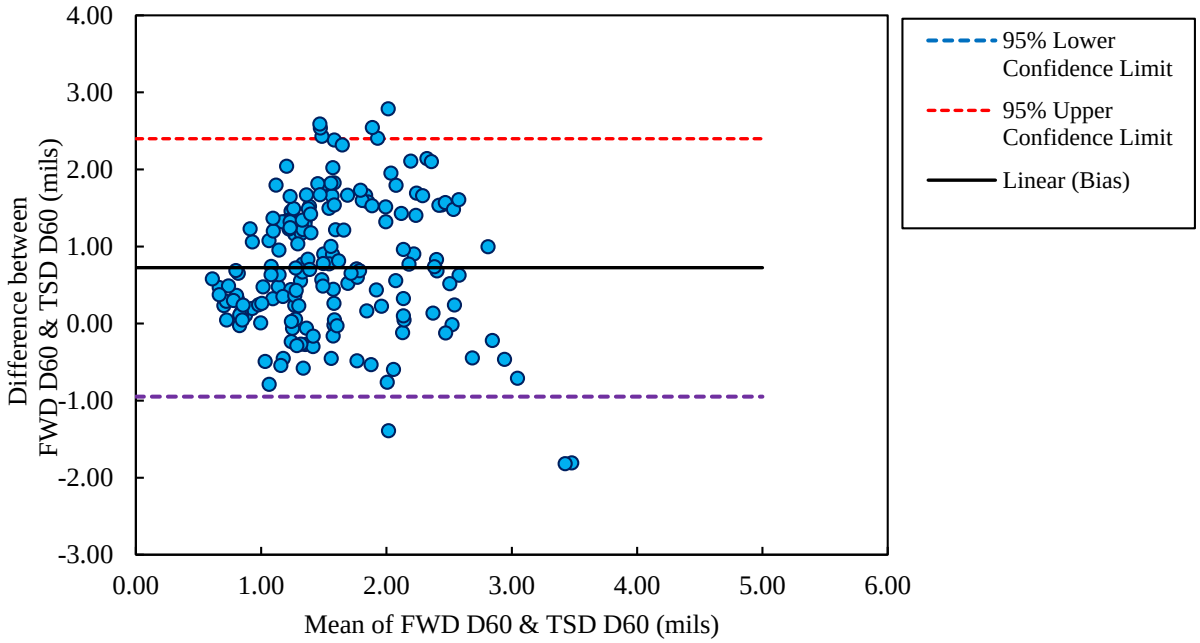

(h) Comparison of FWD D_{60} and TSD D_{60}

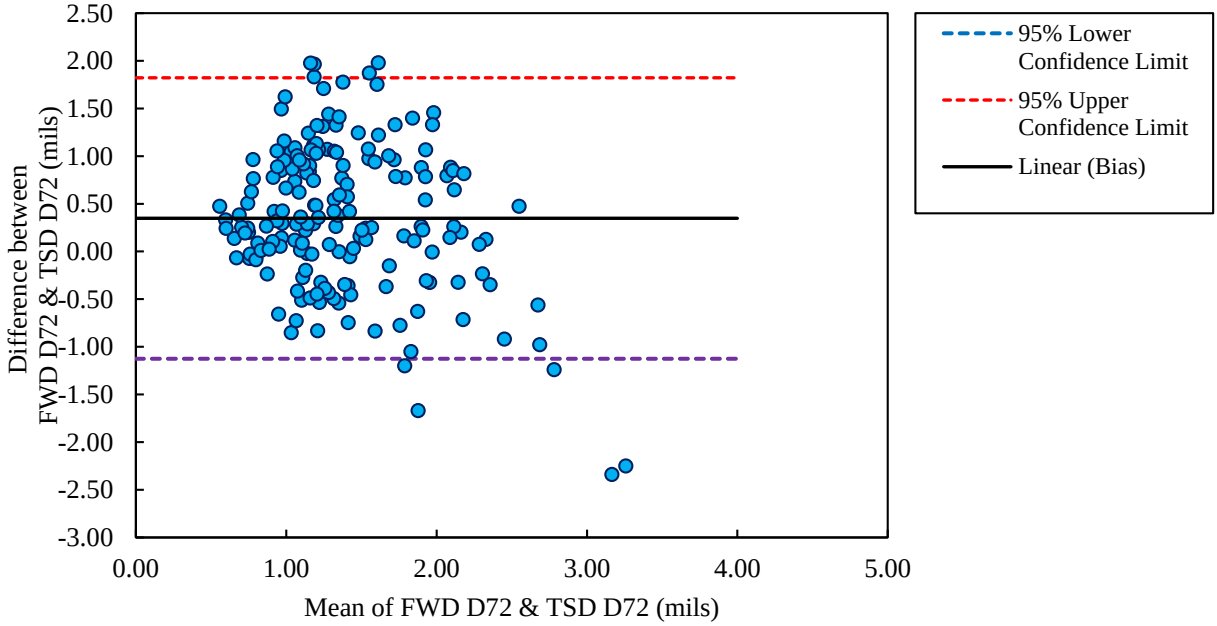

(i) Comparison of FWD D_{72} and TSD D_{72}

Figure 25
Comparison of FWD and TSD measurements using LOA method

FWD and TSD Comparisons for Different Functional Conditions

FWD and TSD measured deflections were compared for different road functional conditions. Roads were divided into four road categories (Poor, Fair, Good, Very Good) based on PCI; see Table 8. Figure 26 shows that TSD and FWD measurements correlated well with more uniform measurements for roads in good functional conditions and more scatterings for roads in poor functional conditions. Similar findings were reached in a previous RWD study in Louisiana *[20]*.

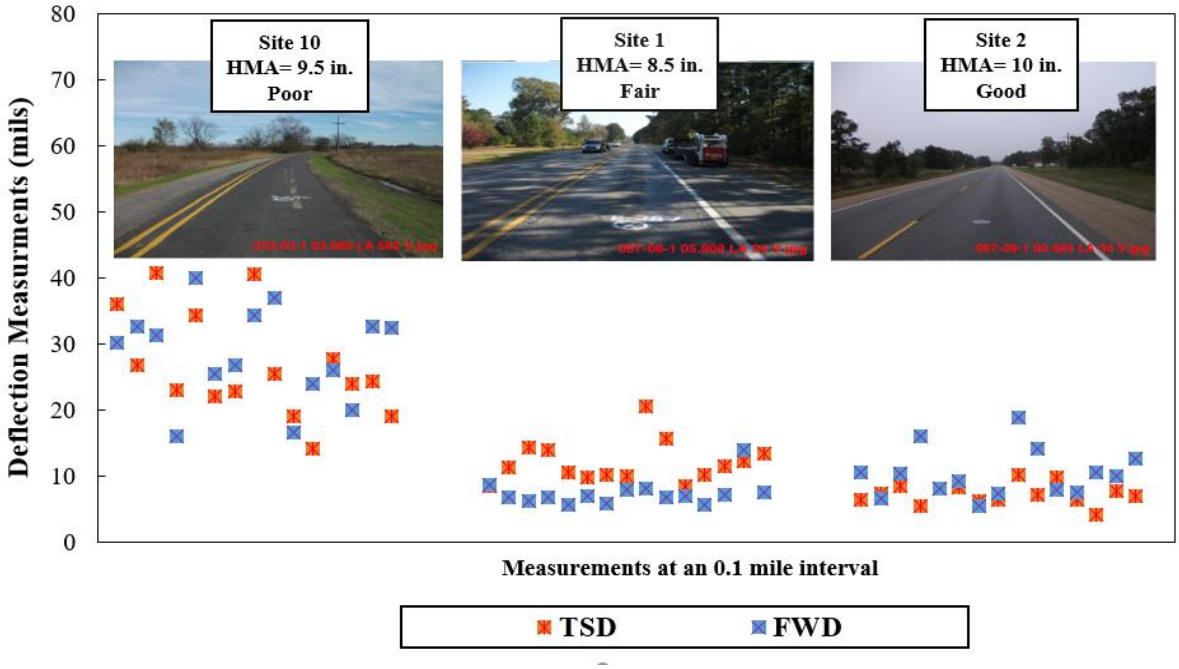

(a)

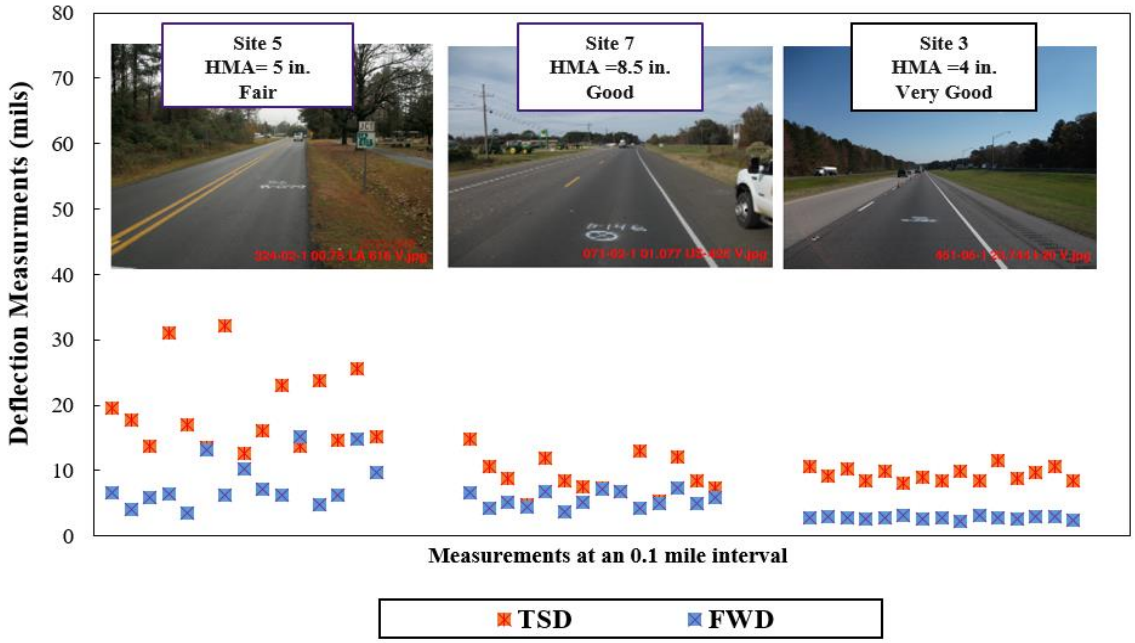

(b)

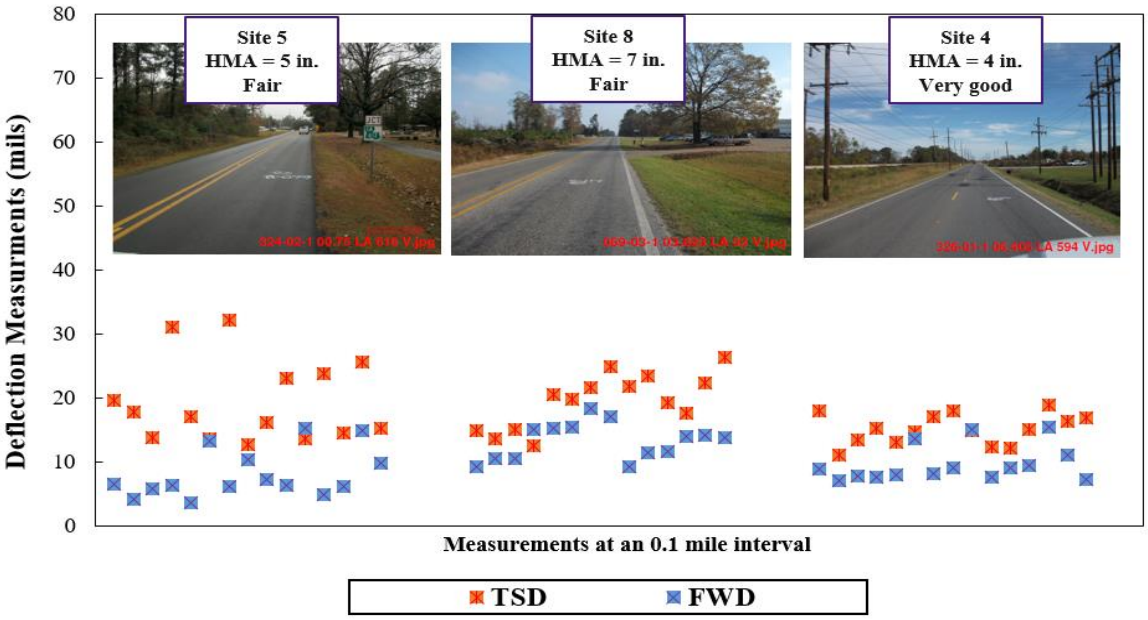

(c)

Figure 26
TSD and FWD comparison plots at different road conditions

Effect of Pavement Roughness in TSD Field Measurements

According to the literature and previous studies in the topic, the effect of pavement roughness is debatable. Studies showed considerable effect of surface roughness in moving load amplification, which would influence the deflection measurements reported by TSD. Yet, studies also found no significant correlation between TSD measurements variation with International Roughness Index (IRI) *[1, 26]*.

In the present study, surface roughness was obtained for the Louisiana sections in terms of IRI and at 0.1-mile interval. To analyze the variation in TSD measurements with IRI, the coefficient of variation (%) for TSD deflection measurements was calculated for each test section. Since FHWA categorizes the pavement section based on IRI as Good if IRI is less than 95 and acceptable if IRI is less than 170, the analysis was conducted by categorizing the control section based on FHWA IRI specifications. Figure 27 indicates that there is a noticeable difference in COV (%) for the two roughness categories. As shown in this figure, the COV (%) was relatively greater for the sections with IRI<170 than the sections with IRI<95. The difference is COV (%) was found to be the largest for the deflections under load (D_0) and the lowest for the far distance deflections (D_{60} and D_{72}). Therefore, it can be reasonably concluded that surface roughness has a notable effect on TSD field measured deflections.

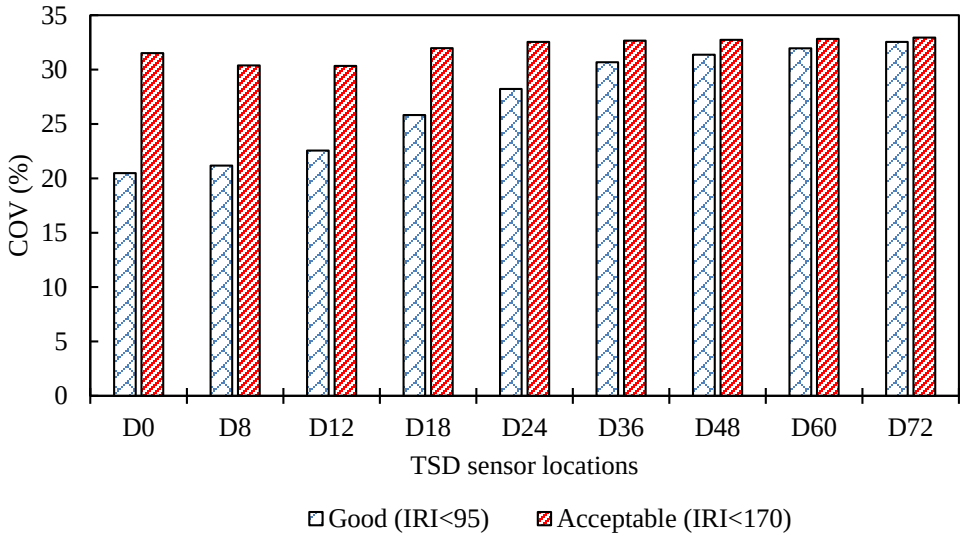

Figure 27
COV(%) comparison for TSD deflections for two roughness categories

Figure 28 presents the variation in COV (%) of loading for each section against the average IRI. As shown in Figure 28, the two variables appear to be correlated with an R^2 of 0.62. It is also noted that the COV (%) in load variation was relatively small with a maximum COV of 4.5%, which can be attributed to the technology advancements in TSD in the last few years. Recent upgrades have introduced new fast acting responsive dynamic servo systems, climate control systems, beam temperature and gyroscopic compensation, significantly improved horizontal velocity measurement, and advancements in laser calibration processes, as well as improved software.

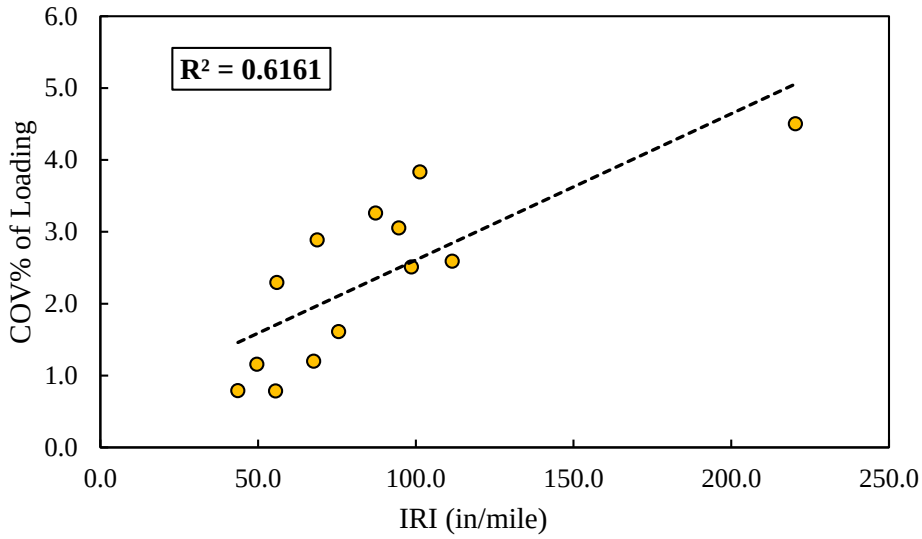

Figure 28
Loading variation with IRI

Effect of TSD Speed on Measured TSD Deflections

In a previous study, it was found that the variation of TSD measurements (i.e., COV) were higher at higher TSD speeds *[26]*. In the present study, the experimental program was conducted at only one speed for every section; therefore, the effect of TSD speed variation could not be assessed with field measurements. Yet, the effect of speed on surface deflections was evaluated using 3D Move simulation. 3D-Move software was selected as it has been shown effective in simulating deflections due to a moving load while considering the vehicle speed and viscoelastic material properties. Deflection variation with speeds was studied at a single location. TSD loading condition and dynamic modulus for AC layer were incorporated as inputs in 3D Move to calculate the corresponding surface deflection at different radial offsets. Simulated deflections were in good agreement with the field-measured deflection at a speed of 25.1 mph. Simulation was conducted at five different speeds. From the simulated results, the increase in vehicle speed caused a decrease in the majority of the deflections, as shown in Table 10 and Figure 29. For a comprehensive evaluation of TSD measurements variation with speed, additional field-testing is recommended.

Table 10
3D Move simulation results with different speed

Speeds (mph)	D0 (mils)	D8 (mils)	D12 (mils)	D18 (mils)	D24 (mils)	D36 (mils)	D48 (mils)	D60 (mils)	D72 (mils)
15	10.85	9.38	8.39	6.99	5.74	3.72	2.30	1.34	0.69
25.1*	10.63	9.13	8.15	6.77	5.55	3.59	2.23	1.28	0.65
30	10.57	9.11	8.14	6.78	5.52	3.61	2.25	1.29	0.66
45	10.43	9.39	8.53	7.23	6.02	3.99	2.51	1.49	0.79
60	10.33	9.01	8.10	6.80	5.58	3.68	2.31	1.34	0.68

** Represents the actual testing speed in this section.*

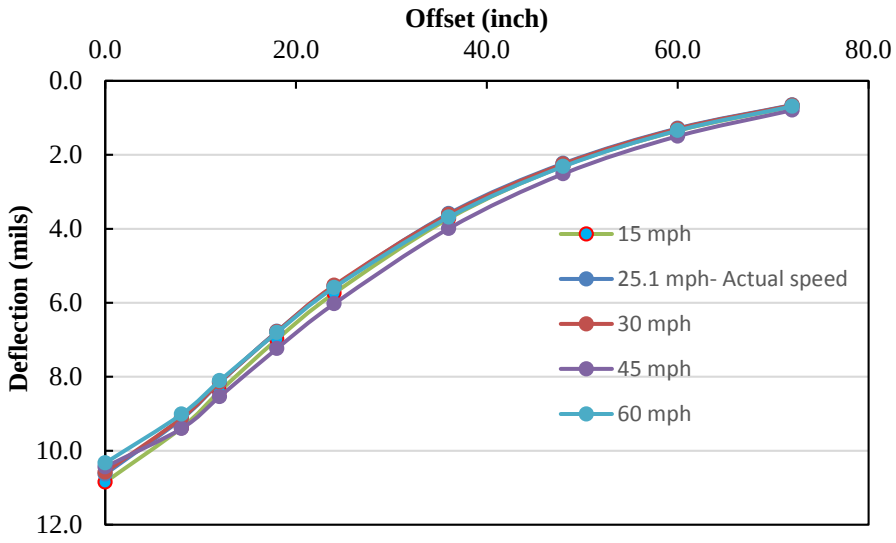

Figure 29
Deflection basin obtained from 3D Move simulation at different speeds

Artificial Neural Network Backcalculation Procedure

A multilayered, feed-forward ANN using a back-propagation error algorithm was selected with a tan-sigmoid transfer function. The network architecture consisted of three layers: an input layer of nine neurons; a hidden layer of five neurons; and a target layer of nine neurons. The input layer was fed with the TSD deflections at the nine aforementioned radial distances while the target layer was fed with the FWD measurements normalized to a load level of 9,000 lbs., as shown in Figure 30. A total of 1,467 data points were used in the model development phase. The data were divided into 70% for training, 15% for validation, and 15% for testing. Training was halted when the validation set error stopped decreasing to

avoid overfitting and to increase the generalization ability of the network. The testing data set had no effect on the training, so it was used to provide an independent measure of the network performance.

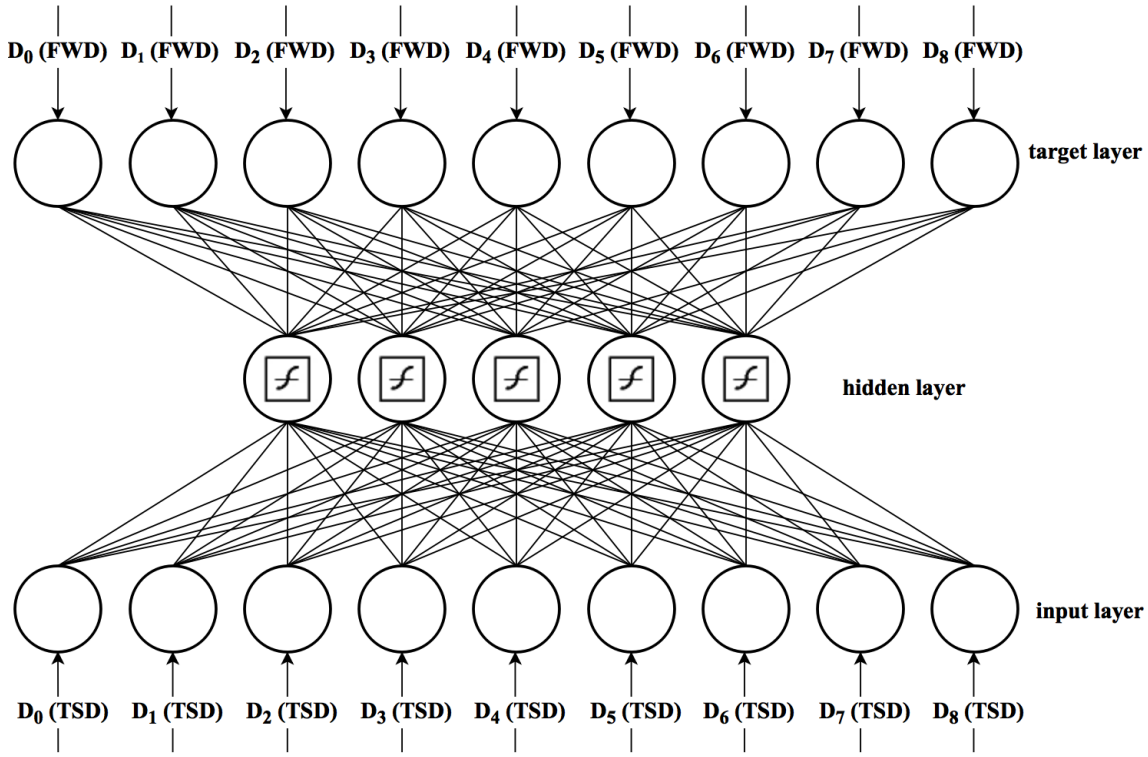

D_0 to D_8 are deflections at the predefined FWD offsets

Figure 30
General layout of the Artificial Neural Network model

The output of the ANN model is the corresponding corrected and normalized FWD deflection basin based on TSD measurements, which were referred to as TSD*. The regression plots of the ANN model for the training, validation, testing, and overall sets are shown in Figure 31. All data processing was performed off-line using a commercial software package (MATLAB R2013a, The MathWorks, Inc.). The MATLAB code is provided in Appendix A for future use of this model. Table 11 shows the root mean square error (RMSE %) values at each radial offset, which were calculated as follows:

$$\text{RMSE} = 100 * \sqrt{\frac{\sum_1^n [\text{Predicted value (TSD*)} - \text{measured value (FWD)}]^2}{n}} \Big/ \frac{\sum_1^n \text{measured value}}{n} \qquad (19)$$

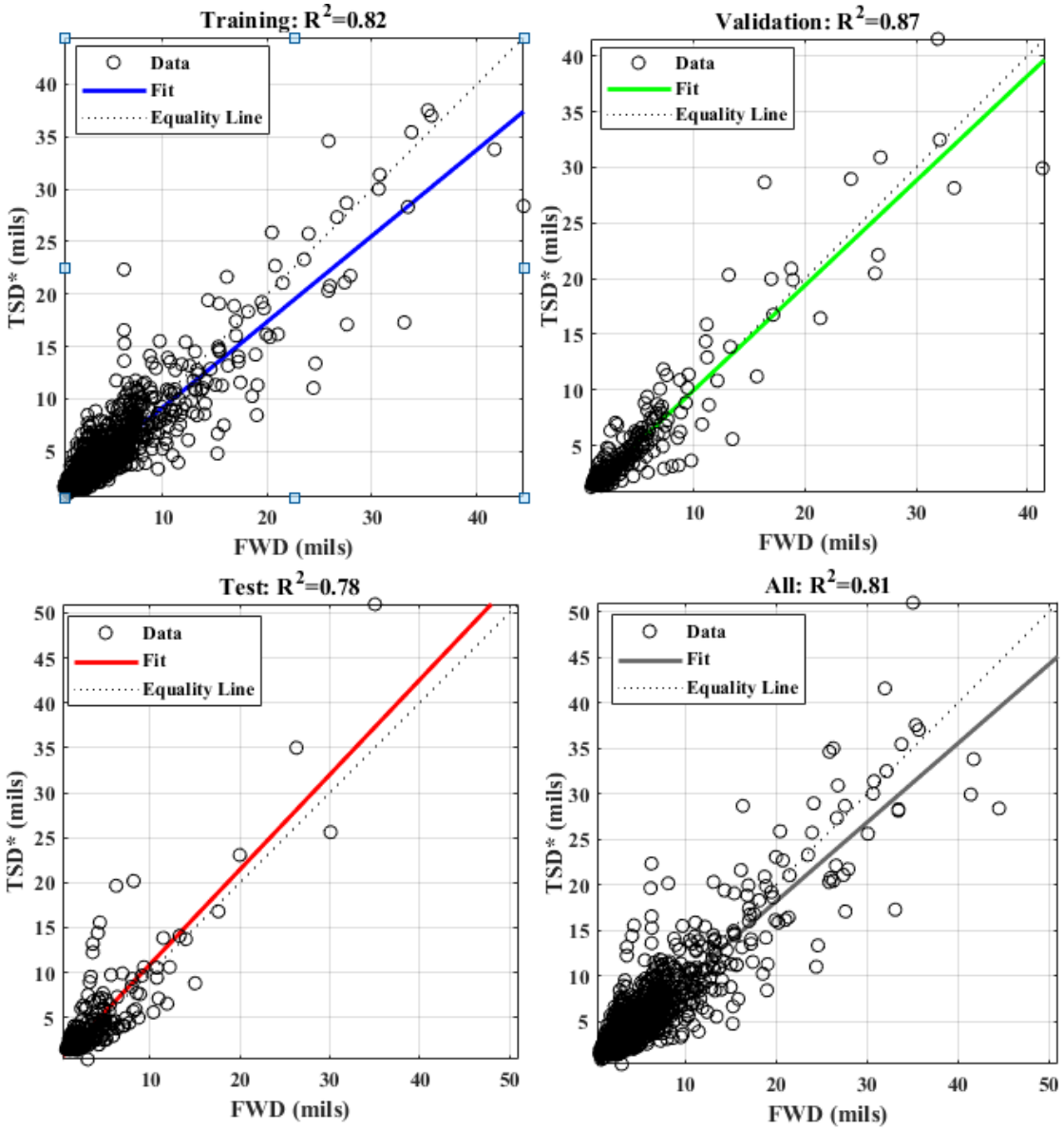

Figure 31
Regression plots of the TSD* vs. the FWD deflection

Table 11
RMSE (%) between FWD and TSD*

Offset Distance, mm	0	203.2	304.8	457.2	609.6	914.4	1219.2	1524	1828.8
RMSE, %	5.4	5.1	4.9	4.7	3.8	5.3	5.3	5.3	5.2

An example of the correlation between FWD, TSD, and TSD* deflections are presented in Figure 32. As shown in this figure, the ANN model was successful in converting the TSD deflection basin to a corresponding FWD deflection basin.

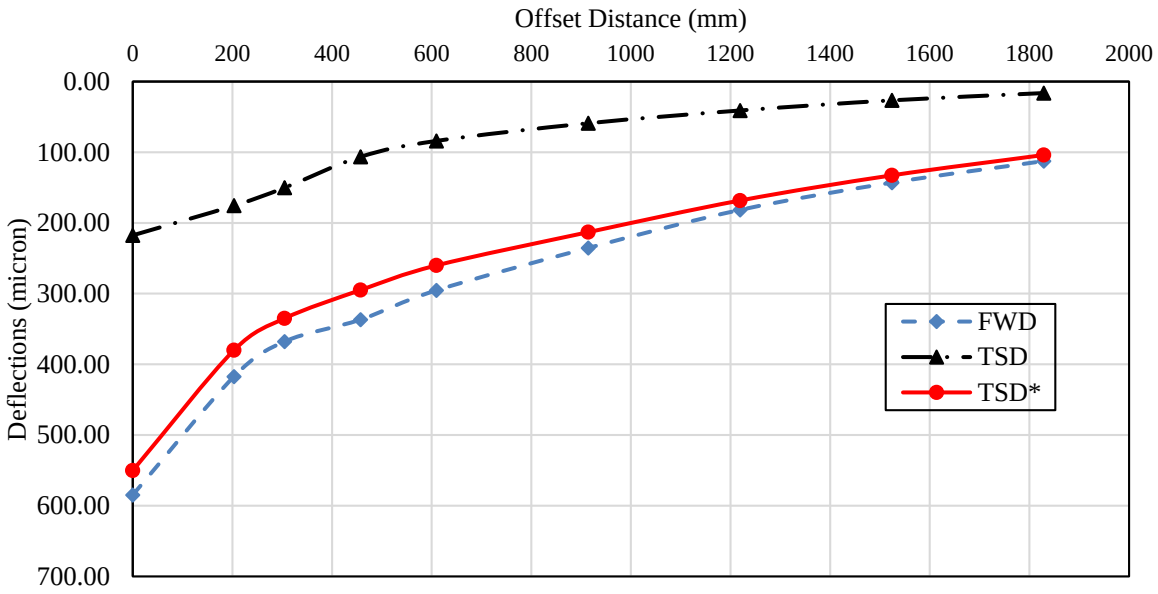

Figure 32
Deflection basins of the FWD, TSD, and TSD* at Station (0+00) Section 67-08

Model Validation

The generalization ability of the presented ANN model was tested and validated using measurements obtained from the testing program conducted at MnROAD. TSD data from 16 flexible pavement testing cells were used as inputs to predict TSD* using the proposed ANN model. The resulted TSD* basin values were then compared with the measured FWD deflections. As shown in Figure 33, the model showed acceptable accuracy with a coefficient of determination (R^2) of 0.9.

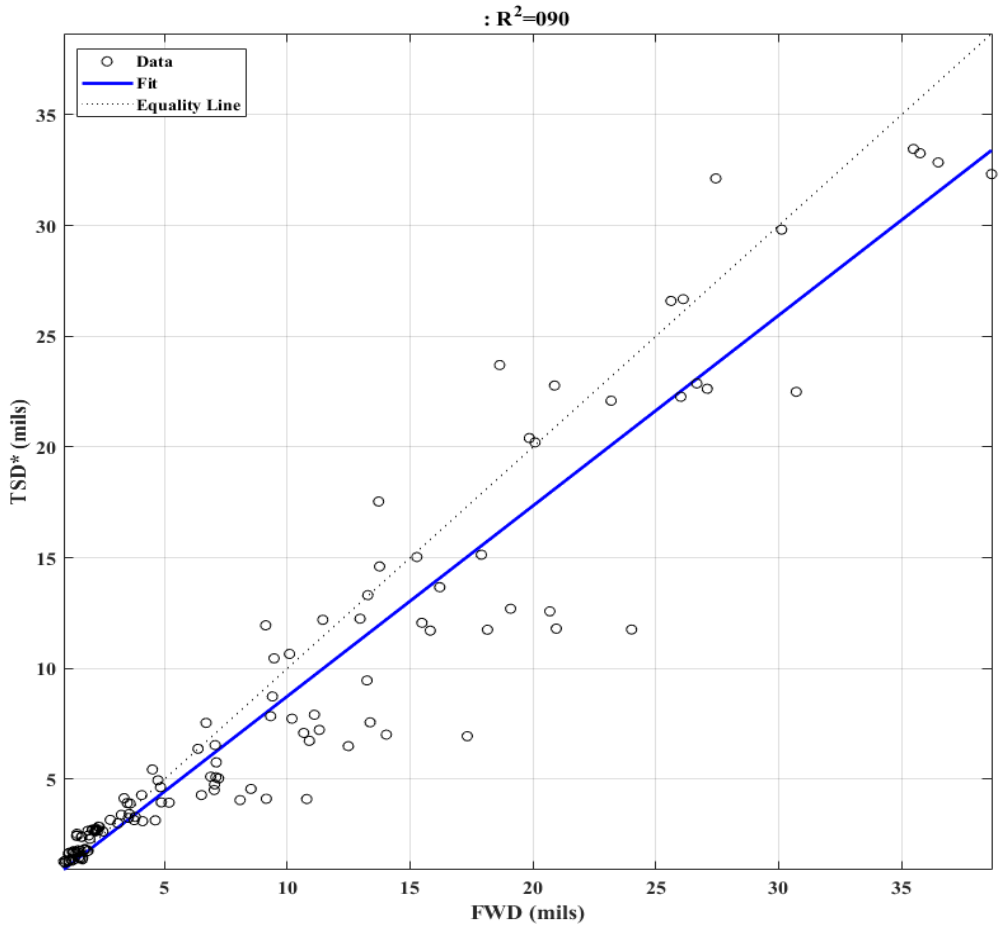

Figure 33
Validation of the ANN model using MnROAD data

Backcalculation Analysis

The Dynatest software ELMOD 6 was used in this study to perform the backcalculation analysis. The ELMOD 6 program provides three methods for conducting the backcalculation of layer moduli (radius of curvature, deflection basin fit, and finite element based method). For the present study, the deflection basin method was used in the backcalculation analysis. The analysis was conducted until a RMSE of 2% or less was achieved.

The backcalculation analyses were conducted using the FWD measurements and the TSD* deflection values. The analyses were conducted for the entire experimental data set (i.e., 13 sections tested in Louisiana and 16 tested in Minnesota). Figure 34 shows the correlation between the backcalculated moduli using the FWD and the TSD*. As shown in this figure, there was a good agreement between the backcalculated moduli from FWD and TSD

deflection measurements. The RMSE was 12.5%, 13.2%, and 10.2% for the AC moduli, base moduli, and subgrade moduli, respectively.

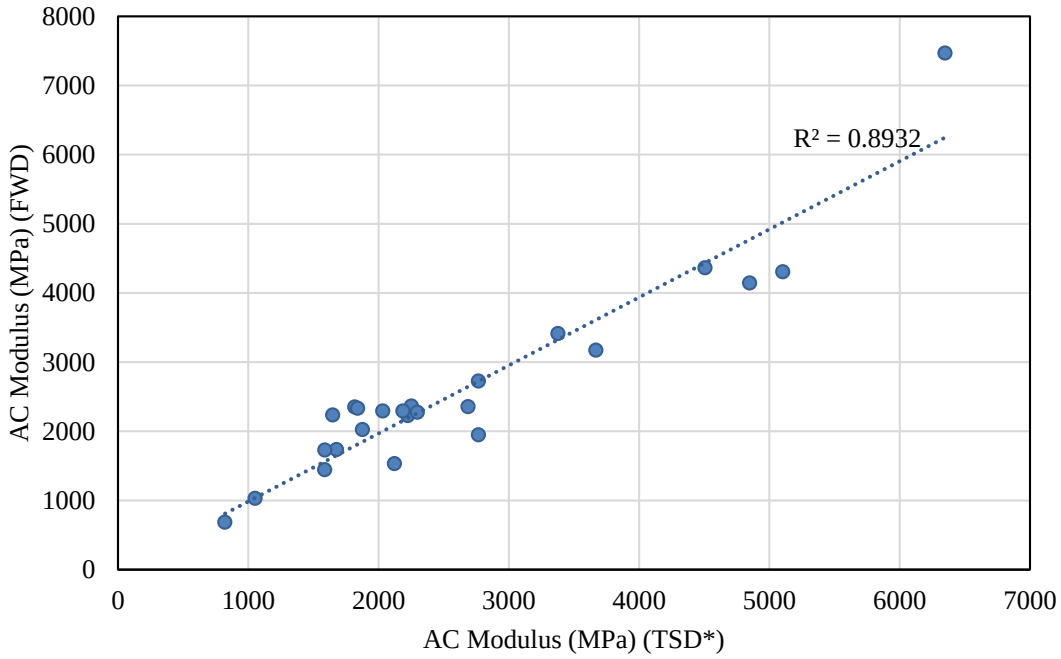

(a) HMA layer

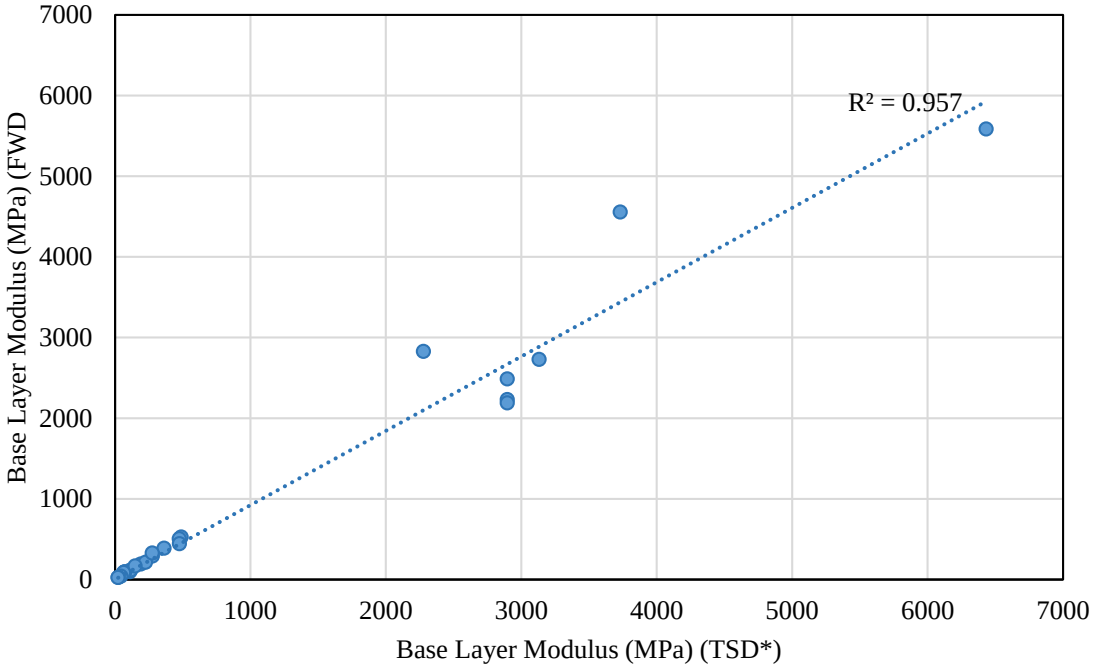

(b) Base layer

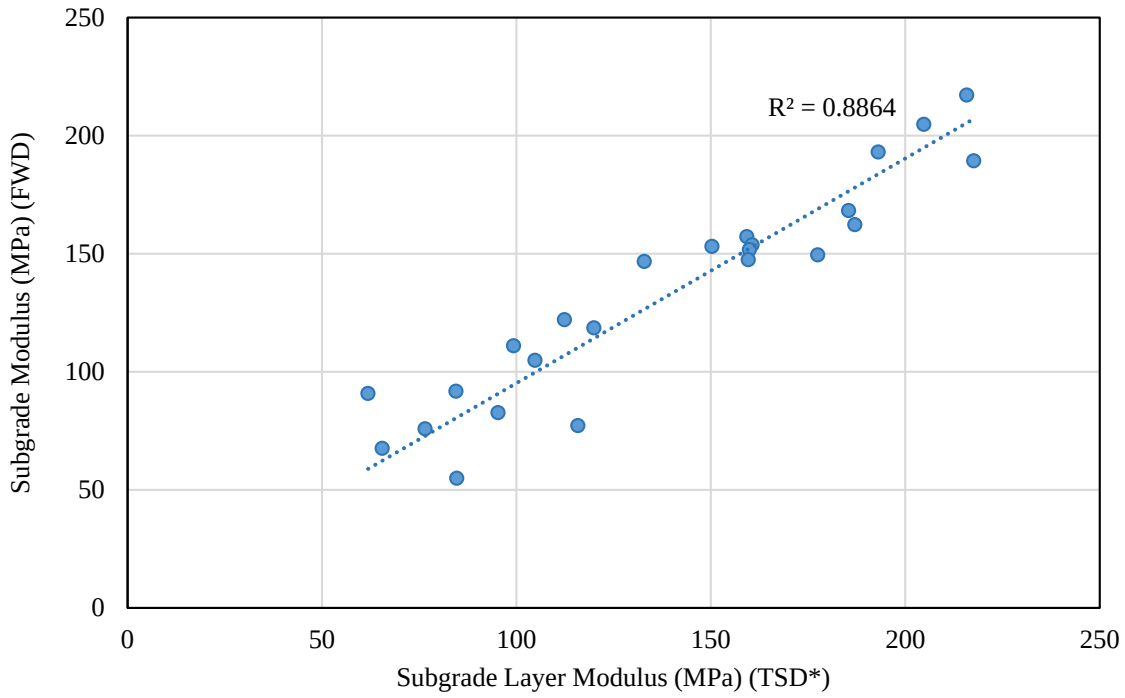

(c) Subgrade layer

Figure 34
Correlation between backcalculated layer moduli Using FWD measurements and TSD*

Comparison of Critical Pavement Responses

To further investigate the proposed approach, critical pavement responses were calculated using 3D Move software for the 16 road segments tested in Minnesota. These responses included the horizontal tensile strain at the bottom of the AC layer (ε_t) and the vertical compressive strain on the top of the subgrade (ε_v). These calculations were conducted using the backcalculated moduli based on FWD measurements and using the backcalculated moduli based on the predicted TSD* values. A static load of 18,000 lbs. was applied on a single axle dual-tire assembly. While the tire pressure was assumed 100 psi, the contact area was considered circular, and the distance between the two tires, center to center, was assumed 14.57 in. Critical pavement responses (ε_t and ε_v) were calculated at three radial offsets; under the center of the tire, under the mid-distance between the tires, and under the tire edge in the Y-Z plane as shown in Figure 35. In the X-Z plane, ε_t and ε_v were calculated under the center of the tire.

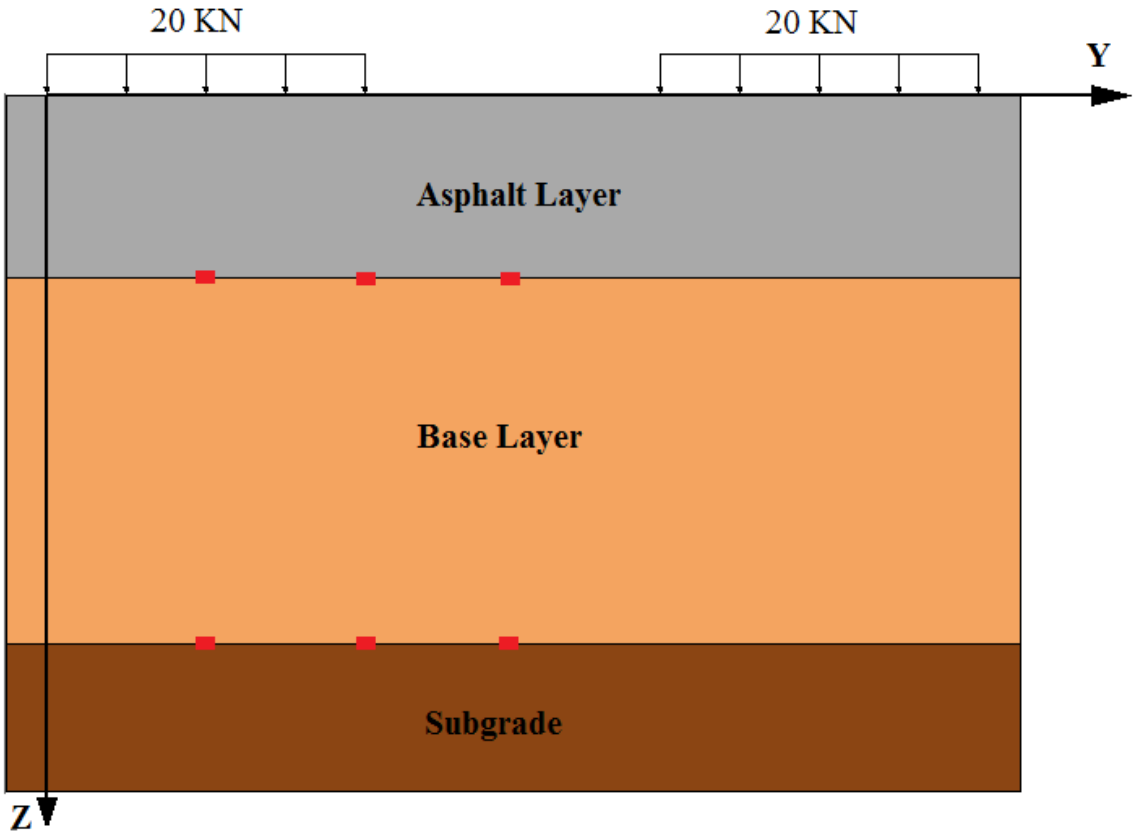

Figure 35
Selected locations for pavement response analysis in the Y-Z plane

From the 3D Move analysis, critical pavement responses calculated based on the FWD measurements, showed good correlation with responses calculated based on the predicted TSD* values. Figure 36 presents these correlations for ε_t at the bottom of the AC layer and for ε_v on the top of the subgrade, both calculated under the center of the tire. Table 12 summarizes the error and the correlation between the pavement responses obtained from the 3D Move analysis.

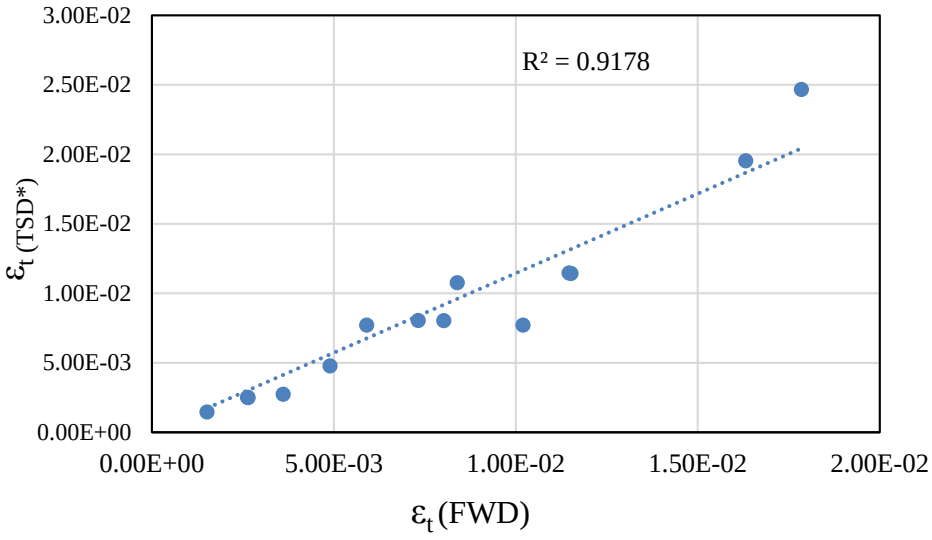

(a)

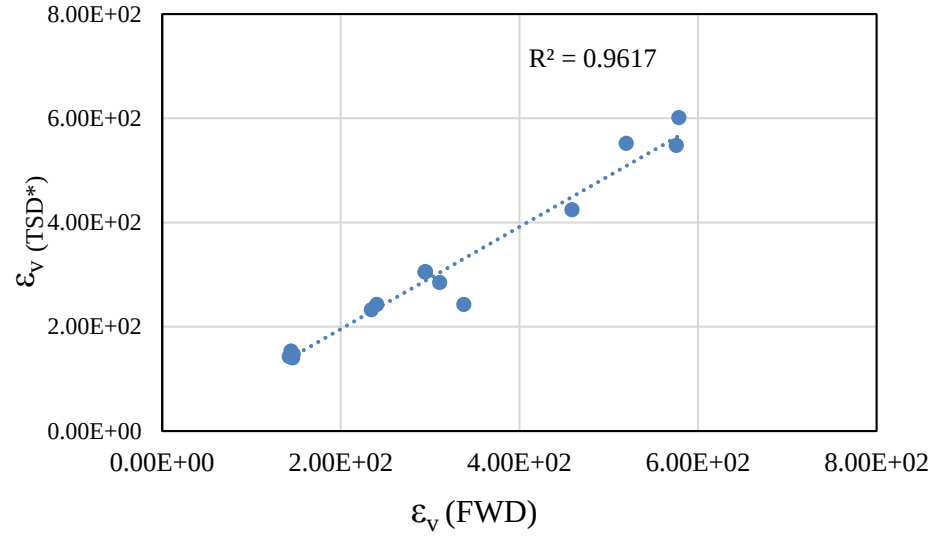

(b)

Figure 36
Correlation between pavement responses calculated under the center of the tire based on FWD measurements and TSD* (a) εt (b) εv

Table 12
Statistics of predicted pavement distresses

	Location					
Criterion	**Tire Center**		**Tire Edge**		**Between Tires**	
Response	ε_t	ε_v	ε_t	ε_v	ε_t	ε_v
R^2	0.92	0.96	0.85	0.96	0.88	0.96
RMSE %	13.8	5.6	18.9	5.3	19.3	5.4

Comparison of Number of Cycles for Fatigue Failure

The calculated tensile strain at the bottom of the HMA layer (ε_t) and the backcalculated HMA moduli (E_{HMA}) were incorporated in the bottom-up fatigue model utilized in Pavement ME *[43]:*

$$N_f = K_{f1} C . C_H \beta_{f1} \left(\frac{1}{\varepsilon_t}\right)^{k_{f2}\beta_{f2}} \left(\frac{1}{E_{HMA}}\right)^{k_{f3}\beta_{f3}} \quad (21)$$

$$C = 10^M \quad (22)$$

$$M = 4.84 \left(\frac{V_b}{V_a V_b} - 0.69\right) \quad (23)$$

$$C_H = \frac{1}{0.000398 + \frac{0.003602}{1 + e^{11.02 - 3.49 hac}}} \quad (24)$$

where,

N_f = Number of cycles for fatigue failure;

K_{f1}, K_{f2}, K_{f3} = Global calibration coefficients (K_{f1}= 0.007566, K_{f2}=3.9492, K_{f3}=1.281);

B_{f1}, β_{f2}, β_{f3} = Local calibration factors (set to 1.0);

V_b= Effective binder content by volume (assumed to be 10%);

V_a = Air voids after construction (assumed to be 7%); and

h_{ac} = thickness of HMA layers.

Equation (21) was utilized to calculate the number of cycles for fatigue failure considering the results obtained from FWD measurements and the results from TSD* values. The comparison showed an RMSE of 16.0% and an R^2 of 0.99. A comparison between N_f based on FWD measurements and TSD* values is shown in Figure 37.

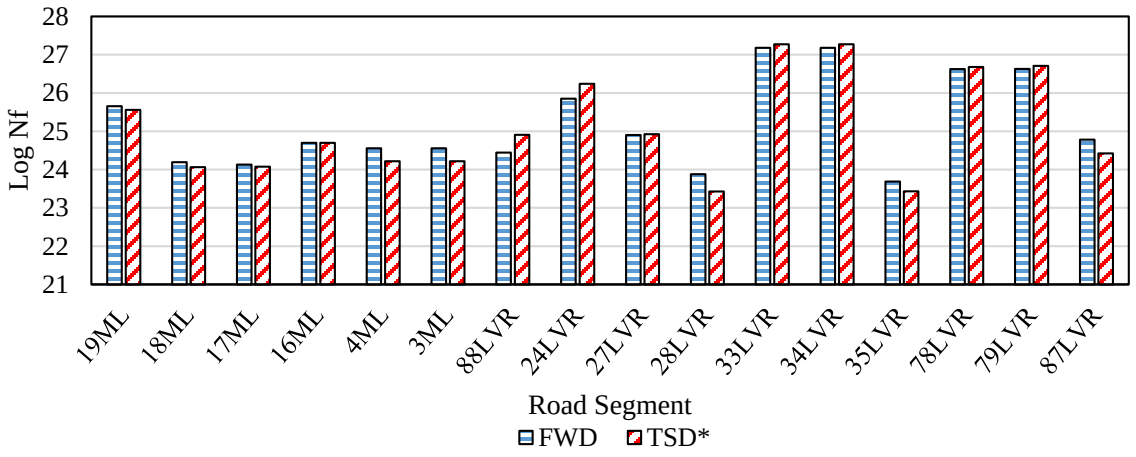

Figure 37
Comparison between N_f calculated based on FWD and TSD* deflection measurements

Structural Health Index Comparison

A recent study conducted by the authors introduced the Structural Health Index (SHI) calculated based on pavement backcalculated layer moduli *[44]*. The SHI was defined based on the estimated loss in SN; it was scaled logistically from zero to 100. A sigmodal function was selected to represent the correlation between the loss in SN (%) and the SHI:

$$SHI = \frac{100}{1+e^{0.15\,(SN\ loss\ \%-30)}} \quad (25)$$

Fitting parameters in the sigmodal model were selected such that pavement sections with loss in SN greater than 50% would have an SHI value close to zero, and sections with minimal or no loss in SN will have an SHI value near 100. The SHI evaluation and validation demonstrated that it responded realistically to sections in poor and in good structural conditions. More details about the development and validation of the SHI have been presented elsewhere *[44]*. In the present study, the SHI was calculated for the MnROAD 16 Road segments based on both FWD measurements and the TSD* values; the average RMSE was found to be 4.6%. Figure 38 presents a comparison between the SHI values for

segments in the main line. As shown in Figure 36, both approaches agreed reasonably well in predicting the SHI.

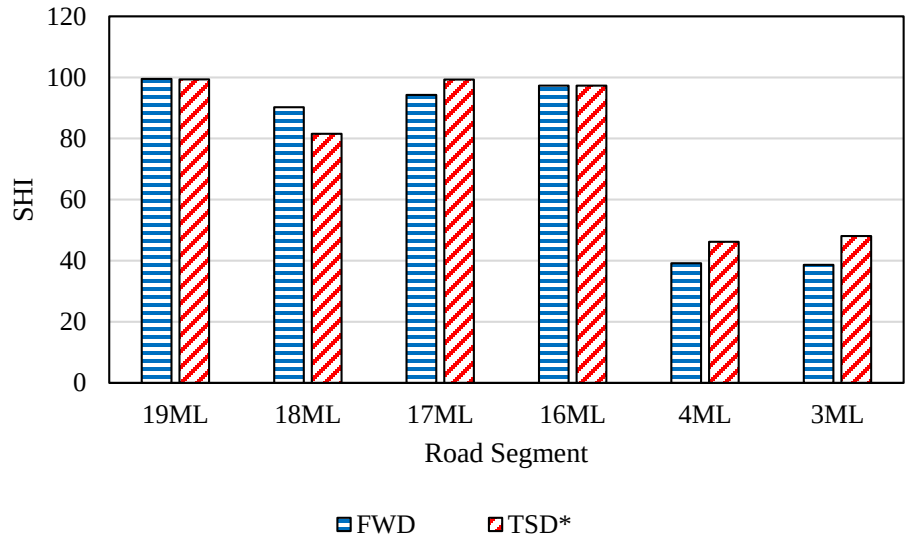

Figure 38
SHI comparison for Main Line segments

Structural Capacity Prediction Model Development

The SN prediction model development along with its validation procedure is discussed in this section. Model development was followed by several statistical analyses to ensure selection of appropriate independent variables and to evaluate their effectiveness in the model. After development, model validation was conducted based on an independent data set.

Pairwise Correlation

Pairwise correlation was conducted among the independent variables to avoid using collinear or multi-collinear independent variables in the model, which may increase the variance of the estimated regression coefficients. All the possible independent variables that may have an influence on the prediction of SN were subjected to pairwise correlation analysis. The correlation coefficient is an indication of the level of collinearity among the independent variables *[45, 46]*. The coefficient is called Pearson's correlation coefficient, which ranges from -1 to +1. A large absolute value indicates high collinearity between those variables. The positive or negative sign represents the positive or negative relationship between the variables. The results of the pairwise correlation analysis is presented in Table 13. A Pearson's coefficient that is greater than 0.6 was considered highly collinear in this analysis.

As shown in this table, most of the deflection measurements were correlated, which was expected as surface deflections tend to increase or to decrease concurrently with the exception of far distance deflections (i.e., D_{60} and D_{72}), which may indicate weakness in the underlying layers and the subgrade. It is worth noting that the final model did not include D_{60} or D_{72} because the use of these variables would limit the application of the model since some TSD surveys do not measure far distance deflections from the load. Moreover, the prediction accuracy was satisfactory with the use of D_{48}, which was deemed more reasonable than the use of D_{60} or D_{72}, even though they showed a better correlation with SN_{FWD}. Based on the results of the analysis, collinear variables were not used. Different combinations of non-collinear variables were considered in the regression analysis.

Table 13
Pearson correlation coefficients

	SN_{FWD}	D0	D8	D12	D18	D24	D36	D48	D60	D72	T_{th}	ADT
SN_{FWD}	1.00	-0.53	-0.33	-0.18	0.02	0.20	0.36	0.40	0.42	0.46	***0.80***	***0.76***
D0	-0.53	1.00	***0.95***	***0.88***	***0.74***	0.58	0.38	0.29	0.21	0.10	-0.24	-0.42
D8	-0.33	***0.95***	1.00	***0.98***	***0. 90***	***0.78***	***0.61***	0.53	0.44	0.32	-0.11	-0.24
D12	-0.18	***0.88***	***0.98***	1.00	***0.97***	***0.89***	***0.75***	***0.67***	0.58	0.46	0.01	-0.10
D18	0.02	***0.74***	***0.90***	***0.97***	1.00	***0.97***	***0.89***	***0.83***	***0.75***	***0.64***	0.14	0.08
D24	0.20	0.58	***0.78***	***0.89***	***0.97***	1.00	***0.97***	***0.93***	***0.87***	***0.77***	0.25	0.24
D36	0.36	0.38	***0.61***	***0.75***	***0.89***	***0.97***	1.00	***0.99***	***0.96***	***0.89***	0.32	0.39
D48	0.40	0.29	0.53	***0.67***	***0.83***	***0.93***	***0.99***	1.00	***0.99***	***0.93***	0.34	0.43
D60	0.42	0.21	0.44	0.58	***0.75***	***0.87***	***0.96***	***0.99***	1.00	***0.95***	0.33	0.45
D72	0.46	0.10	0.32	0.46	***0.64***	***0.77***	***0.89***	***0.93***	***0.95***	1.00	0.35	0.50
T_{th}	***0.80***	-0.24	-0.11	0.01	0.14	0.25	0.32	0.34	0.33	0.35	1.00	0.52
ADT	***0.76***	-0.42	-0.24	-0.10	0.08	0.24	0.39	0.43	0.45	0.50	0.52	1.00

Note: Highly collinear relationships are marked as bold and dark colored.

Regression Analysis and Variance Inflation factor (VIF)

To assess the significance of the independent variables (D_0, D_8, D_{12}, D_{18}, D_{24}, D_{36}, D_{48}, D_{60}, D_{72}, T_{th}, and ADT) on the prediction of the dependent variable (SN), regression analysis was conducted. Independent variables with no significance on the dependent variable were removed from the model to avoid overfitting of the dependent variable. When overfitting occurs, the regression model becomes tailored to fit the random noise in the data set rather than reflecting the actual trends in the measurements. A regression analysis was conducted on several combinations of independent variables using SAS 9.4 software. With 95% confidence level, a P-value less than 0.05 would represent a significant effect. The combination of independent variables that had significant effect on the dependent variable is presented in Table 14.

Table 14
Results of regression analysis and multi-collinearity test

Variable	Pr > |t|	Interpretation	Variance Inflation (VIF)
Intercept	<.0001	Significant	0
D_0	<.0001	Significant	1.86
D_{48}	<.0001	Significant	1.94
T_{th}	<.0001	Significant	2.22
ADT	<.0001	Significant	1.43

To further filter out the multi-collinear independent variables, a second statistical factor known as the 'Variance Inflation Factor (VIF)' was used. Even after pairwise correlation analysis between two variables, there is a possibility of multi-collinearity resulting from the combination of one variable with more than one variable. To address this issue, the most used statistical factor is the variance inflation factor. Because of multi-collinearity, an inflation can occur in the standard error, which is measured by VIF. A maximum VIF value of 5 to 10 is recommended in the literature *[47]*. In this study, the VIF values for the selected independent variables were within the acceptable range (Table 14), which indicates that no multi-collinear independent variables have been used in the model.

Non-Linear Regression Model Development

A non-linear regression model was developed using SAS 9.4 to predict the SN of in-service pavement. The structural number, which is referred to as SN_{TSD}, was predicted based on the statistically significant TSD deflections (D_0 and D_{48}), ADT, and total pavement thickness (T_{th}). About 70% of the data points from Louisiana and 30% of the data points from Idaho were used in the development phase to fit the model; the remaining data points from Louisiana and Idaho were used to validate the fitted model. The model demonstrated an acceptable accuracy with a Coefficient of determination (R^2) of 0.92 in the development phase and with a RMSE of 0.88 as shown in Figure 39. The proposed model is illustrated in equation (26):

$$SN_{TSD} = 18.67 * e^{(-0.013*D_0)} + 8.65 * (D_{48})^{0.11} + 0.18 * (T_{th}) + 0.31 * Ln\,(ADT) - 24.28 \quad (26)$$

where,

SN_{TSD} = SN based on TSD measurements;

D_0 = Deflection of pavement under loaded tire or Center Deflection (mils);

D_{48} = Deflection at 48 in. distance from Center Deflection (mils);

T_{th} = Total layer thickness of pavement (in.); and

ADT = Average Daily Traffic (veh/day).

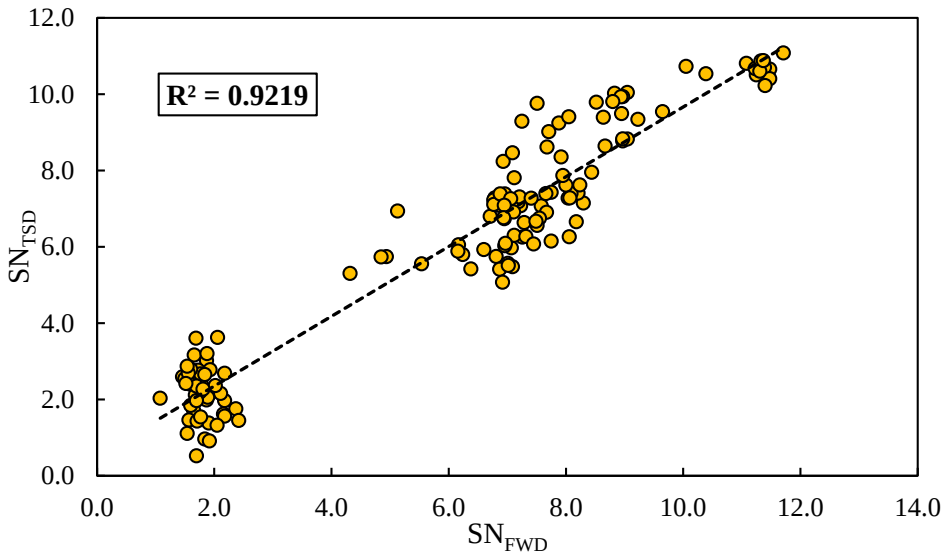

Figure 39
Model fitting in the development phase

Model Validation

An independent TSD and FWD data set was used to validate the model. The use of Idaho data points in the model validation demonstrated the model's compatibility with different climatic regions and construction practices. The model performed satisfactorily in the validation phase with an R^2 of 0.88 and with a RMSE of 1.06, as shown in Figure 40. A good agreement was also found when the average SN_{TSD} for each road section was compared with the average SN_{FWD}; see Figure 41.

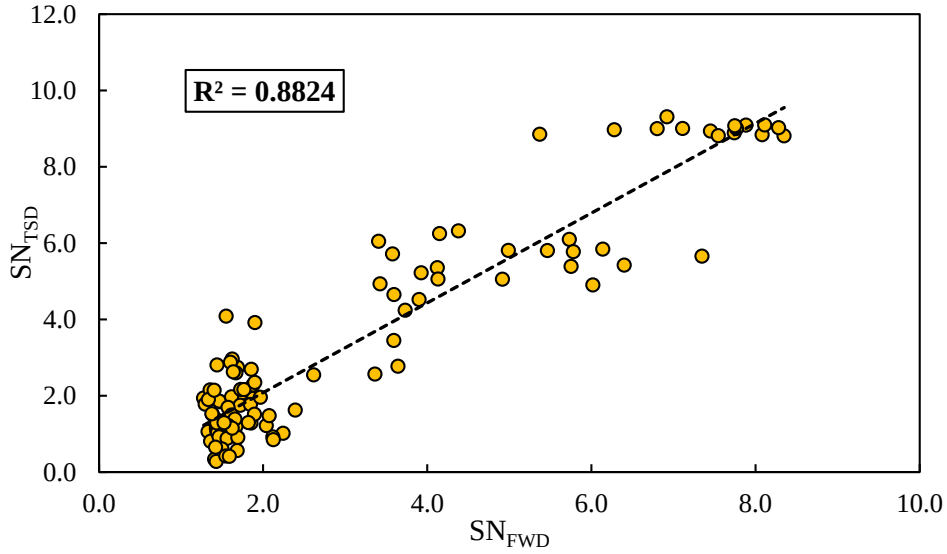

Figure 40
Model fitting in the validation phase

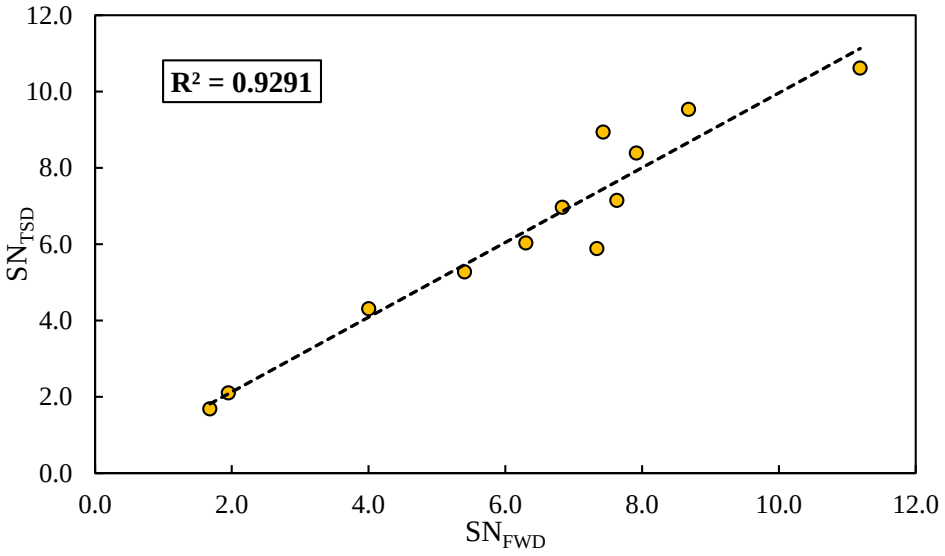

Figure 41
Average SN comparison between TSD and FWD for each section

Table 15 shows the calculated RMSE for each section. It should be noted that the concept of SN is not used for composite pavements in the AASHTO 93 pavement design method; therefore, the tested composite sections (Site ID 3 and 13) were not used in the development and the validation of the model. As shown in this table, RMSE obtained from the model's output was satisfactory within each section.

Table 15
Section wide comparison between predicted and measured SN

Control Section	Route	Log-mile	SN RMSE
067-08	LA 34-1	5.55 - 6.95	0.581
067-09	LA 34-2	3.35 – 4.75	0.168
326-01	LA 594-2	5.05 - 6.45	0.840
324-02	LA 616	3.55 - 4.95	0.607
831-05	LA 821	2.05 - 3.25	0.967
071-02	US 425	1.00 - 2.50	1.029
069-03	LA 33	3.05 - 4.45	1.189
315-02	LA 143	6.00 - 7.50	0.708
333-03	LA 582	3.00 - 4.50	0.827
862-14	LA 589	4.00 - 5.50	1.743
326-01	LA 594-1	2.00 - 3.50	1.268
IDAHO	ID-SH22	Seg 05	0.793

The residual plots are shown in Figure 42 with each independent variable used in the model. The residuals were calculated as the difference between the measured and predicted SN. The plots were drawn for both data sets used in the development and validation phases. As illustrated, the residuals were reasonably scattered and no clear trend is visible in the plots; therefore, the model's estimation can be assumed random with the model inputs.

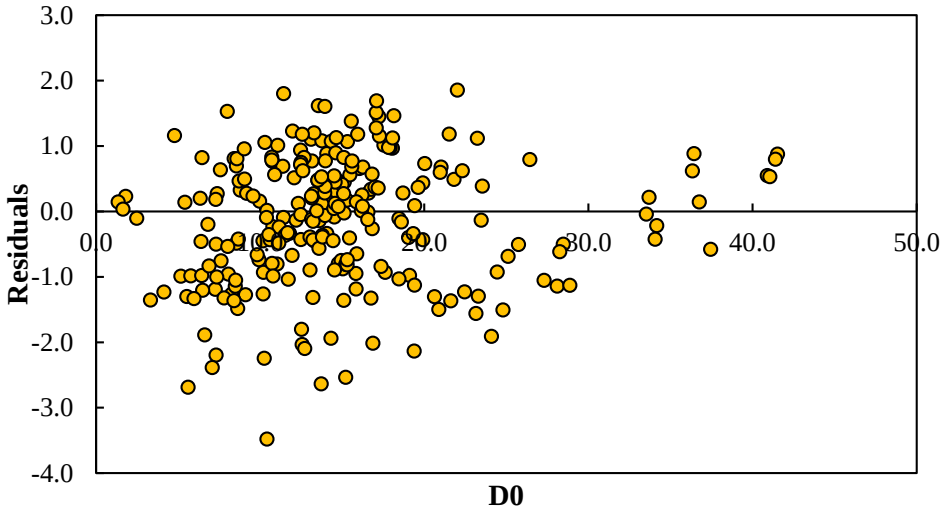

(a)

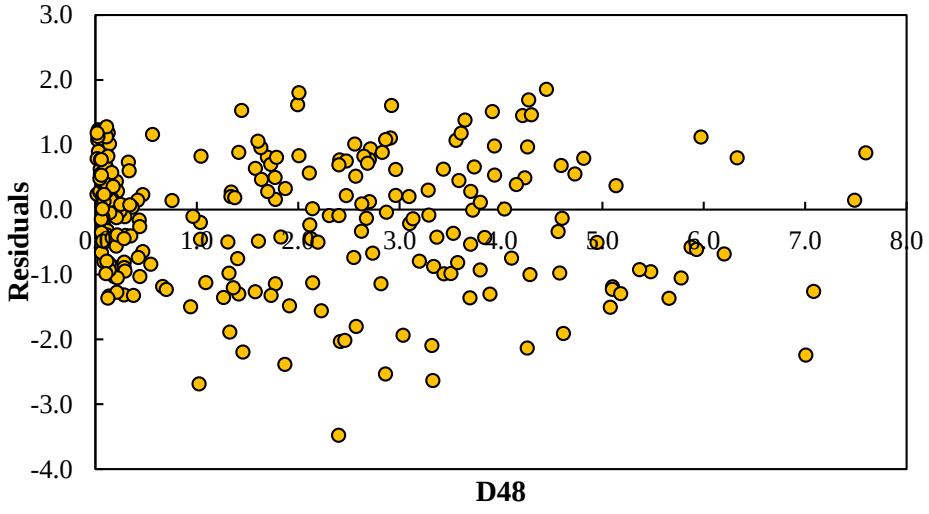

(b)

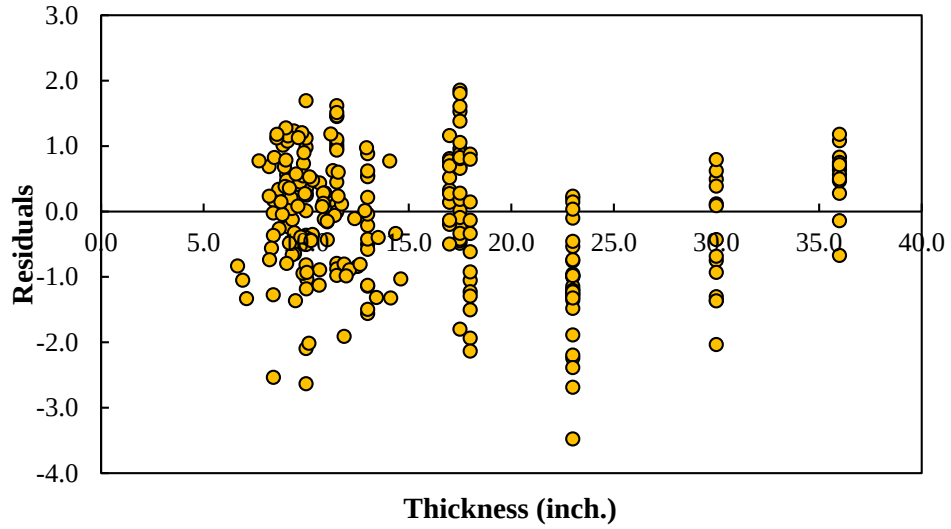

(c)

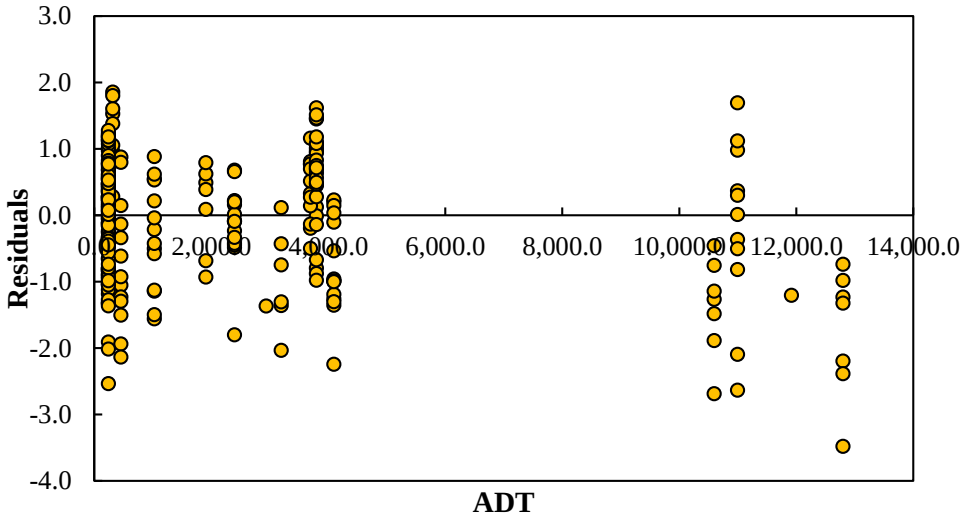

(d)

Figure 42
Residual Plots for the developed model

Longitudinal Profile Comparison

A continuous SN profile was developed from the proposed model at short intervals of 0.01-mile. Longitudinal profiles for SN_{TSD} obtained from the model were compared to SN_{FWD} for both the Louisiana and Idaho control sections. The longitudinal profiles for one Louisiana section and one Idaho section are shown in Figures 43 and 44, respectively. Higher

variability was noted in the Idaho section, possibly due to higher roughness and cracking at the surface as suggested by the lower SN predicted for this section. Past studies concluded that both FWD and RWD test methods resulted in a greater average deflection and scattering in sites in poor conditions *[48]*.

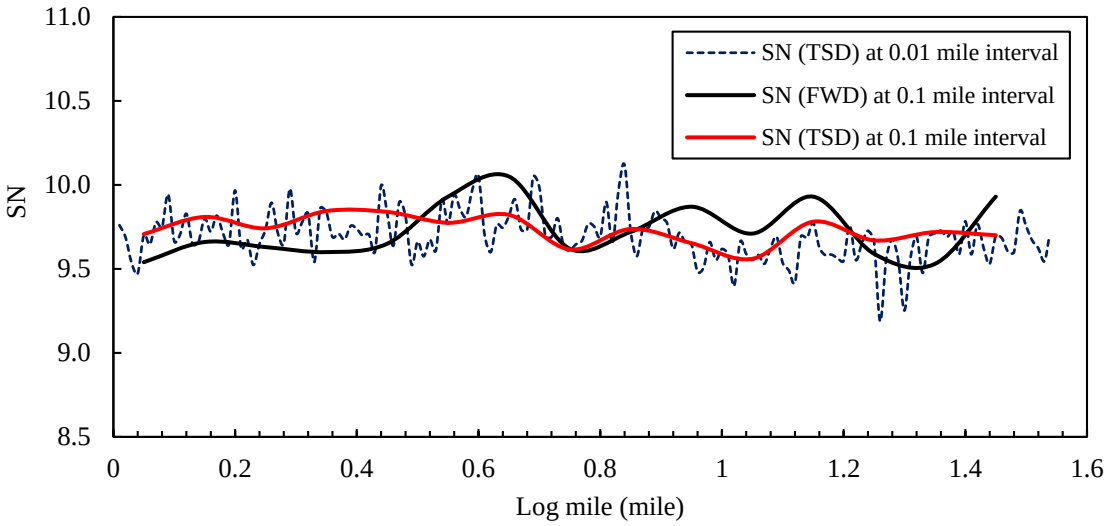

Figure 43
Longitudinal comparison of SN_{TSD} and SN_{FWD} for Louisiana

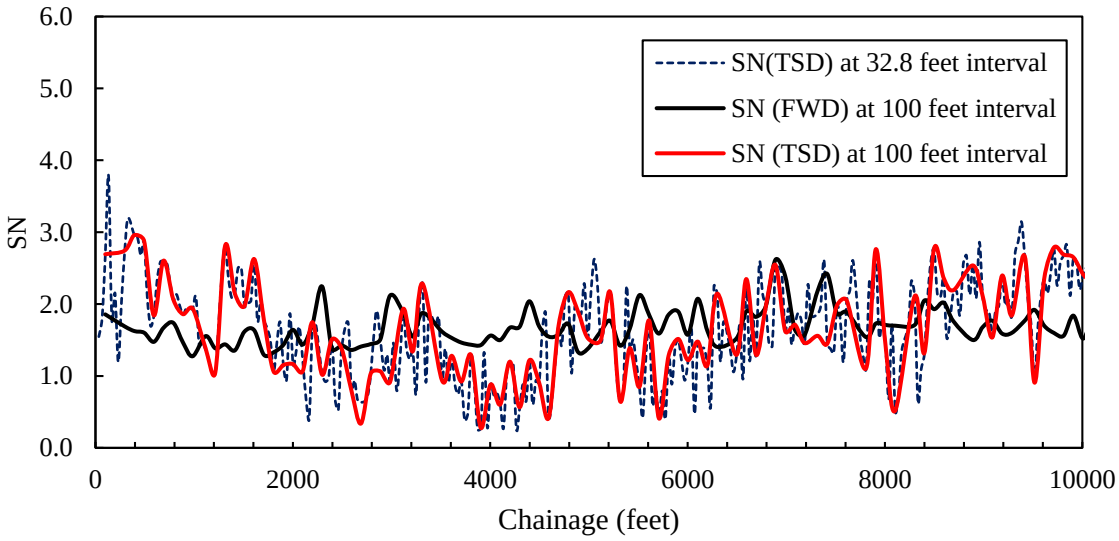

Figure 44
Longitudinal comparison of SN_{TSD} and SN_{FWD} for Idaho

Sensitivity Analysis

A sensitivity analysis was conducted for the proposed model's output as a function of the model's inputs. Sensitivity of the dependent variable (SN_{TSD}) was tested for different input parameters varied within their maximum and minimum values. The average of each of the input parameters was used as the baseline in the sensitivity analysis. From the results of the sensitivity analysis, it was found that the predicted SN_{TSD} was most sensitive to D_0 among all other parameters and the least sensitive to ADT. The change in the predicted SN_{TSD} with the varying input parameters is shown in Figure 45.

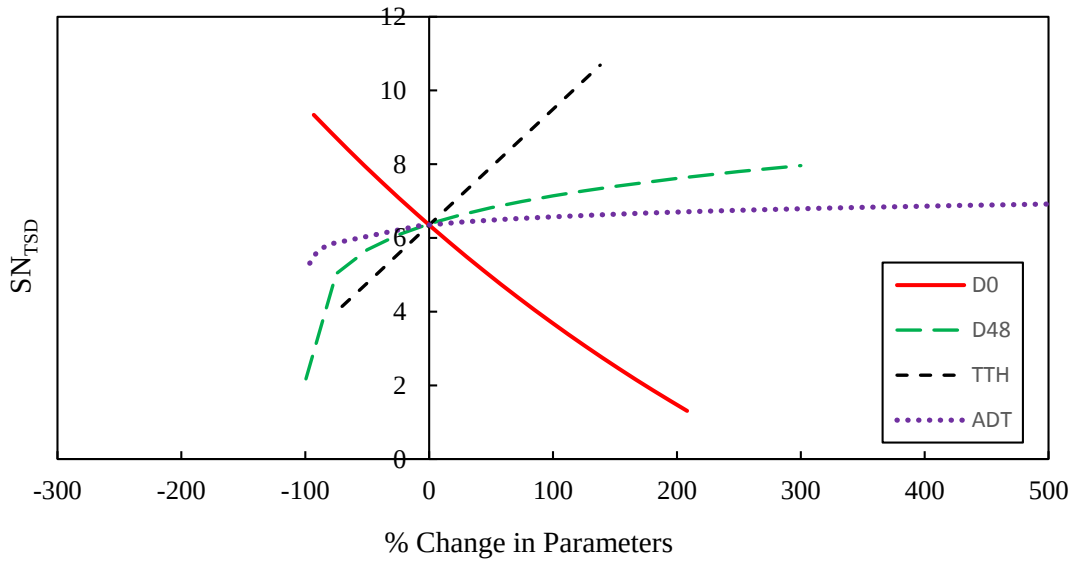

Figure 45
Sensitivity analysis for the SN_{TSD} model

Correlation of Structural Capacity with PMS Functional Indices

An Analysis of Variance was conducted with the measurements from the Louisiana control sections to evaluate the degree of influence of functional indices on in-service structural capacity at a confidence level of 95%. Functional indices considered in the comparison with SN_{TSD} were alligator cracking (ALCR), random cracking (RNDM), patching (PTCH), rutting index (RUT_IND), roughness (RUFF), and Pavement Condition Index (PCI). Road sections were divided into five categories based on asphalt layer(s) thickness and type of base layer (treated and untreated) as shown in Table 16 *[38]*. Thick sections were those that had an AC layer greater than 6 in.; medium sections were those with AC layers between 3 and 6 in.; and

thin sections were those with AC layers less than 3 in. It is noted that there was no thin untreated section tested using TSD in the present study.

Table 16
Classification of the control sections

Asphalt layer thickness	Base layer type
> 6 in.– Thick 3 in. < thickness < 6 in. – Medium < 3 in. – Thin	If Stabilized – Treated If not stabilized- Untreated

The correlation between each of the aforementioned functional indices and structural indices (SN_{TSD}) was evaluated using P-value obtained from the statistical analysis. Since 95% confidence limit was used, a P-value less than 0.05 would represent significant correlation between the condition indices and vice-versa. As shown by the results in Table 17, non-significant statistical relation was found between functional indices and SN in four of the five road categories. Therefore, one may assume that considering a structurally based index in PMS would allow for the identification of road segments that are in need of structural repair and that are not currently identified by the functional indices.

Table 17
Significance of functional indices on SN

Road Category	Functional Indices (Pr > |t|)					
	ALCR	**RNDM**	**PTCH**	**RUT_IND**	**RUFF**	**PCI**
Thick (Treated)	0.7457	*0.0002*	0.4741	0.5430	0.7276	*0.2646*
Thick (Untreated)	*0.0010*	0.2563	0.9565	0.3777	0.7837	0.4982
Medium (Treated)	0.2943	0.0729	*0.0014*	0.1078	0.8731	0.1786
Medium (Untreated)	0.4792	0.6867	NA	0.7065	0.7834	0.8272
Thin (Treated)	0.2205	0.6867	NA	NA	0.1645	0.2347

Note: Non-significant relationships are marked in yellow. NA=Not Available.

Performance Evaluation of the Developed Model

The model's precision and adequacy were evaluated by comparing the percentage loss in SN_{TSDeff} and SN_{FWDeff}. The proposed model's ability in identifying structurally deficient sections was also evaluated as compared to structural deterioration identified from extracted cores and from FWD. Since cores were only available for the Louisiana data set, this analysis was exclusively conducted for the Louisiana road sections.

Calculation of Loss in In-Service SN

To determine the percentage loss in in-service SN, the AASHTO design SN during construction was calculated using equation (27):

$$SN = a_1 * D_1 + a_2 * m_2 * D_2 + a_3 * m_3 * D_3 \quad (27)$$

where,

a_1 = asphalt layer coefficient, a_2 = base layer coefficient, a_3 = subbase layer coefficient;

D_1 = asphalt layer thickness (in.), D_2 = base layer thickness (in.), and D_3 = subbase layer thickness (in.); and

m_2 = base layer drainage coefficient and m_3 = subbase layer drainage coefficient.

The values of the layer coefficients were selected in accordance with LaDOTD design standards: a_1 = 0.42; a_2 = 0.28 for treated (cement stabilized) base and 0.07 for untreated base; a_3 = 0.11 for cement treated subbase and 0.04 for untreated subbase. The values of m_1 and m_2 were considered 1.0 in all cases.

After calculating the design SN of the sections during construction, SN_{TSD} was corrected according to the findings of a study conducted by Wu and Gaspard to account for design and construction practices in the State as follows *[49, 50]:*

$$SN_{eff} = 2.58 \ln (SN_{FWD}) - 0.77 \quad (28)$$

Since the SN_{TSD} model was developed and validated based on SN calculated from FWD deflections, the predicted SN_{TSD} of the road sections were also adjusted through the same model using equation (29):

$$SN_{TSDeff} = 2.58 \ln (SN_{TSD}) - 0.77 \quad (29)$$

The loss in SN_{TSDeff} was then calculated at every 0.1-mile interval using equation (30):

$$\text{Loss in SN}(\%) = \frac{\text{Design SN} - SN_{TSDeff}}{\text{Design SN}} * 100 \quad (30)$$

The percentage loss in SN_{TSDeff} was compared with SN_{FWDeff} at each extracted core location. It is noted that the only control sections considered in this comparison were the ones, which had the cores extracted at almost the same location to ensure precise evaluation of the SN model. The average SN over 1.5-mile was also calculated and compared. As shown in Figures 46 and 47, the estimated percentage loss from the model was in good agreement with the percentage loss predicted from SN_{FWD}.

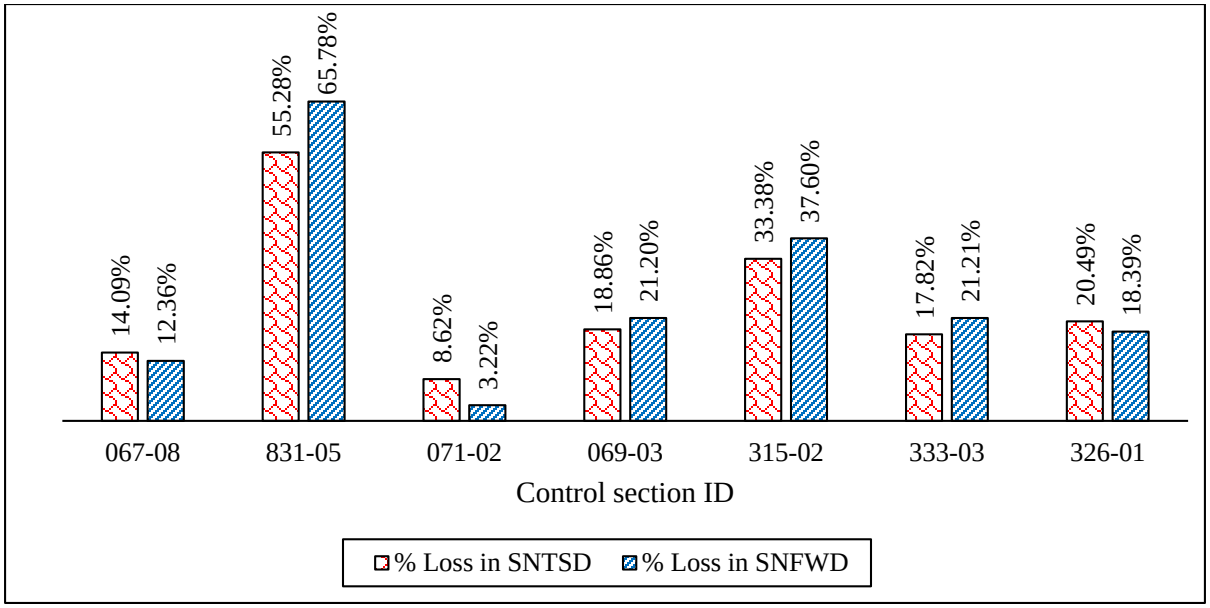

Figure 46
Comparison of loss in in-service SN at core location

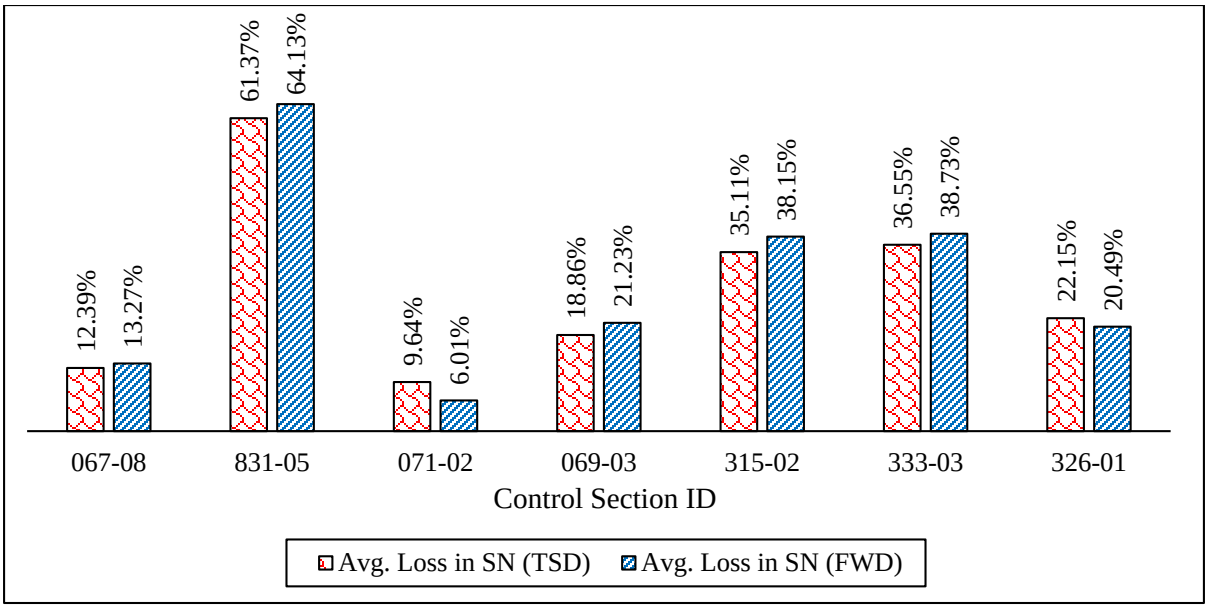

Figure 47
Comparison of loss in average in-service SN

Analysis of the Extracted Cores

In this section, the model's efficiency in identifying structural deficient sections was evaluated. Past studies by the authors used 50% loss of AASHTO SN as the threshold to identify structurally deficient locations *[38]*. In the present study, model's evaluation in identifying structurally deficient locations was also based on a 50% loss in structural capacity. The extracted cores were compared with the estimated loss in SN (%) along with the functional indices at the same locations. A detailed evaluation of four typical road section is presented in the following sections.

Control Section 831-05. The control section is located in Route LA 821 with a length of 8.18-mile located at Lincoln parish in Louisiana District 05. The total layer thickness of this control section from extracted core was found to be 13 in. consisting of three AC layers of 5 in. and a granular base layer of 8 in. After assessment of the extracted core, deterioration (stripping) was detected in the third asphalt layer, which was 2 in. thick as shown in Figure 48. The percentage loss in SN_{TSDeff} at the core location and the average SN (%) loss over 1.5-mile was found 55.3% and 61.4%, respectively. The average Pavement Condition Index (PCI), a combined functional index, for this control section was 92.7 over 1.5 mile and the PCI at the core location was 90.3 indicating excellent functional conditions. Given the average SN loss (%) is greater than 50%, this control section was identified as structurally deficient even with a sound PCI rating.

Figure 48
Control Section 831-05

Control Section 315-02. The control section is located in Route LA 143 with a length of 9.26-mile located at Ouachita parish in Louisiana District 05. The total layer thickness of the control section from extracted core was 23 in. consisting of two AC layers of 9.5 in. on top of a cement stabilized sand clay gravel base layer of 13.5 in. After assessment of the extracted core, debonding was detected between the bottom AC layer and the underlying base layer, as shown in Figure 49. It is to be noted that poor drainage conditions were also detected in this road section. The average percentage loss in SN_{TSDeff} over 1.5-mile and at the core location was 33.4% and 35.1%, respectively. The average PCI for this control section was found to be 92.7 over 1.5 mile and 96.7 at the core location indicating excellent function conditions. Though the predicted structural capacity loss was less than 50%, the model predicted a loss in SN possibly related to the detected debonding between the AC and the base layers.

Figure 49
Control Section 315-02

Control Section 333-03. The control section is located in Route LA 582 with a length of 6.83-mile located at E Carroll parish in Louisiana District 05. The total layer thickness of this control section from the extracted core was 18 in. consisting of five AC layers of 9.5 in. and a granular base layer of 8.5 in. After assessment of the extracted core, deterioration (stripping) was found in the bottom AC layer that was 1.5 in. thick, as shown in Figure 50. The average percentage loss in SN_{TSD} over 1.5-mile was calculated as 36.6% and 17.8% at the core location. Upon further assessment of the control section, it was found that a new overlay was applied since the core extraction and functional survey explaining the adequate structural capacity of the control section. Hence, the model's estimated loss in SN can reasonably be justified. The average PCI in 2015 for this control section was found to be 67.9 over 1.5 mile and the PCI at the core location was 73.6, which was prior to the new overlay.

Figure 50
Control Section 333-03

Summary of the Model's Structural Efficiency Prediction

As discussed in the previous section, the proposed model can reasonably estimate the average loss in in-service SN (%) as compared with the extracted cores. While functionally sound, a number of control sections were identified as structurally deficient as summarized in Table 18.

Table 18
Model's performance evaluation based on extracted cores

Control Section	Avg. PCI	Type of deterioration in Cores	Note	Avg. loss in SN_{TSDeff} (%)	Remarks on Model's efficiency
831-05	92.7	Stripping	N/A	61.4	Identified structurally deficient section
315-02	92.7	Separation	Cement stabilized base layer	33.4	Predicted loss in structural capacity due to debonding
333-03	67.9	Stripping	New overlay applied since core extraction	36.6	Reasonable estimation as new overlay was applied

Note: N/A = not applicable

CONCLUSIONS

The research objective of this study was to assess the feasibility of using TSD measurements at the network-level for pavement conditions structural evaluation in Louisiana and in backcalculation analysis. To achieve the objectives of the study, TSD and FWD measurements were collected in District 05 of Louisiana and data were available from experimental programs conducted at the MnROAD research test facility and in Idaho. TSD measurements were compared with FWD deflection measurements to evaluate the level of agreement and difference between the two devices. Based on this evaluation, a SN predictive model was developed and validated to assess the structural conditions of in-service pavements. The model was then used to identify structurally sound and structurally deficient in-service pavements. Furthermore, a methodology was developed and was validated to backcalculate the layer moduli from TSD measurements. Based on the results of the analysis, the following conclusions may be drawn.

TSD Measurements Evaluation and Comparison with FWD

- Based on ANOVA and Limit of Agreement plots, it can be concluded that the deflection reported by both FWD and TSD for the same locations are statically different, which is reasonable given the differences in loading characteristics and load type between the two devices.
- It is concluded that surface roughness had an effect on TSD loading variation and subsequent field measured deflections. From simulation results conducted using 3D Move, it is also concluded that the increase in vehicle speed caused a decrease in the deflections.

Development of a Methodology to Predict Layer Moduli from TSD Data

- The development of a methodology to incorporate TSD measurements in the backcalculation analysis for predicting pavement layer moduli was successful. The proposed ANN model showed acceptable accuracy in predicting the corresponding FWD deflections (TSD*) from TSD deflection measurements with a coefficient of determination of 0.90.

- The backcalculated moduli from FWD and TSD* deflection measurements were in good agreement. The RMSE was 12.5%, 13.2%, and 10.2% for the AC moduli, base moduli, and subgrade moduli, respectively.
- The ANN model was successfully validated by comparing the critical pavement responses, number of cycles for fatigue failure, and Structural Health Index (SHI) calculated from FWD and TSD* measurements.

Development of a TSD-Based SN Prediction Model

- The present study successfully developed a model to predict in-service SN based on TSD deflections at 0.01-mile interval of a road section. The non-linear regression model showed an acceptable prediction accuracy with a coefficient of determination of 0.92 and RMSE of 0.88 in the development phase and a coefficient of determination of 0.88 and a RMSE of 1.06 in the validation phase. The model was successfully developed and validated with SN calculated based on TSD and FWD deflection data obtained from two contrasting data sets from Louisiana and Idaho.
- The importance of considering structural indices along with functional indices was demonstrated based on ANOVA analysis and extracted cores.
- The estimated percentage loss in structural capacity from the model was in good agreement with the percentage loss calculated from FWD.
- Core samples showed that sections that were predicted to be structurally deficient suffered from asphalt stripping and debonding problems. Yet, some of these sections were in very good conditions according to their functional conditions.

RECOMMENDATIONS

Based on the results and findings of this project, the study recommends the following course of actions for future studies:

- Additional TSD and FWD comparison testing is recommended to be conducted throughout the state of Louisiana to validate and fine-tune the models and procedures presented in this report.
- Research should develop a methodology to incorporate TSD measurements in PMS decision-making processes and in pavement design.
- With the availability of additional measurements, the effects of surface roughness and vehicle speed should be further investigated.
- Cost-effectiveness of TSD measurements should be investigated in future studies.

ACRONYMS, ABBREVIATIONS, AND SYMBOLS

ADT	Average Daily Traffic
AASHTO	American Association of State Highway and Transportation Officials
AC	Asphalt Concrete
ALCR	Alligator Cracking Index
ANOVA	Analysis of Variance
ANN	Artificial Neural Network
ARAN	Automatic Road Analyzer
ARRB	Australian Road Research Board
COV	Co-efficient of Variation
D_0	Maximum Surface Deflection
DOTD	Department of Transportation and Development
FHWA	Federal Highway Administration
ft.	foot (feet)
FWD	Falling Weight Deflectometer
GPR	Ground Penetrating Radar
HMA	Hot Mix Asphalt
IRI	International Roughness Index
in.	inch(es)
ksi	Kilo pounds per square in.
lbs.	pound(s)
LOA	Limit of Agreement
LTRC	Louisiana Transportation Research Center
LVR	Low Volume Road
NHS	National Highway of Significance
PCC	Portland Cement Concrete
PCI	Pavement Condition Index
PMS	Pavement Management System
psi	Pounds per square in.
PTCH	Patching Index
RC	Rehabilitation/Reconstruction
RHS	Rural Highway of Significance
RI	Rolling Wheel Deflectometer Index
RM	Restorative Maintenance

RMSE	Root Mean Square Error
RNDM	Random Cracking Index
RUFF	Roughness Index
RUT	Rutting Index
RWD	Rolling Wheel Deflectometer
SCI	Structural Condition Index
SIP	Structural Index of Pavement
SHI	Structural Health Index
SHRP	Strategic Highway Research Program
SN	Structural Number
SHS	State Highway of Significance
TSD	Traffic Speed Deflectometer
TSDD	Traffic Speed Deflection Devices
VIF	Variance Inflation Factor

REFERENCES

1. Zofka, A., Graczyk, M., and Rafa, J. Qualitative Evaluation of Stochastic Factors Affecting the Traffic Speed Deflectometer Results, *Transportation Research Board 94th Annual Meeting*, 2014.
2. Elseifi, M., and Elbagalati, O. *Assessment of Continuous Deflection Measurement Device in Louisiana*, Louisiana Department of Transportation and Development, Project 14-2P, Interim Report, 2013-2016.
3. Zofka, A., Sudyka, J., Maliszewski, M., and Harasim, P. Alternative Approach for Interpreting Traffic Speed Deflectometer Results, *Transportation Research Record Journal of the Transportation Research Board*, 2014.
4. Katicha, S. W., Bryce, J., Flintsch, G., and Ferne, B. Estimating "True" Variability of Traffic Speed Deflectometer Deflection Slope Measurements, *Journal of Transportation Engineering*, 2014.
5. Irwin, L. H., Orr, D. P., and Atkins, D. *FWD Calibration Center and Operational* 459 *Improvements: Redevelopment of the Calibration Protocol and Equipment*. Publication 460 FHWA-HRT-07-040. FHWA, U.S. Department of Transportation, 2009.
6. Xu, B., Ranji, R. S., and Kim, R. Y. New Relationships between Falling Weight Deflectometer Deflections and Asphalt Pavement Layer Condition Indicators. *In 463 Transportation Research Record: Journal of the Transportation Research Board, No.1806 464 (1)*. Transportation Research Board of the National Academies, Washington. D.C., 2002, pp. 465 48-56.
7. Flintsch, G. W., Ferne, B., Diefenderfer, B., Katicha, S., Bryce, J. and Nell. S., Evaluation of Traffic Speed Continuous Deflection Devices, *In Transportation Research Record: Journal of the Transportation Research Board*. Transportation Research Board of the National Academies, Washington. D.C., 2012, pp. 37-46.
8. Flintsch, G., Katicha, S., Bryce, J., Ferne, B., Nell, S., and Diefenderfer, B. *Assessment of Continuous Pavement Deflection Measuring Technologies*, No. SHRP 2 Report S2-R06F-RW-1. 2013.
9. Chai, G., Manoharan, S., Golding, A., Kelly, G. and Chowdhury, S. Evaluation of the Traffic Speed Deflectometer Data Using Simplified Deflection Model, *6th Transport Research Arena*, April 18-21, 2016.
10. Muller, W. B., and Roberts, J. Revised Approach to Assessing Traffic Speed Deflectometer (TSD) Data and Field Validation of Deflection Bowl Predictions, *International Journal of Pavement Engineering*, vol. 14, no. 4, pp. 388–402, 2013.

11. Elbagalati, O., Mousa, M., Elseifi, M. A., Gaspard, K., and Zhang, Z. Development of a Methodology to Backcalculate Pavement Layer Moduli Using the Traffic Speed Deflectometer, *96th Transportation Research Board Annual Meeting*, 2017.

12. Rasmussen, S., Aagaard, L., Baltzer, S., and Krarup, J. A Comparison of Two Years of Network Level Measurements with the Traffic Speed Deflectometer, *2nd European Transport Research Arena*, Ljubljana, 2008.

13. Katicha, S. W., Loulizi, A., Khoury, J. E., and Flintsch, G. W. An Adaptive False Discovery Rate for Wavelet Denoising of Pavement Continuous Deflection Measurements, *Journal of Computing in Civil Engineering*, 2016.

14. Jenkins, M. Geometric and Absolute Calibration of the English Highways Agency Traffic Speed Deflectometer, *Young Researchers Seminar*, Italy, 2009.

15. Rada, G., Nazarian, S., Daleiden, J., and Yu, T. Moving Pavement Deflection Testing Devices: State of the Technology and Best Uses. Proc., *8th International Conference on Managing Pavement Assets, Santiago, Chile*, 2011.

16. Ferne, B., Langdale, P., Round, N. & Fairclough, R. Development of a Calibration Procedure for the U.K. Highways Agency Traffic-speed Deflectometer, *Transportation Research Record: Journal of the Transportation Research Board*, 2093, 111–17, 2009.

17. Simonin, J. M., Li` evre, D., Rasmussen, S., and Hildebrand, G. Assessment of the Danish High Speed Deflectograph in France, *International Conference on the Bearing Capacity of Roads, Railways and Airfields*, Trondheim, 2005.

18. Katicha, S. W., Bryce, J., Flintsch, G., and Ferne, B. Wavelet Denoising of TSD Deflection Slope Measurements for Improved Pavement Structural Evaluation, *Computer-Aided Civil and Infrastructure Engineering*, October 2013.

19. Nasimifar, M., Thyagarajan, S., and Sivaneswaran, N. Backcalculation of Flexible Pavement Layer Moduli from Traffic Speed Deflectometer Data. *Transportation Research Record: Journal of the Transportation Research Board,* No. 2641, pp. 66–74. http://dx.doi.org/10.3141/2641-09, 2017.

20. Elseifi, M., Khalek, A.M.A., Dasari, K. *Implementation of Rolling Wheel Deflectometer (RWD) in PMS and Pavement Preservation*, LTRC Project Number: 09-2P, Final Report 2009-2011.

21. Rabe, R. Structural Pavement Monitoring with Non-Destructive Measuring Devices-507 Experience from a Pilot Project in Germany, *Presentation at the Ninth International* 508 *Conference on Bearing Capacity of Roads, Railways and Airfields,* BCRRA 2013, Trondheim, 509 Norway.

22. Rada, G. R., and Nazarian, S. *The State-of-the-Technology of Moving Pavement Deflection Testing. Final Report*, FHWA-DTFH61-08-D-00025, U.S. Department of Transportation, Washington, D.C.,2011.

23. Katicha, S., Flintsch, G., Ferne, B. W., and Bryce, J. Limits of Agreement (LOA) Method for Comparing TSD and FWD Measurements, *International Journal of Pavement Engineering*, 2014.

24. Roberts, J., Ai, U., Toole, T., and Martin, T. *Traffic Speed Deflectometer: Data Review and Lessons Learnt*, ISBN 978-1-925037-91-3, Austroads Project No. AT1730, Austroads Publication No. AP-T279-14, October 2014.

25. Katicha, S., Flintsch, G., Shrestha, S., and Thyagarajan, S. *Demonstration of Network Level Structural Evaluation With Traffic Speed Deflectometer: Final Report*, Prepared for the Federal Highway Administration**,** Under Contract # DTFH61-11-D-00009-T-13008, 2017.

26. Rada, G. R., Nazarian, S., Visintine, B. A., Siddharthan, R., and Thyagarajan, S. *Pavement Structural Evaluation at the Network Level: Final Report*. FHWA-HRT-15074, 2016.

27. Kannemeyer, L., Lategan, W., and Mckellar, A. Verification of Traffic Speed Deflectometer Measurements Using Instrumented Pavements in South Africa, *Pavement Evaluation*, Blacksburg, Virginia 2014.

28. Basheer, I. A., and Hajmeer, M. Artificial Neural Networks: Fundamentals, Computing, Design, and Application, *Journal of Microbiological Methods* 43 (2000) 3-31, 2000.

29. Kim, M., Burton, Y. M., Prozzi, J. A., and Murphy, M. Maintenance and Rehabilitation Project Selection Using Artificial Neural Networks. *Transportation Research Board 93rd Annual Meeting*, No. 14-3620, 2014.

30. Ceylan, H., Bayrak, M. B., and Gopalakrishnan, P. Neural Networks Applications in Pavement Engineering: A Recent Survey, *International Journal of Pavement Research and Technology*, 7(6), p.434, 2014.

31. Karlaftis, M., and Vlahogianni, E. Statistical Methods versus Neural Networks in Transportation Research: Differences, Similarities and Some Insights. *Transportation Research Part C: Emerging Technologies*, Vol. 19, No. 3, 2011, pp. 387–399.

32. Plati, C., Georgiou, P. and Papavasiliou, V. Simulating Pavement Structural Condition Using Artificial Neural Networks. *Structure and Infrastructure Engineering*, pp. 1–10, 2015.

33. Lawrence, S., Giles, C.L., and Tsoi, A.C. *Lessons in Neural Network Training: Overfitting may be Harder than Expected*, In AAAI/IAAI (pp. 540-545), 1997.

34. Torrecilla, J. S., Aragon J. M., and Palancar, M. C. Optimization of an Artificial Neural Network by Selecting the Training Function. Application to Olive Oil Mills Waste. *Industrial & Engineering Chemistry Research*, 47, 7072-7080, 2008.

35. Rohde, G.T. Determining Pavement Structural Number from FWD Testing. *Transportation Research Record*, No. 1448, pp. 61-68, 1994.

36. Lukanen, E. O., Stubstad, R., and Briggs, R. *Temperature Predictions and Adjustment Factors for Asphalt Pavement*, No. FHWA-RD-98-085, 2000.

37. Gedafa, D. S., Hossain, M., Miller, R., and Van, T. Network-level Flexible Pavement Structural Evaluation, *Retrieved from http://krex.ksu.edu*, 2014.

38. Elbagalati, O., Elseifi, M.A., Gaspard, K., and Zhang, Z. Prediction of In-service Pavement Structural Capacity Based on Traffic-Speed Deflection Measurements, *Journal of Transportation Engineering*, 2016.

39. Schnoor, H., and Horak, E. Possible Method of Determining Structural Number for Flexible Pavements with the Falling Weight Deflectometer, *Abstracts of the 31st Southern African Transport Conference (SATC 2012)*, 2012. Proceedings ISBN Number: 978-1-920017-53-8.

40. Bland J. M., and Altman D. G. Statistical Methods for Assessing Agreement Between Two Methods of Clinical Measurement, *Lancet*, i: 307–310, 1986.

41. Maser, K., Schmalzer, P., Shaw, W., and Carmichael, A. Integration of Traffic Speed Deflectometer and Ground-Penetrating Radar for Network-Level Roadway Structure Evaluation, *Transportation Research Record: Journal of the Transportation Research Board*, No. 2639, 2017, pp. 55–63.

42. Kim, Y. R., and Park, H. G. *Use of Falling Weight Deflectometer Multi-load Data for Pavement Strength Estimation*. No. FHWA/NC/2002-006, 2002.

43. National Cooperative Highway Research Program (NCHRP). *Guide for Mechanistic-Empirical Design of New and Rehabilitated Structures*, NCHRP Report 01- 37A. *Transportation Research Board*, Washington, DC, 2004.

44. Elbagalati, O., Elseifi, M., Gaspard, K., and Zhang., Z. Development of the Pavement Structural Health Index Based on Falling Weight Deflectometer Testing, *International Journal of Pavement Engineering*, 2016, pp. 1–8.

45. Miller, I., Freund, J. E. *Mathematical Statistics: With Applications*, Pearson Education India, 2004.

46. Freund, R. J., Wilson, W. J., and Sa, P. *Regression Analysis*, Academic Press, 2006.

47. Hair J. F., Black W. C., Babin, B. J., and Anderson, R. E. *Multivariate Data Analysis with Readings*, New Jersey: Prentice Hall 1995.

48. Elseifi, M.A., Abdel-Khalek, A., Gaspard, K., Zhang, Z., and Ismail, S. Evaluation of Continuous Deflection Testing Using the Rolling Wheel Deflectometer in Louisiana, *Journal of Transportation Engineering*, ASCE, Vol. 138, No. 4, 414-422, 2012.

49. Wu, Z., and Gaspard, K. *Mechanistic Flexible Pavement Overlay Design Program*, Report No. FHWA/LA.08/454, 2009.

50. Wu, Z., Zhang, Z., and Abadie, C. Determining Structural Strength of Existing Asphalt Layer Using Condition Survey Data, *International Journal of Pavement Engineering*, 14(7), 2013, pp. 603-611.

APPENDIX A

MATLAB Code for the proposed ANN model:

```
% Solve an Input-Output Fitting problem with a Neural Network
% Script generated by Neural Fitting app
% Created 16-Oct-2017 10:18:54
%
% This script assumes these variables are defined:
%
%   TSD - input data.
%   FWD - target data.

x = TSD;
t = FWD;

% Choose a Training Function
% For a list of all training functions type: help nntrain
% 'trainlm' is usually fastest.
% 'trainbr' takes longer but may be better for challenging problems.
% 'trainscg' uses less memory. Suitable in low memory situations.
trainFcn = 'trainlm';  % Levenberg-Marquardt backpropagation.

% Create a Fitting Network
hiddenLayerSize = 10;
net = fitnet(hiddenLayerSize,trainFcn);

% Choose Input and Output Pre/Post-Processing Functions
% For a list of all processing functions type: help nnprocess
net.input.processFcns = {'removeconstantrows','mapminmax'};
```

```
net.output.processFcns = {'removeconstantrows','mapminmax'};

% Setup Division of Data for Training, Validation, Testing
% For a list of all data division functions type: help nndivide
net.divideFcn = 'dividerand';  % Divide data randomly
net.divideMode = 'sample';  % Divide up every sample
net.divideParam.trainRatio = 70/100;
net.divideParam.valRatio = 15/100;
net.divideParam.testRatio = 15/100;

% Choose a Performance Function
% For a list of all performance functions type: help nnperformance
net.performFcn = 'mse';  % Mean Squared Error

% Choose Plot Functions
% For a list of all plot functions type: help nnplot
net.plotFcns = {'plotperform','plottrainstate','ploterrhist', ...
    'plotregression', 'plotfit'};

% Train the Network
[net,tr] = train(net,x,t);

% Test the Network
y = net(x);
e = gsubtract(t,y);
performance = perform(net,t,y)

% Recalculate Training, Validation and Test Performance
trainTargets = t .* tr.trainMask{1};
```

```
valTargets = t .* tr.valMask{1};
testTargets = t .* tr.testMask{1};
trainPerformance = perform(net,trainTargets,y)
valPerformance = perform(net,valTargets,y)
testPerformance = perform(net,testTargets,y)

% View the Network
view(net)

% Plots
% Uncomment these lines to enable various plots.
%figure, plotperform(tr)
%figure, plottrainstate(tr)
%figure, ploterrhist(e)
%figure, plotregression(t,y)
%figure, plotfit(net,x,t)

% Deployment
% Change the (false) values to (true) to enable the following code blocks.
% See the help for each generation function for more information.
if (false)
    % Generate MATLAB function for neural network for application
    % deployment in MATLAB scripts or with MATLAB Compiler and Builder
    % tools, or simply to examine the calculations your trained neural
    % network performs.
    genFunction(net,'myNeuralNetworkFunction');
    y = myNeuralNetworkFunction(x);
end
if (false)
    % Generate a matrix-only MATLAB function for neural network code
```

```
    % generation with MATLAB Coder tools.
    genFunction(net,'myNeuralNetworkFunction','MatrixOnly','yes');
    y = myNeuralNetworkFunction(x);
end
if (false)
    % Generate a Simulink diagram for simulation or deployment with.
    % Simulink Coder tools.
    gensim(net);
end
```

This public document is published at a total cost of $250
42 copies of this public document were published in this first printing at a cost of $250. The total cost of all printings of this document including reprints is $250. This document was published by Louisiana Transportation Research Center to report and publish research findings as required in R.S. 48:105. This material was duplicated in accordance with standards for printing by state agencies established pursuant to R.S. 43:31. Printing of this material was purchased in accordance with the provisions of Title 43 of the Louisiana Revised Statutes.